

November 2020

## New Mechanisms that Control FACT Histone Chaperone and Transcription-mediated Genome Stability

Angelo Vincenzo de Vivo Diaz  
*University of South Florida*

Follow this and additional works at: <https://digitalcommons.usf.edu/etd>

 Part of the [Cell Biology Commons](#), and the [Molecular Biology Commons](#)

---

### Scholar Commons Citation

de Vivo Diaz, Angelo Vincenzo, "New Mechanisms that Control FACT Histone Chaperone and Transcription-mediated Genome Stability" (2020). *USF Tampa Graduate Theses and Dissertations*.  
<https://digitalcommons.usf.edu/etd/9566>

This Dissertation is brought to you for free and open access by the USF Graduate Theses and Dissertations at Digital Commons @ University of South Florida. It has been accepted for inclusion in USF Tampa Graduate Theses and Dissertations by an authorized administrator of Digital Commons @ University of South Florida. For more information, please contact [scholarcommons@usf.edu](mailto:scholarcommons@usf.edu).

New Mechanisms that Control FACT Histone Chaperone and Transcription-  
mediated Genome Stability

by

Angelo Vincenzo de Vivo Diaz

A dissertation submitted in partial fulfillment  
of the requirement for the degree of  
Doctor of Philosophy  
Department of Cell, Microbiology and Molecular Biology  
College of Arts and Sciences  
University of South Florida

Major Professor: Younghoon Kee, Ph.D.  
Gary Daughdrill, Ph.D.  
Sandra Westerheide, Ph.D.  
Meera Nanjundan, Ph.D.

Date of Approval:  
October 26, 2020

Keywords: OTUD5, UBR5, SPT16, TRC

Copyright © 2020, Angelo Vincenzo de Vivo Diaz

## Dedication

I would like to dedicate this work to my parents, who without their support I would not have been able to get through graduate school. Their love, advice and understanding enabled me to push forward.

## Acknowledgments

I would like to acknowledge several people, starting with Dr. Younghoon Kee. His guidance and constant push to better myself was crucial to both better myself as a person and grow as a researcher. His mentorship will be crucial for me moving forward into my career. I would also like to thank fellow lab members for their help: Anthony Sanchez, who started with me in the program and was a great person to discuss our work – I learned a lot from our discussions. Dr. Jeonghyeon Kim, our former post doc who patiently trained me and set a high standard of work. Jose Yegres, former technician, the amount of work you helped me with was invaluable. I would also like to thank former lab technician and my best friend Sylvia Emly, who in addition of providing help with crucial experiments; she was the best person I could have hoped for - I couldn't have done this without her help.

I would also like to thank my committee members for their helpful insight and constructive criticism: Drs. Meera Nanjunda, Sandy Westerheide, and Gary Daughdrill. Many thanks to Robert Hill, who was in charge of the core facilities and trained me on many different equipment and helped troubleshoot many experiments.

## Table of Contents

List of Tables .....	iii
List of Figures .....	iv
Abstract.....	vi
Chapter 1: Introduction.....	1
Ubiquitination as a Cellular Signal .....	1
E3 Ligases and UBR5 .....	3
Deubiquitinating enzymes.....	4
OTU deubiquitinases and OTUD5 .....	5
DNA damage response .....	6
Transcriptional regulation at DNA breaks .....	7
Transcriptional – Replication Conflict and the formation of R-loops .....	8
The nucleosome and Histone Chaperones.....	10
The FACT Complex.....	10
Structure and Domains of SPT16 and SSRP1 .....	11
Mechanisms and Regulation of FACT Activity .....	13
Acetylation and Histone deacetylases 1 and 2.....	15
Chapter 2: Methods ..	17
Cell lines, plasmids, and chemicals .....	17
RNAi .....	17
Western Blots and antibodies .....	19
Immunoprecipitation and Mass Spectrometry Analysis .....	19
Immunofluorescence and Image Quantification .....	20
Proximity Ligation Assay .....	22
EdU Labeling.....	23
Cell Fractionation Assay.....	23
Clonogenic Survival Assay .....	23
Protein Purification and <i>in vitro</i> binding.....	24
Limited Proteolysis .....	25
Cell Cycle Analysis .....	25
Chromatin Immunoprecipitation .....	25
End Point PCR Analysis .....	26
qPCR Analysis .....	27
Chapter 3: The OTUD5-UBR5 complex regulates FACT-mediated transcription at damaged chromatin .....	28
Introduction .....	28
Results .....	29
OTUD5 is a regulator of UBR5 stability and foci formation .....	30
OTUD5 localizes to chromatin and double strand breaks.....	36
Mapping the interaction site between OTUD5 and UBR5.....	39

OTUD5 regulates transcriptional repression at double strand Breaks.....	42
OTUD5 interacts with histone chaperone SPT16 .....	45
OTUD5 interacts with SPT16 through its C-terminus .....	49
Identification of a nuclear localization signal in OTUD5 .....	51
OTUD5 regulates SPT16 enrichment.....	53
Transcriptional repression at DSB is dependent on SPT16.....	54
Interaction deficient OTUD5 mutants cannot rescue the transcriptional phenotype .....	55
Cancer associated OTUD5 missense mutation disrupts FACT association .....	56
OTUD5 depletion causes genome instability.....	57
Discussion.....	60
Future Directions .....	61
 Chapter 4: Uncoupling of OTUD5/FACT reveals replication stress and genomic instability .....	63
Introduction .....	63
Results .....	64
OTUD5 depletion causes replication stress.....	64
OTUD5 depletion causes R-loop formation and accumulation at CFS.....	67
Validation of OTUD5 <sup>D537A</sup> knock in cell line.....	69
OTUD5 is a direct binding partner of SPT16 .....	75
OTUD5 <sup>D537A</sup> knock in in cell line exhibit TRC.....	77
SPT16 interacts with HDAC1/HDAC2 through OTUD5 .....	81
Discussion.....	83
Future Directions .....	84
 Works Cited .....	86
 Appendix I: Supplementary Information.....	99

List of Tables

Table 1. List of siRNA used and companies who engineered the sequences..... 18

Table 2. List of primers used for end point analysis and qPCR analysis of CHIP .....27

## List of Figures

Figure 1. Review of Ubiquitination.....	4
Figure 2. Schematic of the FACT Complex .....	12
Figure 3. UBR5 protein levels are dependent on OTUD5 expression. ....	30
Figure 4. Western blot cycloheximide chase for UBR5 stability. ....	31
Figure 5. UBR5 foci is dependent on OTUD5.....	32
Figure 6. Genomic sequencing of OTUD5 Knock Out cell lines.....	33
Figure 7. OTUD5 KO cell lines confirm UBR5 stability is dependent on OTUD5 .....	33
Figure 8. OTUD5 promotes UBR5 stability by preventing its proteasomal degradation .....	35
Figure 9. UBR5 and OTUD5 directly bind.....	36
Figure 10. OTUD5 localizes to double strand break site.....	37
Figure 11. OTUD5 is enriched at the chromatin after DSB .....	38
Figure 12. OTUD5 and UBR5 interact in the nucleus at DSB sites.....	39
Figure 13. Prediction of Natural Disordered Regions Score of OTUD5 protein.....	39
Figure 14. Limited Proteolysis of OTUD5 .....	40
Figure 15. Mapping the interaction site of OTUD5-UBR5 .....	41
Figure 16. The N-Terminus of OTUD5 is required for UBR5 interaction and stability .....	41
Figure 17. OTUD5 WT, but not OTUD5 $\Delta$ N17, interact with UBR5.....	42
Figure 18. Schematic for pTuner263 reporter cell line .....	43
Figure 19. OTUD5 and UBR5 depletion leads to de-repression of transcription at double strand breaks.....	44
Figure 20. OTUD5 and UBR5 depletion lead to RNA Pol II overlap with $\gamma$ H2AX .....	44
Figure 21. 5-EU stain in OTUD5, UBR5 KO cell lines reveal that transcription is not repressed at DSB sites.....	45



Figure 22. siRNA verification of de-repression phenotype .....	46
Figure 23. OTUD5 binds to SPT16.....	47
Figure 24. OTUD5 co-localizes with SPT16 at DSBs .....	48
Figure 25. Verification Proximity Ligation Assay signal.....	49
Figure 26. OTUD5 binds SPT16 through its UIM.....	50
Figure 27. Recombinant GST-OTUD5 $\Delta$ UIM does not bind to SPT16.....	51
Figure 28. The interaction deficient mutant localizes to DSBs .....	52
Figure 29. Localization study OTUD5 fragments .....	53
Figure 30. SPT16 foci is enlarged when OTUD5 or UBR5 are depleted.....	54
Figure 31. SPT16 depletion reverses OTUD5, UBR5 depletion phenotype .....	55
Figure 32. Interaction deficient mutant do not repress transcription.....	56
Figure 33. UIM mutant D537A does not repress transcription .....	58
Figure 34. OTUD5 depletion causes genomic instability .....	59
Figure 35. OTUD5 depletion increases G1 bodies .....	65
Figure 36. OTUD5 depletion causes accumulation of 53BP1 at CFS.....	66
Figure 37. OTUD5 knockdown shows replication stress.....	66
Figure 38. OTUD5 depletion leads to aberrant transcription at CFS.....	67
Figure 39. PLA analysis of OTUD5, UBR5 depleted cells reveals TRC phenotype .....	68
Figure 40. OTUD5 binding to UBR5 / SPT16 is important to prevent replication stress.....	69
Figure 41. Genomic sequencing of OTUD5 <sup>D537A</sup> Knock in cell lines.....	70
Figure 42. Validation of OTUD5 <sup>D537A</sup> Knock in cell line .....	71
Figure 43. OTUD5 <sup>D537A</sup> Knock in clones show increased replication defects .....	72
Figure 44. OTUD5 <sup>D537A</sup> Knock in cell lines have increased G1 bodies.....	73
Figure 45. OTUD5 <sup>D537A</sup> Knock in cell lines show spontaneous $\gamma$ H2AX foci.....	74
Figure 46. OTUD5 <sup>D537A</sup> Knock in cell lines are sensitive to a variety of different damage .....	75

Figure 47. OTUD5 binds directly to SPT16 .....	76
Figure 48. The C-term of OTUD5 is sufficient to bind SPT16 .....	77
Figure 49. SPT16 accumulates at CFSs in OTUD5 D537A Knock in cells .....	78
Figure 50. R-loop formation at CFS is increased in cells with unregulated transcription .....	79
Figure 51. OTUD5 <sup>D537A</sup> knock in cell line show increased PLA signal between replication fork and transcription .....	80
Figure 52. OTUD5 D537A knock in cell have increased FANCD2 foci .....	81
Figure 53. OTUD5 mediates the interaction of HDAC1/2 with SPT16 .....	82
Figure 54. PLA analysis between SPT16 and HDAC1/2 reveals lack of signal in OTUD5 D537A Knock in cell line .....	83
Figure 1A. FACT histone Eviction Model.....	99
Figure 2A. Model for Repression.....	100

## Abstract

The Role of deubiquitinating enzymes (DUBs) in transcription, replication and genome integrity is not one that has been extensively researched. OTU DUBs are a particular class of enzyme with very little known about them.

OTUD5 is a cysteine protease in the OTU family responsible to processing lysine 48 and lysine 63 ubiquitin chains. Recently, it has been implicated in to play a role in transcription through its binding partner UBR5. OTUD5 has also been shown to interact with proteins such as PDCD5 and p53, potentially have great importance in cell fate. In this study, I describe new discovered functions for OTUD5 in regards to transcriptional regulation at double strand breaks through a novel interaction with the histone chaperone FACT complex and the downstream effects of OTUD5 has by preventing Transcription-Replication Conflict (TRC). I provide evidence for the UBR5/OTUD5/FACT complex and how they bind to each other: OTUD5 binds UBR5 through its disordered N-terminal tail while the UIM of OTUD5 binds directly to SPT16. I describe a new pathway where FACT/OTUD5 interact with histone deacetylases 1 and 2 (HDAC1/2) to coordinate transcriptional repression both at double strand breaks and at the replication for in order to maintain genomic integrity.

## Chapter 1: Introduction

### **Ubiquitination as a Cellular Signal**

Ubiquitination is one of several post-translational modifications that can occur within a cell. Ubiquitination is accomplished in a series of steps carried out by multiple proteins working in a step-wise mechanism. The enzymes involved in this process are divided into three categories: E1 enzymes (ubiquitin activating enzymes), E2 enzymes (ubiquitin conjugating enzymes), and finally E3 enzymes (ubiquitin ligases) (1). Ubiquitin is covalently conjugated to proteins using lysine residues within the substrate (2). There are seven known types of ubiquitin chains, but not all of them have been characterized. But just as ubiquitin can be conjugated to a protein, ubiquitin signals can also be removed (3). This is accomplished by deubiquitinating enzymes (DUBs), a group of enzymes that identify and remove either a single ubiquitin or entire ubiquitin chains (4).

Ubiquitination occurs in several steps: ubiquitin activating enzymes utilize ATP to first bind ubiquitin molecules which are then passed on to a respective ubiquitin conjugating enzyme. The E2 will then form a complex with an ubiquitin ligase, which recognizes the final substrate and catalyzes the “ligation” of ubiquitin and the substrate (5). The process may then be repeated to target a new molecule resulting in monoubiquitination or be repeated on the same ubiquitin molecule to form polyubiquitination chains, each with different effect (6). Therefore, it is important to identify and characterize the enzymes that add different combinations of ubiquitin to their substrates.

Monoubiquitination can happen in two different methods which lead to different effects: monoubiquitination at a single lysine of a substrate and multiple mono-ubiquitination on multiple

lysines on a single substrate (7). For example, the E3 ubiquitin ligase RNF8 is known to monoubiquitinate histone H2AX in response to DNA damage (8). This modification results in the recruitment of DNA damage repair proteins. On the other hand, multiple monoubiquitinated proteins have been observed, such is the case of Receptor Tyrosine Kinase, where multi-mono ubiquitination results in its localization from the cellular membrane into the cytosol which leads to degradation by lysosomes (9).

On the other hand, polyubiquitination is vastly more complex. There are seven different chain conformations that can be formed, all with different cellular fate (10). Although not all seven ubiquitin chains have been studied equally, there is enough data to determine function (5). Lysine 6 ubiquitin chains still remain unclear, but they are implicated in DNA damage, and it is known that at least BRCA1 forms these chains (11). Lysine 11 ubiquitin chains shows similar function to Lysine 48 chains, but seem to be more specific to cell cycle (3). Lys 11 chains, like Lys 48 chains, are recognized by the proteasome and rapidly degraded (5). Lysines 27, 29, and 33 have proven to be more difficult to characterize due to their proximity, resulting in lack of data. However, Lys 29 and 33 ubiquitin chains have been implicated in blocking phosphorylation sites, although the exact mechanism is still unclear. Lysine 48 polyubiquitin chains are the most studied and abundant of the ubiquitin chains. The most known of the ubiquitin chains, a protein tagged with this modification will be degraded by the proteasome. However, an E3 ubiquitin ligase/deubiquitinase complex that regulates each other has not been identified in humans, yet there have been reports in other organisms such as yeast (12). Lastly, Lysine 63 ubiquitin chains are the second most studied types of ubiquitin chains. They are involved in several cellular responses, with different functions in depending on the situation (5). Some of the known functions of Lys 63 chains include when certain receptors have to be internalized, as a recruitment signal for DNA damage response promoted by the E3 ligases RNF8

(monoubiquitination) and RNF 168 (extending the monoubiquitination to a polyubiquitin chain) or activation and regulation of the NF- $\kappa$ B pathway (13).

The Ubiquitin Proteasome System (UPS) is central to regulation of protein stability and plays a regulatory role in many cellular pathways. Ubiquitination is used as an important post-translational modification to regulate cellular processes such as cell cycle, apoptosis, transcription and DNA damage, among others (14). Ubiquitin, a 9 kDa globular protein, is covalently attached to many proteins resulting in either in monoubiquitination or polyubiquitination in form of ubiquitin chains (15). Because of the formation of these polymers, the complexity of ubiquitination is greater than other post-translational modification, such as phosphorylation or methylation. While ubiquitination is widely studied, many aspects related to ubiquitin ligases and deubiquitinases remain unclear (16).

Finally, the proteasome is a protein complex composed of three main subunits (one 20S subunit and 2 19S subunits) the 19S proteasome recognizes Lys 11 and 48 ubiquitin chains proteins marked for degradation and which then proceed to interact with the 20S subunit that contains the sites for proteolysis (17). The proteins must therefore be denatured and deubiquitinated in order to be degraded. Unfortunately, not much is known about the mechanism and the order of reactions within the proteasome (18).

### **E3 ubiquitin ligases and UBR5**

E3 ligases recruit E2 ubiquitin-conjugating enzymes in order to finalize the ubiquitination process and modify the final substrate. This process is illustrated in Figure 1. Amongst E3 ubiquitin ligases there exist three different families: HECT (homologous to E6AP C terminus) E3 ligases, RING (really interesting new gene) E3 ligases, and RBR (RING-between-RING) E3 ligases (19). Amongst E3 ligases, UBR5 (Ubiquitin Protein Ligase E3 Component N-Recognin

5, also known as EDD) is a HECT E3 ligase of 2799 amino acids (20). UBR5 has been implicated in several different mechanisms: in cancer, it has been found that the catalytic site of UBR5 is often mutated, however, UBR5 null mice are embryonic lethal resulting in difficulties in studies (21). Other UBR5 studies have found interaction with several proteins, such as ATM, APC, CHK2, CDK9, RNF168, TFIIS, and TOPBP1, amongst other proteins (22). These interactions link UBR5 to DNA damage response and repair, transcriptional regulation, cell cycle regulation, and WNT signaling pathways (23). In a 2016 study, *Sanchez et al* found UBR5 foci to be dependent on the RING E3 ubiquitin ligases BMI1, and that transcriptional repression at damage sites was impaired in the absence of UBR5 (24).

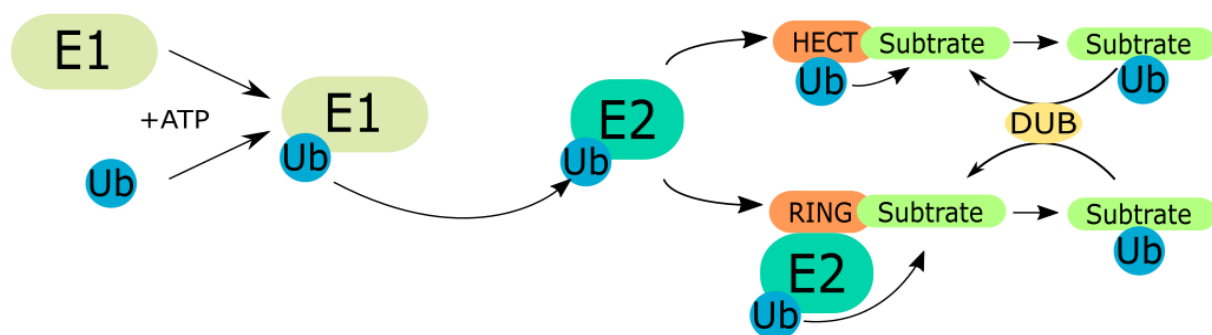


**Figure 1 – Review of Ubiquitination.** Enzymatic cascade of ubiquitination transfer. E1 enzymes, along with ATP first bind with ubiquitin (Ub) to then transfer the conjugated ubiquitin to an E2 conjugating enzyme to finally interact with an E3 ubiquitin ligase. RING E3 transfer the ubiquitin from the E2 to the substrate directly while HECT E3 transfer the ubiquitin to their HECT domain first. Deubiquitinating enzymes (DUB) reverse this process by cleaving ubiquitin chains.

## Deubiquitinating enzymes

Deubiquitinating enzymes (DUBs) have recently emerged as important regulator in the form of ubiquitin chain proteases. As such, they are a central part of the UPS, balancing protein degradation within the cell (1). Not many DUBs have been characterized, however, we do know of their importance. For example, USP22, a DUB within the Ubiquitin Specific Protease family of DUBs, has been found to be an important regulator of ubiquitination status of histone H2A and

H2B (25). Additionally, USP22 has been implicated to function with Myc, regulating expression of proteins such as p53 and p21, inhibiting cell proliferation and even arresting cell cycle. For this reason, USP22 is often overexpressed in cancer and is often used as a marker when screening patients (26). Many other DUBs have been implicated in cellular pathways such as gene silencing, cell cycle control, and DNA damage response (3). Because of the limited knowledge we possess, investigating DUBs is an important undertaking in order to further our knowledge on cellular regulation.

Among domains commonly found within DUBs, the Ubiquitin binding motif (UIM) has been found to be important for the ability to bind ubiquitin chains, giving specificity to the DUB (4). This motif is composed of a short sequence of amino acids that is mostly conserved (27). In a study performed by Kommander, he found that by removing the Ubiquitin Binding Domain of OTUD1 and testing the ability to cleave different ubiquitin chains. When the wild type and the mutant OTUD1 were mixed with different chains, it was observed that OTUD1 loses specificity of ubiquitin chains (4). Thus we can conclude that the UIM is crucial for properly identifying and targeting of the substrate.

### **OTU Deubiquitinases and OTUD5**

Within the classifications of DUBs is the OTU (Ovarian Tumor) domain containing family of DUBs. OTUs are characterized for using a cysteine residue as their catalytic residue and thus, are considered cysteine proteases (they fall within the same family of the previously described USP22). Currently, only 16 DUBs have been classified as OTU members (28). Among the OTU members, OTU Domain containing protein 5 (OTUD5) is a 573 amino acid long protein. OTUD5 (also referred to as deubiquitinating enzyme A, or DUBA) has been implicated in regulation of ubiquitination status of p53 and its interacting protein PDCD5 (29). OTUD5 has



also been implicated in regulation of transcription of type 1 interferon (IFN-1) through TRAF3, by cleaving the K63 ubiquitin chains found on TRAF3 (30). The study found that the ubiquitin interacting motif of OTUD5 was critical in this interaction, highlighting the importance of UIM when interacting with other proteins. Another link to transcription is through ROR $\gamma$ t, a transcriptional factor involved in differentiation of T Helper type 17 cells. Here, OTUD5 stabilizes the E3 ubiquitin ligase UBR5 which is responsible for the ubiquitination of ROR $\gamma$ t, leading to suppression of transcription (31). However, its role beyond these proteins has not been studied.

Related to OTUD5 and DUBs, E3 ubiquitin ligases play an important role as they catalyze ubiquitin chain formation. HECT domain containing E3 ligases must be tightly regulated, and while they have been studied, not every E3 ubiquitin ligase has been fully characterized. In yeast, it is known for E3 ubiquitin ligases to form regulatory complexes with DUBs. However, this type of interaction has not been observed in humans, yet many of the E3 ligases have homologs in humans, which lead us to hypothesize that OTUD5 forms a mutually regulatory complex with an E3 ubiquitin ligase.

## **DNA Damage Response**

Responding to DNA damage in a precise and timely manner is of utmost importance for cell viability. For this reason, many different pathways have evolved such as Non-Homologous End Joining or Homologous Recombination; each one of these pathways is specific to certain types of damage and tightly regulated (32).

When a double strand break is detected, activation of the ATM/ATR signaling cascade is crucial for repair. ATM/ATR identify double strand break lesions and will phosphorylate histone H2AX, leading to recruitment of 53BP1 or BRCA1 to start either Nonhomologous Recombination (NHEJ) or Homologous Recombination Repair (HRR) respectively (33).

Homologous Recombination (HR) is a DNA damage response involved in repairing double strand breaks (DSB) by using a homologous DNA sequence. The HR pathway is also involved in maintenance of telomeres, segregation of chromosomes during meiosis and reinitiation of stalled replication forks (34).

The protein involved in initiating homologous recombination is BRCA1, an E3 ubiquitin ligase often mutated in breast and ovarian cancers (35). Since we know that ubiquitin ligases are involved in homologous recombination, we can also predict that deubiquitinases are also involved. P53 is required for BRCA1 activity (36, 37), linking OTUD5 to homologous recombination as a possible regulator of homologous recombination repair.

### **Transcriptional regulation at DNA breaks**

While it is known that transcription is stalled during DNA damage for repair to take place, the downstream mechanism of transcriptional stalling remains unclear (38). However, it is known that there are multiple mechanisms related to transcriptional repression at DNA lesion sites. For instance, Polycomb Repressive Complex 1 (PRC1) has been linked to transcriptional repression at DSBs (39, 40) and a study from our lab suggested a collaboration with UBR5 in such process (24, 41). Although this study involved a regulation of FACT histone chaperone, how the regulation is achieved by Polycomb or UBR5 remains unknown.

Other regulatory factors have also been found to repress transcription at DNA damage. Most notably, ATM is a key upstream regulator for repression of transcription (42). Other factors such as DYRK1B, a factor required for double strand break repair on actively transcribed chromatin. DYRK1B is a kinase that silences transcription by phosphorylating EHMT2, a methyltransferase responsible for regulating H3K9 methylation which is crucial for transcriptional repression (43). Another factor that was recently discovered to repress

transcription at double strand breaks is cohesin. Cohesin is most known for sister chromatid cohesion during cell division, but in a study by Meisendberg a new function independent of chromatin cohesion was found (44). The cohesin complex, particularly SA2 and PBAF were found to be essential for transcriptional repression at double strand breaks and failure to repress transcription leads to genome wide rearrangement.

While OTUD5 has been linked to transcription regulation and DNA damage response, however its role in both DNA damage response and transcription has been poorly characterized. Additionally, the binding partners of OTUD5 remain mostly elusive. By determining binding partners, the cellular role of OTUD5 will become clearer. Here we investigate the role of OTUD5 in transcriptional regulation as a transcriptional repressor and the downstream effects of DNA damage in an OTUD5 depleted cell line (45).

### **Transcription-Replication Conflict and the formation of R-loops**

Whenever the cell begins the process of replication, transcription of genes must be regulated for DNA to be replicated and prepared for cell division. Conflict between transcription and replication has been shown to be a source of intrinsic genome instability (46). These conflicts arise when a replication fork encounters an elongating RNA polymerase as the replication fork cannot progress past it. These conflicts can arise in two different forms: head on collisions and co-directional collisions (47). In head on collisions, a major impediment for both machineries is the formation of positive supercoiling in DNA that would eventually cause both replication and transcription to stall (48). However, this does not occur in co-directional collisions as the negative and positive supercoiling formed would lead to no change in supercoiling.

Because Transcription-Replication Conflict (TRC) can have profound effect on the genome, mammalian cells have developed various mechanisms to avoid such encounters (49).

For example, rDNA replication and transcription are spatially separated to avoid collisions between the two machineries (50). Other regions of the genome are separated temporally. While the transcription machinery may indeed be a physical obstacle to the replication fork, other transcriptional byproducts could cause conflict to arise. Indirect effects such as DNA supercoiling, formation of DNA:RNA hybrids (commonly referred to as R-loops), and formation of secondary DNA structures can all be a challenge for replication (51, 52).

R-loops are transient DNA:RNA hybrids that are formed as a result of transcription and negative supercoiling (53). R-loops have been linked to immunoglobulin class switch recombination in B-cells, gene expression (by silencing genes) and regulating chromatin structure. Degradation of R-loops is often done by two enzymes found in the human genome: RNaseH1 and RNaseH2 (51, 54) while the unwinding of these structures is carried out by RNA-DNA helicases such as DHX9 or SETX (55, 56). However, presence of R-loops can also lead to more negative effects such as replication fork collapse, DNA damage and chromosome rearrangement. In a study by Sollier, it was concluded that R-loops, in the absence of functional R-loops processing proteins such as Topoisomerase I, are processed into double strand breaks by the Transcription Coupled Nucleotide Excision Repair (TC-NER) proteins XPG and XPF, providing insight into how R-loops lead into genomic instability (57). Another study by Castellano-Pozo also found that in R-loop regions, histones accumulate markers that lead to chromatin compaction which would provide an additional barrier for the replication fork to overcome (54). Here, we investigate how the OTUD5-SPT16 interaction is crucial to regulate transcription at DNA lesion sites and how uncoupling OTUD5-SPT16 leads to formation of R-loops and genomic instability.

Another factor that could lead to TRC is trapped RNA Polymerase II molecules (stable but transcriptionally inactive RNA Polymerase II molecule formed due to backtracking). Backtracked RNA Polymerase II can also lead to stalling of other RNA polymerase on the same

DNA template, causing these complexes to accumulate (58). Clearing a large number of RNA polymerase is indeed a challenge, and there have been studies that suggest that the replication fork slows down when it approaches highly transcribed genes (59).

### **The Nucleosome and Histone Chaperones**

Nucleosome assembly is completed by first having the histone (H3-H4)<sub>2</sub> tetramer binds DNA followed by the two histone dimers (H2A-H2B) binding to the tetramer (60). Histone H1 then completes the densely packed chromatin structure by bringing together multiple nucleosomes (61). This process is aided by the histone chaperones. Histone chaperones are a group of protein that bind histone and regulate nucleosome assembly. They are essential genes due to their role in relaxing densely packed chromatin for DNA to be readily available for cellular processes such as replication or transcription. These proteins can be classified by which histones they bind either H3-H4 chaperones or as H2A-H2B chaperone (62). However, some histone chaperones fall into both classification, such as the histone chaperone complex FACT (facilitates chromatin transcription) (62, 63).

### **The FACT Complex**

The human FACT (facilitates chromatin transactions) complex was originally identified as a heterodimer and purified from HeLa cells extract by Reinberg's group in an effort to identify factors required for transcribing DNA bound to histones. In this publication, it was found that the complex co-eluted with two polypeptides, one of 140kDa and one of 80kDa and when added to chromatin in vitro, it facilitated transcription only after initiation (63). Further work by Reinberg identifies the factors that make up FACT by purifying the complex. They found that the 140kDa protein was a human homologue of the *Saccharomyces cerevisiae* Spt16/Cdc68, a protein

previously implicated in transcription and cell cycle progression (64). Thus, it was named SPT16 (Suppressor of Ty protein 16). The 80kDa protein was identified as the previously known protein SSRP1 (Structure Specific Recognition Protein 1) by peptide analysis and by western blotting (65).

Both subunits of FACT have homologues of yeast proteins that are also found as a heterodimer. Human SPT16 (from here on referred to as hSPT16) shares 36% similarity with yeast SPT16 (from here on referred to as ySpt16) (66), while the yeast homologue for SSRP1 is actually two proteins, one named Pob3, an essential yeast protein for transcription due to its role in elongation and the other protein being Nhp6 (non histone protein 6) . Therefore the yFACT is composed of three proteins as opposed to the two components of hFACT (67, 68). In the initial study where hFACT was discovered, a third protein was eluted with SPT16 and SSRP1 but it was determined to be non-essential for FACT activity.

### **Structure and domains of SPT16 and SSRP1**

SPT16 has several domains that have been identified. At its N terminus, SPT16 has a negatively charged, intrinsically disordered N-Terminal Domain (NTD) which spans amino acids 1-431 in hSPT16 and amino acids 1-447 in ySPT16. While the NTD has been initially shown to be non-essential in yeast, there is data that suggest that the residues Ser83 and Lys86 are required for SPT16 binding to Histone H3 and H4 (69). Additionally, introduction of mutations to the NTD disrupts interaction with the H2A C-terminal “docking” domain, resulting in lethality in yeast (70). From amino acid 431-606 in hSPT16 and 447-630 in ySPT16 the Dimerization Domain (DD) is found. SPT16 uses the DD in conjunction with the NTD/DD of SSRP1/Pob3 to become a heterodimer (71). The Middle Domain (MD) located from amino acids 644-933 in hSPT16 and 630-959 in ySPT16 has been suggested to help in stabilizing the DD and therefore

helps maintain the stability between SPT16 and SSRP1/Pob3. However, the general fold and structure of the MD remains unknown (72). Lastly, the C-Terminal Domain (933-1047 in hSPT16; 959-1035 in ySPT16) is a highly conserved region found amongst many other histone chaperones and believed to interact with the histone core complex (71). In fact, removal of the CTD in hSPT16 prevents interaction with the histone core and chaperone activity. The CTD of both humans and yeast is highly acidic, however only hSPT16 has a positively charged, mostly arginine and lysine, region that is hypothesized to grant greater regulation that ySPT16 does not have (63). However, its exact function remains unknown.

### SPT16:

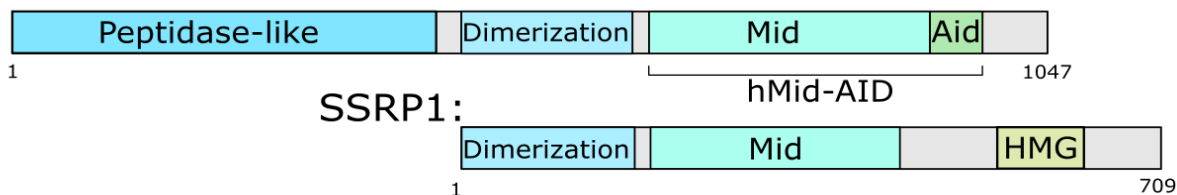


**Figure 2 - Schematic of the FACT Complex.** Domain organization of each component of the hFACT complex (SPT16 and SSRP1). These two proteins form a dimer using their dimerization domain. The mid domain (amino acids 644-930 in SPT16) has an important function in recognition of histones. The AID domain (amino acid 931-988 in SPT16) is key in proper FACT function due to its acidic composition.

SSRP1 contains three domains: the NTD/DD, the MD and the HMG-1 domain (73). The NTD/DD and the MD domain serve similar functions as their counterpart in SPT16: they allow heterodimerization to form the FACT complex. The NTD spans amino acid 1-177 while the MD spans amino acid 196-430. The HMG-1 domain (High Mobility Group) of SSRP1 spans amino acid 534-624 and is responsible for DNA binding for recognition and re-organization of chromatin (74). This HMG1 domain is similar to the protein Nhp6, the third member of yFACT and acts functionally the same as SSRP1 HMG1 (71).

## Mechanism and Regulation of FACT Activity

While the exact mechanism of FACT-induced chromatin remodeling remains undiscovered, two models have been proposed: the dimer eviction model and the non-eviction model. The dimer eviction model proposes that first FACT binds to nucleosomes through SPT16 acidic C terminal tail, displacing the histone H2A-H2B dimer, allowing other factors to interact with DNA. After such events have taken place, FACT reinserts the H2A-H2B dimer to once again have an intact nucleosome (75). This is evident by *in vitro* studies showing FACT binding not only to nucleosomes, but to the histone H2A-H2B dimer alone. Additional studies show a lack of H2A deposition at site of DNA damage when FACT is not functional.

The second model, the global accessibility model or non-eviction model, based on the yFACT data states that Nhp6 binds to nucleosome which recruits SPT16/Pob3 complex causing reorganization of the nucleosome complex in a non-cannonical conformation such that it allows factors access to DNA. Finally, yFACT restores the conformation of the nucleosome (76). While both models have been shown to occur *in vitro*, there is no data regarding if these models are exclusive or both act in a combinatory method. Additionally, the method of recruitment to chromatin remains unclear (77).

Regulation of FACT activity is less understood, however there is data that suggest how FACT activity is controlled within the cell. It has been shown that FACT is not required to initiation of transcription but it is essential for elongation (78). Studies have proposed models where FACT recognizes transcriptional block (RNA Polymerase II stalling) (79) and is then recruited to these sites, along with other factors that result in monoubiquitination of Histone H2B (K120) and this signals for histone H2A-H2B displacement by FACT; this process is repeated as needed (80). It has also been shown that FACT is required for deposition of the Histone variant MacroH2A1.2 in order to protect areas from replication stress, primarily in fragile sites within the genome, and is required in order to have proper BRCA1 mediated DNA repair (81). This



model implicates that FACT recruitment is dependent on phosphorylation of histone variant H2AX (S139), triggering a signal for MacroH2A2.1 deposition by FACT.

Additional data suggest that ySPT16 is ubiquitinated by the cullin Rtt101. Removal of Rtt101 results in reduced binding affinity between FACT and the helicase MCM, resulting in replication defects in yeast (82). Our studies suggest that the E3 ligase UBR5 interacts with and represses FACT enrichment at damaged chromatin. How this occurs is unclear, although UBR5 is able to ubiquitinate hSPT16 *in vitro* (24).

Little is known about hFACT post translational modifications, particularly which residues are modified. A series of analysis by mass spectrometry could be used to identify which residues are modified, followed by introduction of mutations into the using CRISPR could allow us to more fully understand how FACT is regulated. Additionally, many of the experiments done regarding structure of SPT16 and SSRP1 have been *in vitro* studies. It is speculated that *in vitro* data reflects *in vivo* studies, but this has not been done experimentally. For instance, the crystal structure of SSRP1 has been solved and from this data has been gathered to understand how domains interact with DNA and histones (73), but these experiments are isolated to test tube reactions without taking into consideration other factors that would be present *in vivo*. By finding specific residues within these domains and then introducing mutations we can corroborate the *in vitro* studies with *in vivo* data. Another aspect to consider is that while cellular models might provide a more realistic expectation, we still ignore the organism as a whole. Creating stable mice or zebrafish models, while they are different species and may have slight difference than humans, could result in a more accurate representation of how the changes introduce affect the organism as a whole and could give insights into disease progression or tumor formation. While the structure of FACT has been studied significantly, there is still little data on the localization requirements hFACT has. An experiment could be proposed to test each individual domain's localization ability. For instance, does the MD of SPT16 alone localize to sites of damage, or is

there a greater requirement we are not aware of? This could be studied by introducing each domain into cells with either a GFP tag to do live cell imaging, or any other tag to do indirect fluorescence to observe localization of each domain.

## **Acetylation and Histone Deacetylases 1 and 2**

Acetylation is a common post translational modification that plays a regulatory role in cellular processes (83). Acetylation is controlled by two types of enzymes, acetyltransferases of which there are 18 identified proteins, and deacetylases enzymes of which 18 have also been identified (84). Acetylation is most associated with active gene expression as acetylation of the N-terminal tail of histones H3 and H4 interferes with the electrostatic relation between the histone core complex and DNA resulting in chromatin relaxation (85). Inversely, removal of acetylation would result in chromatin condensation. For this role, acetyltransferases and deacetylases are commonly referred to as histone acetyltransferases (HATs) and histone deacetylases (HDACs).

In a recent publication, Beck shows that OTUD5 binds HDAC2 through its C terminus. HDAC2 shares 83% similarity with HDAC1 and they are often found together as part of a larger protein complex (86). The most studied and characterized protein complexes in which HDAC1 and HDAC2 are found are the Sin3, where they bind to Sin3A/B, the NuRD complex where they bind MTA1-3, and the CoREST complex where they bind CoREST1-3 (87, 88). While HDAC1/2 do not directly bind to DNA, members of the protein complexes have DNA binding domains that allow HDAC1/2 to interact with the chromatin (89). For instance, NuRD complex member MBD2 is a methyl-DNA binding protein and Mia $\alpha/\beta$  contain PhD finger and chromodomains. Due to the role HDAC1/2 play in chromatin regulation and the recently found interaction between OTUD5 and HDAC2, we investigated the possibility of a SPT16/OTUD5/HDAC2 complex. Indeed,

SPT16 does indirectly interact with HDAC1/2 through OTUD5. Whether this interaction is limited to HDAC1/2 or extends to other complexes of HDAC1/2 (such as the NuRD complex) remains to be further investigated. However, this interaction could be key in regulating transcriptional repression at sites of DNA damage.

## Chapter 2: Methods

### **Cell lines, plasmids and chemicals**

HeLa, 293T and U2OS cells were cultured in Dulbecco's Modified Eagle Medium (DMEM) supplemented with 10% Fetal Bovine Serum (FBS) and L-glutamine. HeLa S3 cells were cultured in Joklik media supplemented with 8% FBS and L-glutamine. HeLa CRISPR-Cas9 UBR5 KO and OTUD5 KO were generated using the CRISPR-Cas9 plasmid (purchased from SantaCruz) and the Double Nickase (Cas9 D10A) OTUD5 KO cell lines were generated cells were generated using the Double Nickase plasmid purchased from SantaCruz. The cells were transfected with plasmids and transiently selected with Puromycin (1ug/ml) for 48 hours and surviving cells were isolated into single cells and allowed to grow. Clones were checked for expression using western blot technique. Selected clones were then sequenced at the genomic region targeted by the CRISPR by Washington University to confirm knock-out. Knock in cell lines were generated by Washington University Core facility using CRISPR guided by gRNA. Knock in cell line were verified using genomic sequencing.

### **RNAi**

Cells were cultured in medium without antibiotics and transfected once with 20 nM siRNA (final concentrations) using the RNAiMAX (Invitrogen) reagent following the manufacturer's protocol. Table 1 shows the siRNA sequences used.

**Table 1 – List of siRNA used and companies who engineered the sequences. These siRNAs were the ones used throughout the experiments presented in the following two chapters.**

<b>Target</b>	<b>Sequence (5' - 3')</b>	<b>Company</b>
<b>UBR5 #1</b>	CAGGUAUGCUUGAGAAAUAU	Qiagen
<b>UBR5 #2</b>	GAAUGUAUUGGAACAGGCUACUAU	Qiagen
<b>SPT16</b>	ACCGGAGUAAUCCGAAACUGA	Qiagen
<b>OTUD5 #1</b>	GGCCGGCUUGGACAAUGAATT	Qiagen
<b>OTUD5 #2</b>	GGGUGCCGAAGAIAGACAATT	Qiagen
<b>OTUB1</b>	CTCCGACTACCTTGTGGTCTA	Bioneer
<b>OTUB2</b>	TTCCGTTTACCTGCTCTATAA	Bioneer
<b>OTUD1</b>	CTGGTGTACCTTCATCTATGA	Bioneer
<b>OTUD2</b>	GAGUACUGUGACUGGAUCA	Bioneer
<b>OTUD3</b>	CAGAAGCGAAGCAGAGGCGAA	Bioneer
<b>OTUD4</b>	CTGTATGAGAAGGTATTTAAA	Bioneer
<b>OTUD6A</b>	AAGAGTGAACAGCAGCGCATA	Bioneer
<b>OTUD6B</b>	GGUCAUUGAUAGCAAGUAATT	Bioneer
<b>OTUD7A</b>	CACAAGUCGCAGACCUACA	Bioneer
<b>OTUD7B</b>	GGUCAUUGAUAGCAAGUAATT	Bioneer
<b>TRABID</b>	CACCUUAAAAGAUCUCAUCU	Bioneer

**Table 1. (continued)**

<b>OTULIN</b>	<b>CGUAUGCCCUUGAUUGGUU</b>	<b>Bioneer</b>
<b>VCPIP1</b>	CUGGUAACCCACACCUUGA	Bioneer
<b>A20</b>	CUCAGUUUCGGGAGAUCAU	Bioneer
<b>BRCA1</b>	CUGAAACCAUACAGCUUCA	Bioneer

### **Western blots and antibodies**

Cell extracts were run on sodium dodecyl sulfate polyacrylamide gel electrophoresis (SDS-PAGE) gels and then transferred to a PVDF membrane (Bio-Rad). Membranes were probed with primary antibodies overnight at 4C, followed by incubation of HRP-conjugated secondary antibodies (Cell Signaling Technologies) for 1 hour. The bound antibodies were viewed via Pierce ECL Western Blotting Substrate (Thermo Scientific). The following primary antibodies were used: -SPT16, -SSRP1, -UBR5, -H2A, -Rpb1, -H2AX, -OTUD5, -53BP1, -SIRT3 rabbit polyclonal antibodies from Cell Signaling Technologies; -NELF-E, -RPB1 (CTD pSer2) rabbit polyclonal antibodies from Abcam; -53BP1 goat polyclonal and -FLAG mouse monoclonal antibodies from Sigma Aldrich; -H2AX and -Tubulin mouse monoclonal antibodies from Millipore; -SPT16 and -GST mouse monoclonal antibodies from Santa Cruz Biotechnologies.

### **Immunoprecipitation and mass spectrometry analysis**

293T or HeLa cells stably expressing the transgene (FLAG -OTUD5) or transiently transfected with plasmids grown to 70–80% confluency were harvested by scraping. The pellets were lysed with the Lysis buffer (25 mM Tris pH 7.4, 0.5% NP40, 100 mM NaCl, 0.1 mM ethylenediaminetetraacetic acid (EDTA) supplemented with protease inhibitor cocktail solution)

for 10–15 minutes on ice. The lysates were cleared by centrifuging for 30 minutes at 14 000 RPM, and 10% of the supernatant was collected for 'input' samples while the remaining volume was incubated overnight with the antiFLAG M2 agarose (Sigma Aldrich) at 4°C while rotating. The M2 beads were washed three times with the lysis buffer before elution by boiling at 95°C for 3 minutes in 1× Laemli buffer. For the mass spec sample, the bound proteins were eluted with the phosphate-buffered saline (PBS) containing 4% SDS. The eluate was processed using the FASP method, digested with trypsin-LysC and desalted using HYPERSEP C18 columns. Peptides were separated on an Acclaim PepMap C18 (75 m × 50 cm) UPLC column (Thermo) using an EASY-nLC 1000 with gradient times of 60–90 minutes (2–40% acetonitrile in 0.1% formic acid). Mass spectrometry analysis was performed by a hybrid quadrupoleOrbitrap (Q Exactive Plus, Thermo) or hybrid linear ion trap-Orbitrap (Orbitrap XL) using a top 10 data-dependent acquisition method. For LC-MS/MS analysis using the Q Exactive, full scan and MS/MS resolution was 70 000 and 17 500, respectively. For LC-MS/MS analysis using the Orbitrap XL, full scan mass resolution was 60 000 (Orbitrap detection) with parallel MS/MS acquisition performed in the linear ion trap. Protein identifications were assigned through MaxQuant (version 1.5.0.30) using the UniProt Homo sapiens database. Carbamidomethyl (C) was set as a fixed modification and acetyl (protein N-terminus) and oxidation (M) were set as variable modifications. Trypsin/P was designated as the digestion enzyme with the possibility of two missed cleavages. A mass tolerance of 20 ppm (first search)/4.5 ppm (recalibrated second search) was used for precursor ions while fragment ion mass tolerance was 20 ppm and 0.6 Da for Q Exactive and Orbitrap XL data, respectively. All proteins were identified at a false discovery rate of < 1% at the protein and peptide level.

## Immunofluorescence and image quantification

Cells were seeded in 12-well plates onto coverslips and treated with indicated siRNA and damage treatments. For UV irradiation, cells were irradiated with 15–100 J/m<sup>2</sup> UVC (UV stratalinker 2400), depending on the type of experiments. For inhibitor treatments, ATM inhibitor (KU60019, 1 M), ATR inhibitor (AZ20, 100 nM), PARP inhibitor (ABT888, 5 M), DNA-PK inhibitor (NU7441, 1 M) were treated for 12 hours prior to fixing. The PTuner 263 cells (provided by Dr Roger Greenberg) were seeded on coverslips in 12-well plates at ~30% confluence; indicated siRNAs were treated at 20 nM for 48 hours. Stabilization of the Fok1-mCherry fusion protein was induced with the addition of 4-hydroxytamoxifen (1 M) and Shield-1 (1 M) to the cell growth medium 3 hours prior to fixing. Transcription of YFP-MS2 was induced with the addition of tetracycline (1 g/ml) to the growth medium 3 hours prior to fixing. Cells were fixed and stained for indicated antibodies following standard procedures. For rescue experiments, siRNA was treated 72 hours prior to fixation, and plasmids were transfected 24 hours prior to fixation. For fixation, coverslips were washed twice with ice-cold PBS and fixed for 10 minutes in the dark with cold 4% paraformaldehyde. Fixed cells were permeabilized for 5 minutes with 0.25% Triton, and incubated with primary antibodies (diluted in PBS for 1:300–1:500) for 1–2 hours in the dark, then with secondary antibodies (diluted in PBS for 1:1000) for 1 hour in the dark, followed by incubating with Vectashield mounting medium containing DAPI (Vector Laboratories Inc). Images were collected by a Zeiss Axiovert 200 microscope equipped with a Perkin Elmer ERS spinning disk confocal imager and a 63x/1.45NA oil objective using Volocity software (Perkin Elmer). All fluorescence quantification was performed using Image J. To measure relative fluorescence intensity (RFI), the fluorescence channel of interest was imported into Image J. The raw integrated density of the nucleus was measured and normalized to background in the image. The raw density measurements were normalized to a value of 10 (arbitrary) to the highest reading. Pearson's overlap correlations were obtained with the use of



the 'Colocalization finder' plugin for Image J. Full color images were imported into Image J and the channels were split into blue, red and green; the red and green channels were analyzed and the degree of colocalization was determined. All Pearson's correlation graphs are representative of at least three independent experiments, error bars represent standard error. For measuring the SPT16/H2AX foci area the pixel areas were automatically selected using the 'wand tracing tool' in the Image J. For vector quantification, single color images are opened in Image J, the straight line section tool is used to draw a transect of 250 pixels across the area of interest. The 'plot profile' function in the 'analyze' menu is used to measure the raw gray value across the transect. The raw gray values for each pixel is exported into Microsoft excel, the values are normalized to the highest raw value in the sample set using a 1–10 scale (RFI). These values are plotted for each pixel to obtain a fluorescence profile for the area of the selection.

### **Proximity ligation assay**

Proximity ligation assays were performed using the Duolink kit from Sigma Aldrich; cells were grown in a 12-well format on coverslips. Cells were fixed and permeabilized according to the standard immunofluorescence protocol (previously described), primary antibodies were added at a 1:500 dilution in PBS and incubated for 1 hour at room temperature. Proximity ligation assay (PLA) minus and plus probes were diluted 1:5 in the provided dilution buffer, 30  $\mu$ l of the probe reaction was added to each coverslip and incubated for 1 hour at 37°C; the coverslips were washed twice with buffer A. The provided ligation buffer was diluted 1:5 in water, the ligase was added at a 1:30 dilution; the ligation reaction was left at 37°C for 30 minutes before washing twice with wash buffer A. The provided amplification buffer was diluted 1:5 in water before adding the provided polymerase at a 1:80 ratio, the amplification reaction was left at 37°C for 100 minutes, the reaction was quenched by washing twice with buffer B. The coverslips were mounted on slides with DAPI containing mounting medium.

## **EDU Labeling**

Cells were seeded on a coverslip and treated as indicated. Edu was added at 10uM final concentration for 15 minutes prior to fixing for 10 minutes with 4% paraformaldehyde. Cells were washed twice with cold PBS and then permeabilized with 0.25% Triton X-100 in PBS. Cells were washed twice with cold PBS and Edu was labeled using Clik chemistry reaction by incubating with  $\text{CuSO}_4$  (2 mM), Azide-Biotin (10uM), and ascorbic acid (10mM) for 1 hour at room temperature. Cells were washed 3 times with PBS and PLA was performed as described above.

## **Cell fractionation assay**

Cells with or without Bleomycin (10 M) treatment for ~16 hours were harvested from 6 cm plates. Cells were lysed by 10 minutes incubation on ice with buffer containing 20 mM Tris (pH 7.4), 0.5% NP40 and 100 mM NaCl, then the lysate was subject to gentle centrifugation (5 minutes at 3000 RPM). The supernatant was collected and cleared by high-speed centrifugation (10 minutes at 14 000 RPM) and the cleared supernatant was preserved as 'S100' fraction. The remaining pellet was gently washed twice with the same buffer, then resuspended with Laemmli buffer (P fraction). P fraction protein loading amount was normalized proportional to the amount measured in S100 fractions.

## **Clonogenic survival assay**

HeLa and U2OS cells were seeded into 24-well plates (100 cells per well) and treated with indicated siRNAs for 48 hours, then treated with indicated drugs with indicated concentrations, then allowed to grow for ~10 days. The plating efficiencies (the number of cells

that survive in the absence of drug treatment) were roughly equal between the groups. The cells were fixed with 10% methanol, 10% Acetic acid solution for 15 minutes at room temperature, followed by staining with crystal violet. Crystal violet was then dissolved with Sorensen buffer (0.1M sodium citrate, 50% ethanol), then the colorimetric intensity of each solution was quantified using Gen5 software on a Synergy 2 (BioTek, Winooksi, VT, USA) plate reader (OD at 595 nm). Error bars are representative of three independent experiments.

### **Protein purification and in vitro binding assay**

OTUD5 cDNA was cloned into pGEX-6p vector and transformed into BL21 Escherichia coli. strain. Protein expression was induced by addition of IPTG at a final concentration of 300 M for 4 hours. Cells were harvested and lysed using the ice-cold Lysis buffer (150 mM NaCl, 1% Triton, 20 mM Tris pH 7.4, 0.1% EDTA, supplemented with PMSF and protease inhibitor cocktail) while rotating in 4°C. Resuspended pellets were sonicated three rounds (40 seconds pulse), and the lysate was cleared by centrifugation (20 000 RPM for 40 minutes). Glutathione beads (GE Healthcare) was added to the supernatant and incubated by rotating for 2 hours at 4°C. Beads were then washed three times with lysis buffer. Bound proteins were eluted with the Elution buffer (50 mM glutathione, 200 mM NaCl, 50 mM Tris) or treated overnight rotating at 4°C with Precision Protease to remove protein of interest from the beads. For UBR5 purification, pDEST10-6xHis-UBR5 plasmid was transformed into DH10bac for bacmid creation. Protein purification was performed as according to the Bac-to-Bac Baculovirus Expression System (Invitrogen). In brief, bacmid was transfected into SF9 cells and the virus in supernatant was harvested 72 hours later. Virus was amplified by infecting SF9 cells two more rounds. Infected (P3) cells were harvested and lysed using lysis buffer (25 mM Tris pH 7.4, 0.5% NP40, 100 mM NaCl plus protease inhibitor cocktail), and cleared by high speed centrifugation (20,000 RPM for 40 minutes). The supernatant was incubated with Ni<sup>2+</sup> Sepharose (Qiagen) for 2 hours, washed

three times, and eluted with the Elution buffer (20 mM Tris pH 7.4, 250 mM Imidazole). For the binding assays, purified proteins were mixed in 50 mM Tris buffer on a 1:1 stoichiometric ratio and allowed to incubate by rotation overnight at 4°C. The Ni<sup>2+</sup> beads were added and allowed to incubate for additional 2 hours by rotating at 4°C. Beads were washed three times before eluting with 2× Laemli buffer and analyzed via gel electrophoresis and Coomassie stain.

### **Limited proteolysis**

Purified OTUD5 (5 g) was mixed with Trypsin (Sigma Aldrich) at a 1:100 ratio of protease:protein and incubated in 100 mM Tris pH 8.5 for indicated times. The same amount of bovine serum albumin was used for control. Reaction was quenched by addition of 4× Laemli buffer and boiling for 5 minutes. Samples were run on SDS-PAGE and the gel was stained with Imperial Protein Stain (Thermo Fisher).

### **Cell cycle analysis**

U2OS cells were treated with siRNAs for 72 hours. Sixteen hours prior to harvesting, indicated cells were irradiated with Bleomycin (5 M). Cells were harvested with trypsin and fixed with 70% Ethanol for 1 hour in darkness, washed with PBS and incubated with Propidium Iodide and RNase (25 g/ml) for 1 hour. Cell-cycle analysis was carried out in Accuri C6 Flow Cytometer and data was analyzed using BD Accuri C6 Software.

### **Chromatin Immunoprecipitation**

Cells were grown to confluency in 10cm dishes, treated with indicated conditions, and crosslinked with formaldehyde (1.42% final concentration) for 10 minutes. Reaction was

quenched using Glycine (125mM final concentration) for 5 minutes. Cells were washed twice using cold PBS with 0.5mM PMSF and then harvested by scrapping. Collected cells were washed twice by gently resuspending with FA lysis buffer (50mM HEPES-KOH pH 7.6, 140mM NaCl, 1% Triton X-100, 0.1 Sodium Deoxycholate) with Inhibitor proteases cocktail added and allowing 1 minute incubation on ice, followed by high speed centrifugation. Cells were lysed using FA lysis buffer with Inhibitor proteases cocktail added and incubating on ice for 10 minutes, followed by 8 rounds of sonication with 45% amplitude for 10 seconds allowing sample to rest on ice for 1 minute between rounds. Lysed sample was centrifuged at high speed and 4C. Supernatant was moved to new tube and each sample was normalized using Bradford assay. Each sample was then divided into input, no abs and IP samples. Input sample is frozen and kept at -20C. 400uL of FA buffer was added to no abs and IP sample and primary antibody was added to IP sample only and incubated overnight on a rotator at 4C. Protein A/G agarose beads was added and allowed to incubate in rotator at 4C for 2 hours. Samples were then washed using PCR FA buffer 3 times by gently resuspending and low speed centrifugation. FA buffer was removed without removing A/G beads and 400uL of ChIP Elution buffer (1% SDS, 100mM Sodium bicarbonate) was added to Input, No Abs, and IP samples and incubated for 1 hour on a rotator at room temperature. Samples were then centrifuged at high speed and supernatant moved to a new tube. RNaseA was added to each tube at a final concentration of 50ug/ml and allowed to incubate for 2 hours at 65C. Proteinase K was then added to each sample at a final concentration of 250ug/ml and allowed to incubate overnight at 65C. DNA was then purified by using PCR purification kit (Bioneer) on each sample.

### **End Point PCR analysis**

ChIP DNA was analyzed using End point PCR analysis. PCR reactions were set up for each sample using the following master mixture: 10uL HF buffer (Invitrogen), 0.5ul Phusion

polymerase (Invitrogen), 2ul of forward primer, 2ul of reverse primer, 2ul of dNTPs (10mM mixture, Invitrogen), 22.5 PCR grade water (GenDepot). 10uL of DNA (obtained from ChIP protocol) was used for each reaction. The following primers were used:

**Table 2 – List of primers used for end point analysis and qPCR analysis of ChIP samples.** Primers used in this study to investigate accumulation of proteins at chromatin fragile sites.

<b>Primer</b>	<b>Sequence (5' - 3')</b>
<b>Fra3B Central Fw</b>	5' tgttggaatgtaactctatcccat 3'
<b>Fra3B Central Rv</b>	5' atatctcatcaagaccgctgca 3'
<b>Fra3B Distal Fw</b>	5' caatggcttaagcagacatggt 3'
<b>Fra3B Distal Rv</b>	5' agtgaatggcatggctggaatg 3'
<b>Fra7H Fw</b>	5' taatgcgtccccttgtagct 3'
<b>Fra7H Rv</b>	5' ggcagatttagtccctcagc 3'
<b>Fra16D Fw</b>	5' gatctgccttcaaagactac 3'
<b>Fra16D Rv</b>	5' caaccaccatttctcactctc 3'
<b>GAPDH Fw</b>	5' ccctctggtggtggcccctt 3'
<b>GAPDH Rv</b>	5' ggcgcccagacacccaatcc 3'

### qPCR Analysis

PCR experiments were performed on appliedbiosystems Quantstudio3 thermocycler using amfiSure qGreen qPCR mastermix (GenDEPOT Q5603-001). QPCR reaction were set up to a final volume of 50ul using 15ng of template DNA. The PCR cycles used consisted of a 95C denaturalization step (15 seconds), followed by annealing and extention steps (1 minute) at 60C. 35 cycles were repeated. Measurements were acquired after every cycle. Quantification was performed using DELTACT of the untreated sample and the experimental sample for each primer set. Target specificity was confirmed by melt curve analysis as well as end point analysis. Cq confidence of samples quantified was greater than 0.98. Primers used are listed in Table 2.

Chapter 3: The OTUD5-UBR5 complex regulates FACT-mediated transcription at damaged  
chromatin

**Introduction**

Deubiquitinating enzymes (DUBs) are important regulators of many biological processes. DUBs process ubiquitin precursors to release free ubiquitins, cleave ubiquitin chains from substrates or edit chains to modify the functional outcome. DUBs are subject to various forms of regulations, such as phosphorylation and being bound to co-factors, which can regulate catalytic activity, stability or localization (28, 90). DUBs are also often physically coupled to E3 ubiquitin ligases, with different functional consequences; a DUB may counteract E3 activity on substrate ubiquitination or promote E3 activity by stabilizing the E3 itself (91, 92). Among the several types of DUBs is the subfamily of OTU (Ovarian Tumor) DUBs, which are cysteine proteases that regulate various biological processes including the immune signaling responses (4). Of note, some of the OTU family members such as OTUB1, OTUB2, OTUD4 participate in the regulation of DNA repair or DNA damage responses (11, 93–96). In response to genotoxic stresses, various mechanisms operate to maintain the genome and transcriptome integrity. One such response is the rapid arrest of transcription at or nearby the DNA lesions. The transcriptional arrest may facilitate the access of DNA repair machineries to the lesions enabling the repair processes, which is followed by resumption of transcription upon recovery. Transcription obstacles, including DNA damage, can also lead to ubiquitination and degradation of elongating RNA polymerases as a last resort (97). DNA lesions such as UV-induced CPDs induce direct stalling of RNA polymerases in cis, triggering transcription-coupled nucleotide excision repair, but transcription arrest can also occur distant from DNA breakage sites (98, 99), through kinases or protein-modifying activities. For example, Ataxia Telangiectasia Mutated (ATM), Poly ADP-Ribose Polymerase (PARP) and DNA-dependent Protein Kinase (DNA-PK)

repress transcription near or distant from double strand break (DSB) sites (100) Ataxia Telangiectasia and Rad3- related (ATR) induces transcription repression at stalled replication forks (101). A Polycomb gene repressor component BMI1 also regulates damage-associated transcriptional repression (both DSB and UV-induced lesions), and it may do so by inducing histone H2A ubiquitination, or at least in part in collaboration with UBR5 E3 ligase. For the latter, the proposed mechanism involves UBR5-induced repression of FACT histone chaperone complex and arrest of RNA Pol II elongation at UVC or nuclease-induced DSB lesions (24). Here we identify that the OTUD5 DUB is a new regulator of the DNA damage-induced transcriptional repression. Through a DUB siRNA screen, we found that OTUD5 is a specific DUB that stabilizes and promotes foci formation of UBR5. Both UBR5 and OTUD5 localizes to DSB lesions, where they interact. Similar to UBR5 depletion, OTUD5-depleted cells show misregulation of the FACT-dependent Pol II elongation and histone H2A deposition at damaged chromatin. Through mapping analysis, we found that OTUD5 associates with UBR5 and the FACT component SPT16 through the disordered N- and C-termini, respectively. When the either interaction-deficient OTUD5 mutant is expressed in OTUD5 KO cells, the cells are defective in arresting Pol II elongation and nascent RNA synthesis, underscoring the importance of the engagement of the UBR5–OTUD5 complex with SPT16 in transcription repression. We have further identified that a cancer-associated missense mutation in the UIM of OTUD5 abrogates the association of OTUD5 with the FACT components SPT16 and SSRP1, and that this leads to loss of the transcriptional repression at the damaged sites. Our work provides a new insight into the FACT-mediated transcription during the DNA damage response.



## Results

Using siRNA targeting OTUD5, we explored the phenotype of OTUD5 depleted cells.

### OTUD5 is a regulator of UBR5 stability and foci formation

In order to identify a deubiquitinating enzyme (DUB) that regulates UBR5 stability and damage-inducible foci formation of the E3 ligase, I screened different siRNAs that target human DUBs of the cysteine proteases family by measuring the amount of UBR5 protein by western blot as a readout, compared to scramble siRNA treated sample. Among the siRNAs used for targeting ~80 DUBs, siRNA targeting OTUD5 drastically reduced the level of UBR5 (Figure 3). Of all of the siRNA tested, only OTUD5 had a drastic effect on reducing UBR5 protein levels.

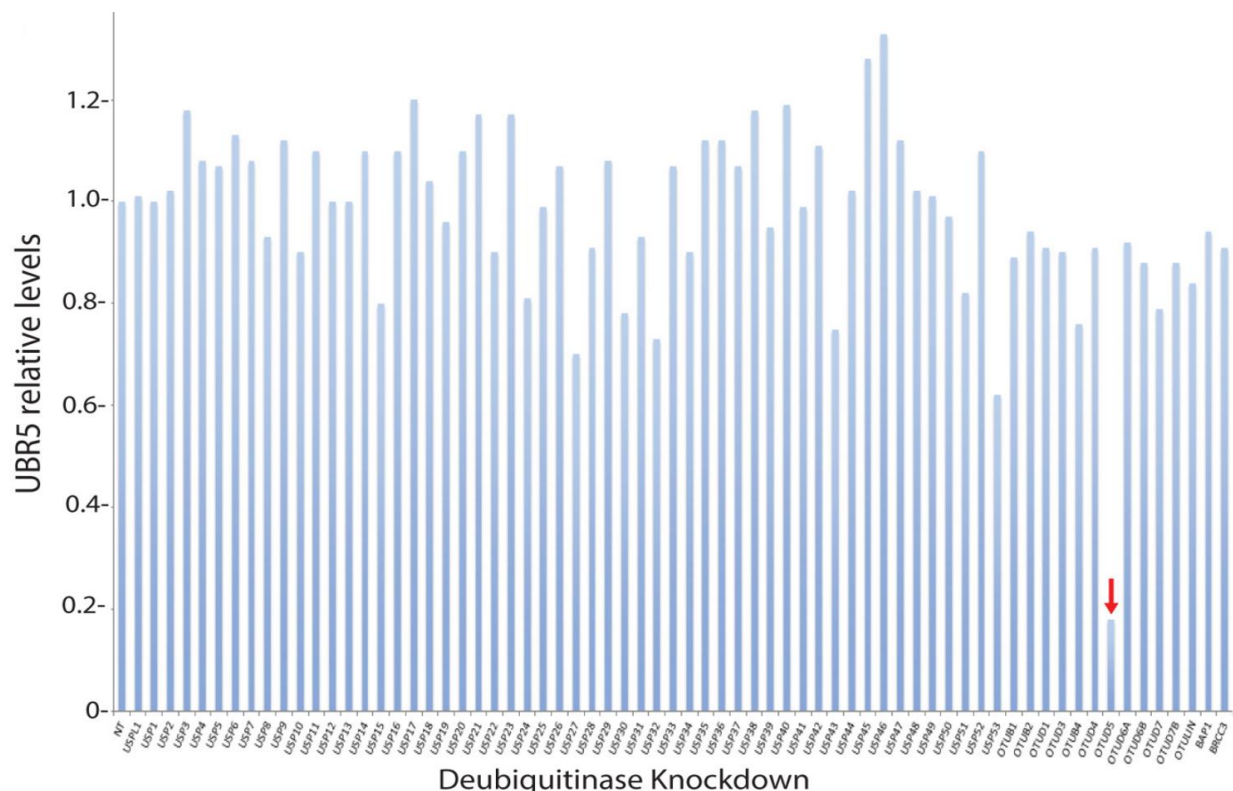


**Figure 3 – UBR5 protein levels are dependent on OTUD5 expression.** UBR5 protein levels were screened for in samples treated by different siRNA targeting human DUBs. Samples were collected and analysed using western blotting technique. UBR5 protein level was determined by measuring the intensity of each band using ImageJ and normalizing to control. Reprinted from “The OTUD5-UBR5 complex regulated FACT-mediated transcription at damaged chromatin” by de Vivo et al, 2018, Nucleic Acid Research.

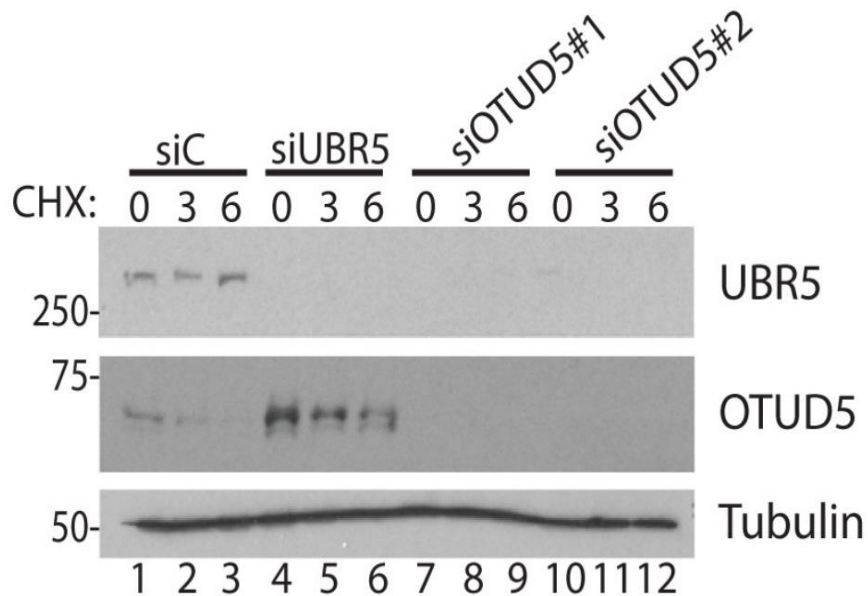


**Figure 4 – Western blot cycloheximide chase for UBR5 stability.** siRNA scramble (siC), siUBR5, siOTUD5 #1 and #2 followed cycloheximide treatment (10  $\mu$ M) for 0, 3, or 6 hours was done to determine UBR5 levels. Reprinted from “The OTUD5-UBR5 complex regulated FACT-mediated transcription at damaged chromatin” by de Vivo et al, 2018, Nucleic Acid Research.

The initial screen was further validated by treatment of two different siRNAs targeting OTUD5 (Figure 4). OTUD5 protein levels were increased in siUBR5 condition, indicating that UBR5 may also regulate OTUD5 protein levels. Previously, we showed in Sanchez *et al.* that UBR5 localizes to the UV-C induced  $\gamma$ -H2AX foci when cells were irradiated through micropore filters (17). UV-C induced foci of UBR5 was also abrogated by OTUD5 siRNA treatment (Figure 6 top).

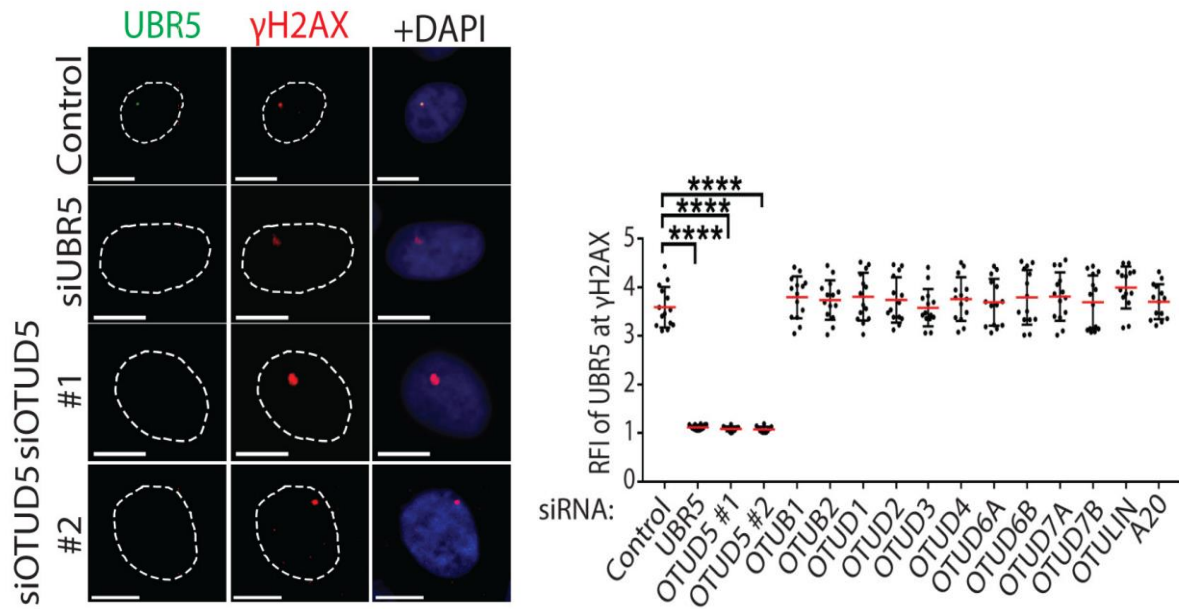


**Figure 5 – UBR5 foci is dependent on OTUD5.** Foci for UBR5 was observed using immunofluorescent microscopy. Cells were treated with indicated siRNA for 72 hours followed by UV-C (100J/m<sup>2</sup>) through a micropore filter (3μm) and allowed to recover. Cells were stained using antibodies targeting UBR5 and γ-H2AX (Right). Relative Fluorescent Intensity was measure using ImageJ. Quantification from three independent experiments (Left). Reprinted from “The OTUD5-UBR5 complex regulated FACT-mediated transcription at damaged chromatin” by de Vivo et al, 2018, Nucleic Acid Research.

The observed reduced foci is specific to OTUD5 depletion as depletion of other OTU DUB members had no effect (Figure 5). To further investigate the effect of OTUD5 depletion has on UBR5, I generated two independent HeLa OTUD5 knockout clones (one generated with conventional CRISPR-Cas9 method and the other with the Double Nickase (Cas9 D10A mutant); genomic sequencing analysis for both clones confirmed that both alleles had out-of-frame mutations (Figure 6).

OTUD5 KO, Cas9

	WT	.GGAGTGGACTAGCCGGTCCCCGCGGCA	GC GGAGTTCAGCCTCGTCACCTGA.	
OTUD5 KO	Allele 1	.GGAGTGGACTAGCCGGTCCCCGCGG	-A GC GGAGTTCAGCCTCGTCACCTGA.	1 nucleotide deletion
	Allele 2	.GGAGTGGACTAGCCGGTCCCCGCGGC	ACAGC GGAGTTCAGCCTCGTCACCTGA.	2 nucleotide insertion

OTUD5 KO, Double Nickase

	WT	CCAGGACA	TGCATGAGGTTGTGCGAAAGCATTGCAT	GGACTATCTGGTGA.		
OTUD5 KO	Allele 1	CCAGGACA	GACATGTCATGAGGT	-----GCAT	GGACTATCTGGTGA	10 nucleotide deletion
	Allele 2	CCAGGACA	TGCATGAGGTTGTGCGAAAGCATTGCAT	TGCAT	GGACTATCTGGTGA	5 nucleotide insertion

**Figure 6 – Genomic sequencing of OTUD5 Knock Out cell lines.** OTUD5 knockout cell lines were generated by transfecting HeLa cells with gRNA targeting OTUD5 gene and either CRISPR-Cas9 or CRISPR-Cas9 D10A. Cells were selected using puromycin and single clones were amplified. Cell lines were then sequenced to confirm knockout. Reprinted from “The OTUD5-UBR5 complex regulated FACT-mediated transcription at damaged chromatin” by de Vivo et al, 2018, Nucleic Acid Research.

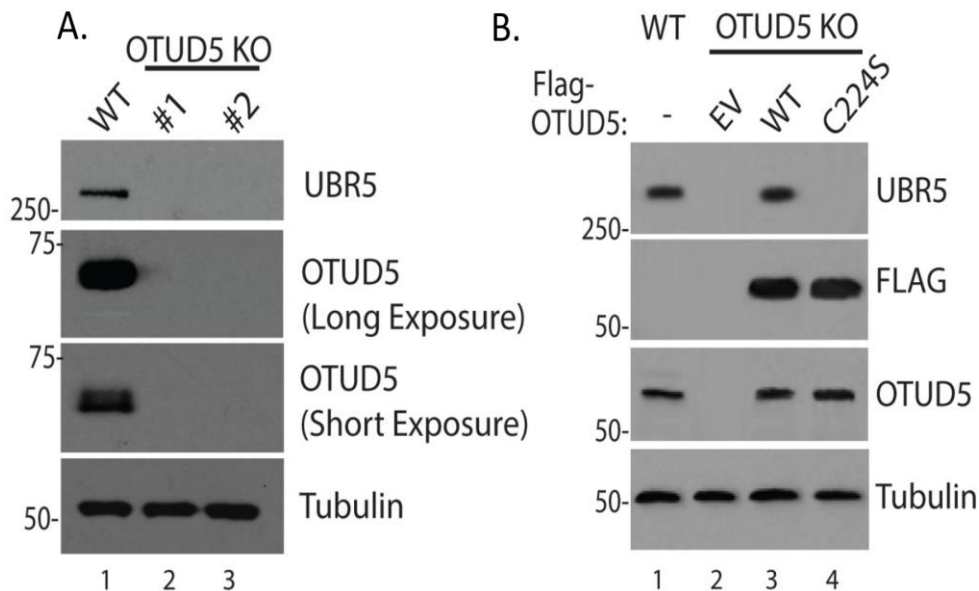


**Figure 7 – OTUD5 KO cell lines confirm UBR5 stability is dependent on OTUD5.** **A.** OTUD5 Knockout CRISPR/CAS9 generated cells also lack UBR5 protein levels, indicating that UBR5 protein stability is dependent on OTUD5 expression. **B.** UBR5 protein levels are recovered when Wild Type (WT) OTUD5 is reintroduced into the Knockout cell line but not when catalytic inactive 3xFlag OTUD5 (C224S) mutant is introduced. Reprinted from “The OTUD5-UBR5 complex regulated FACT-mediated transcription at damaged chromatin” by de Vivo et al, 2018, Nucleic Acid Research.

In both clones, OTUD5 protein levels were completely abolished. Similarly, UBR5 protein levels were depleted (Figure 7A).

The depleted UBR5 proteins were effectively rescued by reintroducing FLAG-OTUD5 wild-type (WT), but not when the catalytically inactive OTUD5 mutant (C224S) was introduced (Figure 7B), suggesting that the deubiquitinating activity of OTUD5 is necessary for preserving the UBR5 stability. Since ubiquitination of UBR5 has been reported in proteomic studies coupled with our OTUD5 knockdown results, we hypothesized that OTUD5 may be the deubiquitinase responsible for removing ubiquitin chain on UBR5 to promote UBR5 stability. In fact when UBR5 polyubiquitination was tested by knocking down OTUD5 and inhibiting the proteasome, we observed increased polyubiquitination in UBR5 (Figure 8A).

UBR5 polyubiquitination appears to be self-catalyzed, as FLAG-UBR5 WT was much less stable than the catalytically inactive C2768A mutant, in the absence of OTUD5 (Figure 8B).

In an immunoprecipitation experiment we found that UBR5 co-precipitates with OTUD5 (Figure 9A). By using BL21 cells and vectors containing a recombinant DNA sequence for GST-OTUD5 and another vector with recombinant 6xHis-UBR5, both proteins were purified and the binding was tested. Using Precision Protease, the GST tag of OTUD5 was cleaved off by targeting a linker site between GST and OTUD5. Then, the purified recombinant OTUD5 and UBR5 proteins were tested and found that they interact *in vitro* (Figure 9B), suggesting that this interaction is in fact direct. Altogether, these results suggest that OTUD5 is a specific stabilizer of UBR5.

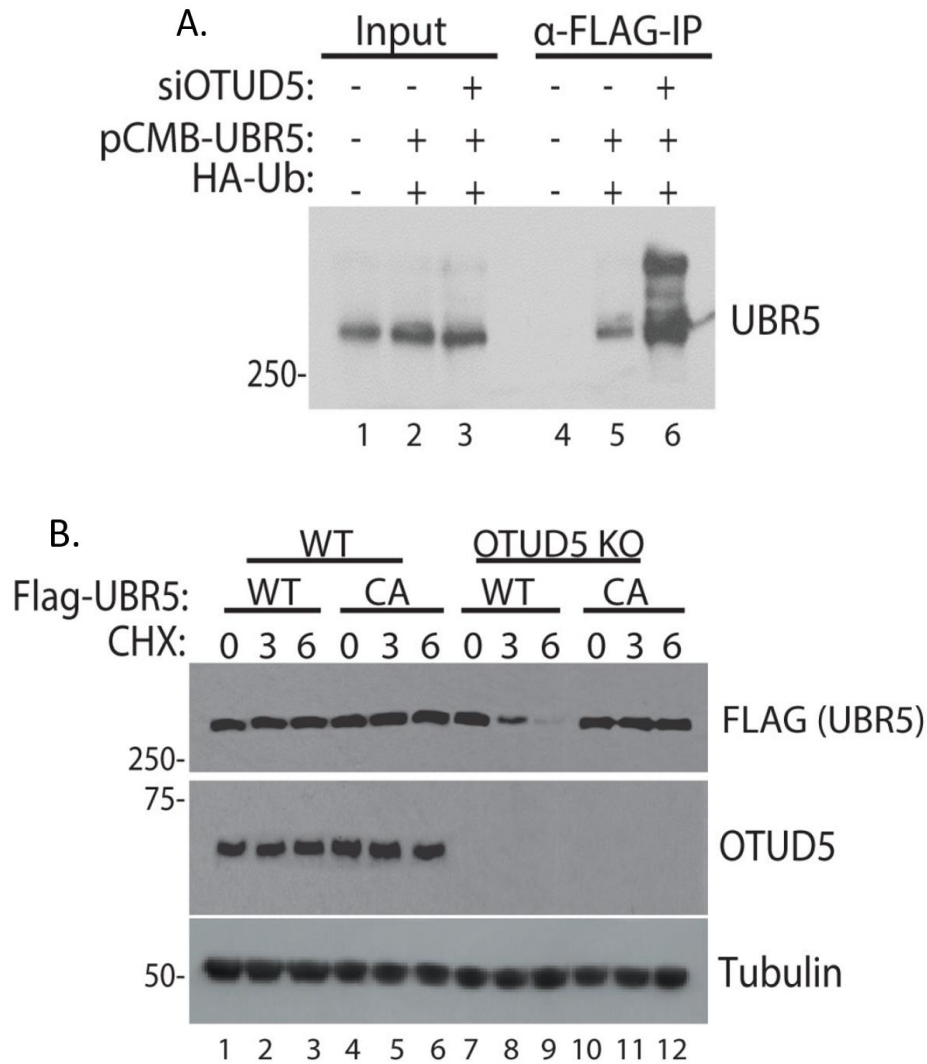


**Figure 8 – OTUD5 promotes UBR5 stability by preventing its proteasomal degradation. A.** Ubiquitination of UBR5 is increased when OTUD5 is depleted. UBR5 and ubiquitin was overexpressed by transfecting HeLa cells with pCMB-UBR5 and HA-ubiquitin and treating with MG132 for 8 hours. **B.** Wild type and OTUD5 KO cells were transfected with either WT or CA mutant (catalytically inactive) UBR5. Half life of UBR5 was observed by treatment of cycloheximide (CHX) for indicated time. Catalytic inactive UBR5 was not degraded, suggesting UBR5 self regulates its protein levels. Reprinted from “The OTUD5-UBR5 complex regulated FACT-mediated transcription at damaged chromatin” by de Vivo et al, 2018, Nucleic Acid Research.

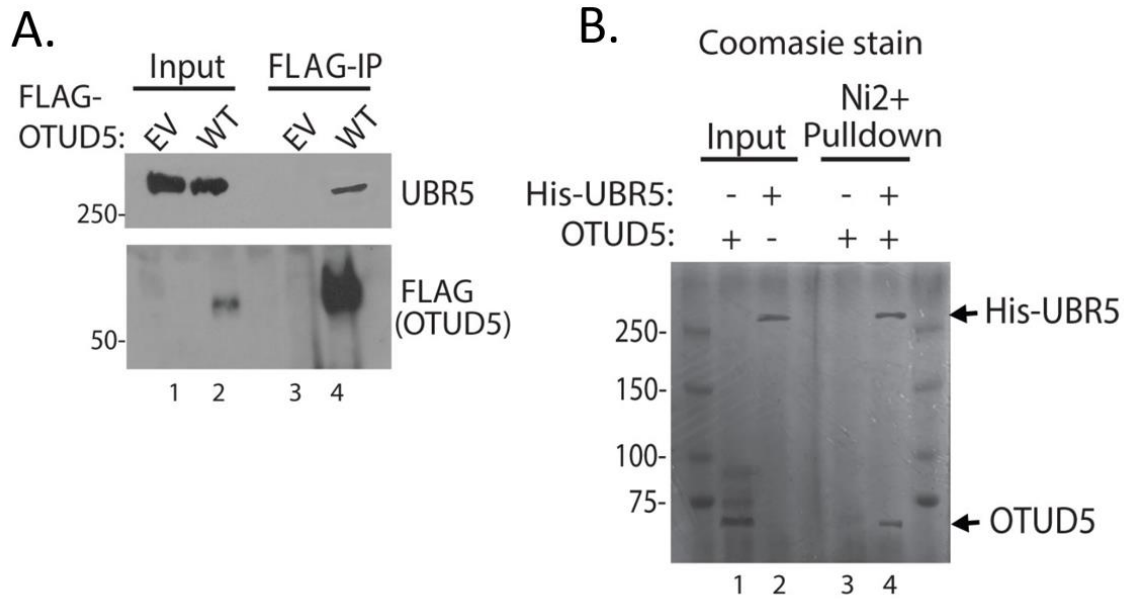


**Figure 9 – UBR5 and OTUD5 directly bind.** **A.** Immunoprecipitation of FLAG-OTUD5 reveals binding to UBR5. **B.** In vitro binding analysis of UBR5 and OTUD5. Purified recombinant OTUD5 and 6xHis UBR5 proteins were mixed and using Ni<sup>2+</sup> beads they were pull-down. Lane 1 – Purified OTUD5. Lane 2 – Purified 6xHis-UBR5. Lane 3 – Purified OTUD5 and Ni<sup>2+</sup> beads. Lane 4 – Purified OTUD5, 6xHis-UBR5 and Ni<sup>2+</sup> beads. Reprinted from “The OTUD5-UBR5 complex regulated FACT-mediated transcription at damaged chromatin” by de Vivo et al, 2018, Nucleic Acid Research.

### OTUD5 localizes to chromatin and double strand breaks

As UBR5 has been shown to localize to damaged chromatin sites and OTUD5 regulates the UBR5 foci, we reasoned that OTUD5 itself may localize to the damaged chromatin. Indeed, we have observed this in several ways; foci of endogenous OTUD5 and GFP-OTUD5 were detected at UVC-induced H2AX spots (Figure 10A and 10B, respectively). GFP-OTUD5 and endogenous OTUD5 were also observed at Fok1 nuclease-induced DSB sites (Figure 10C and 10D, respectively).

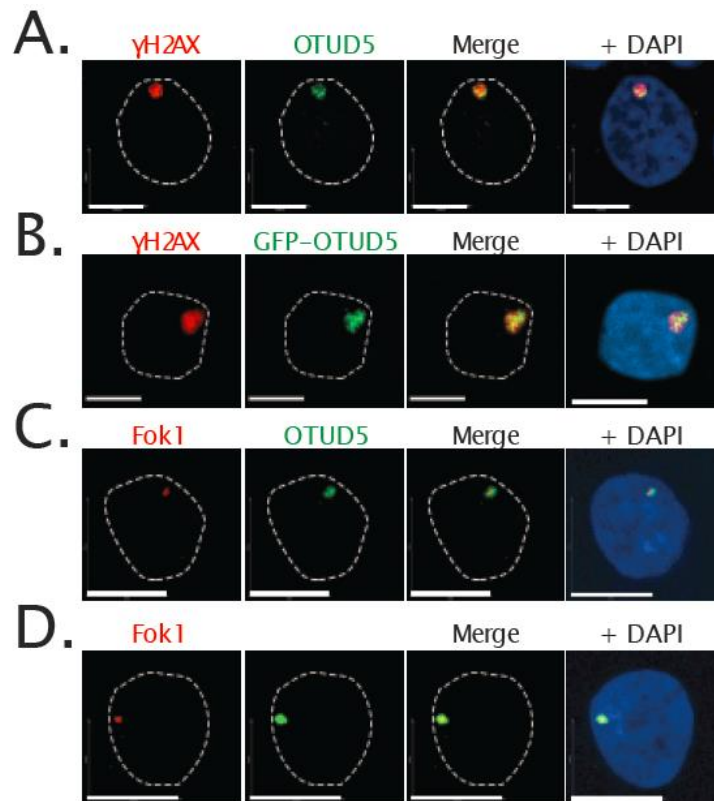


**Figure 10 – OTUD5 localizes to double strand break site.** **A.** Endogenous OTUD5 localizes to UV-C induced  $\gamma$ H2AX (3 $\mu$ m micropore filter) in HeLa cells. **B.** GFP-OTUD5 localizes to UV-C induced  $\gamma$ H2AX (3 $\mu$ m micropore filter) in HeLa cells. **C.** Endogenous OTUD5 localizes to mCherry-LacI-Fok1 fusion protein after pTuner 263 U2OS cells are induced with Shield-1 and 4-OHT. **D.** GFP-OTUD5 localizes to mCherry-LacI-Fok1 fusion protein after pTuner 263 U2OS cells are induced with Shield-1 and 4-OHT. Reprinted from “The OTUD5-UBR5 complex regulated FACT-mediated transcription at damaged chromatin” by de Vivo et al, 2018, Nucleic Acid Research.

To further verify OTUD5 being present in the nucleus, I used cell fractionation assay to determine the location of OTUD5 within the cell. Here, I found that both UBR5 and OTUD5 localize into the chromatin-enriched fraction when the cells were treated with Bleomycin, a double strand break inducing chemical agent (Figure 11A).



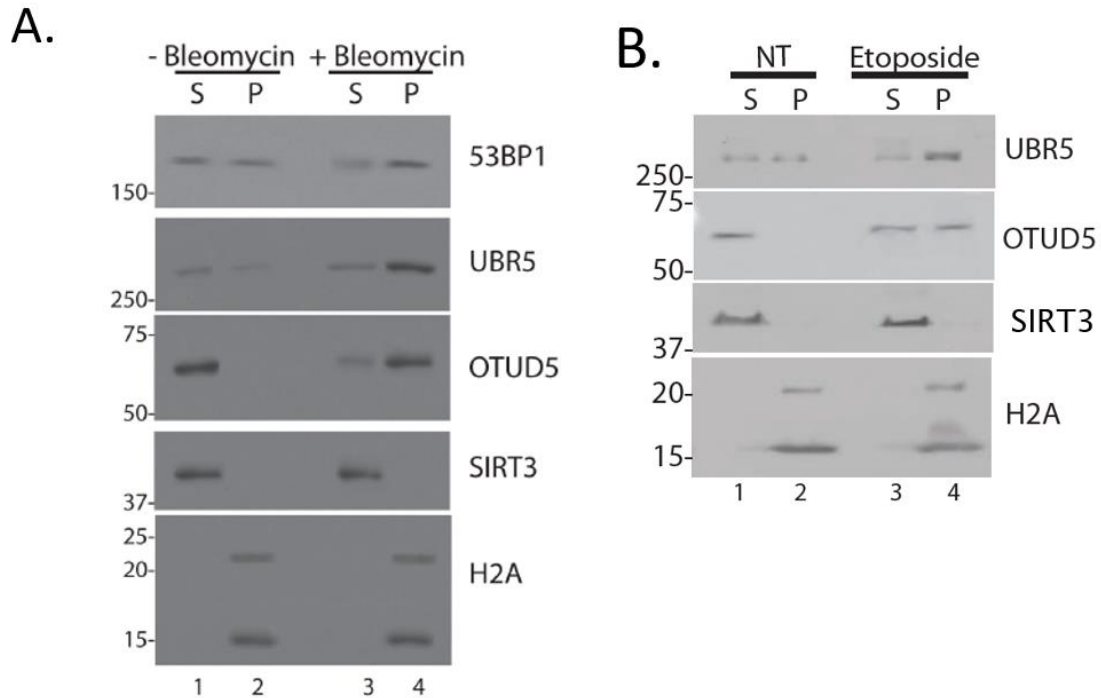


**Figure 11 – OTUD5 is enriched at the chromatin after DSB.** **A.** Cell fractionation assay shows OTUD5 and UBR5 localizing to the P fraction after Bleomycin treatment. **B.** Cell fractionation assay shows OTUD5 and UBR5 localizing to the P fraction after etoposide treatment.

Similar results were observed when testing Etoposide, a Topoisomerase II inhibitor (Figure 11B). Since both OTUD5 and UBR5 localize at DSB lesions, we wished to test whether the interaction occurs at the damaged chromatin spots. PLA detected the interaction between UBR5 and OTUD5 at damaged chromatin in situ, and that the interaction spots partially coincide with the DNA DSB marker 53BP1 (Figure 12), suggesting that at least a fraction of the interaction indeed occurs at damage (DSB) sites. Altogether, these results show that both UBR5 and OTUD5 localizes to damaged chromatin sites, particularly in DSB lesions, where they interact.

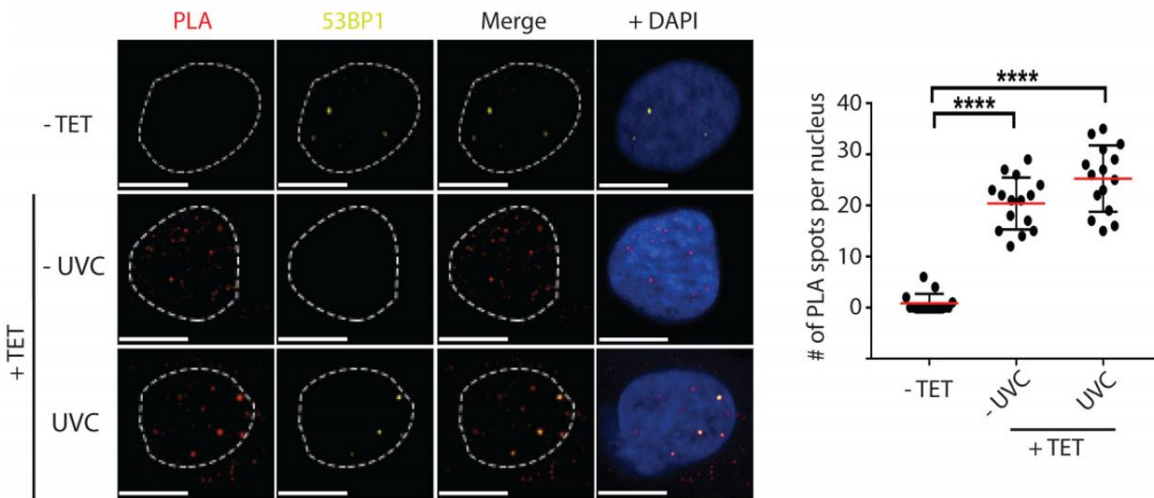


**Figure 12 – OTUD5 and UBR5 interact in the nucleus at DSB sites.** PLA between FLAG (OTUD5) and UBR5 shows interaction at sites of double strand break damage in DOX-inducible FLAG OTUD5 HeLa cells. C. Quantification of B. Reprinted from “The OTUD5-UBR5 complex regulated FACT-mediated transcription at damaged chromatin” by de Vivo et al, 2018, Nucleic Acid Research.

### Mapping the Interaction site between OTUD5 and UBR5

To further investigate the interaction between OTUD5 and UBR5, we began to wonder how they physically interact. To do this, we first looked at the structure of OTUD5 (PONDR Score) to determine possible sites that OTUD5 could use to bind UBR5 (Figure 13).

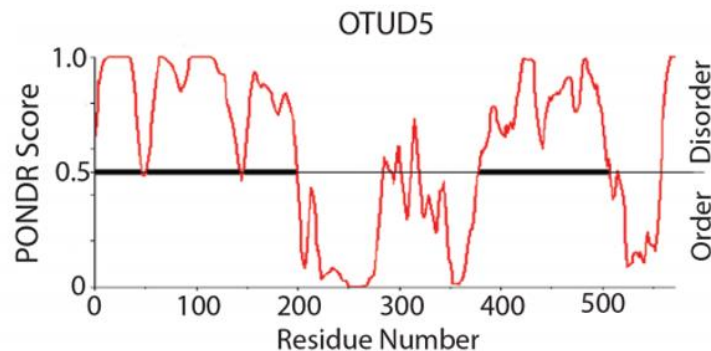


**Figure 13. Prediction of Natural Disordered Regions Score of OTUD5 protein.** Using the amino acid sequence of OTUD5, the PONDR score was determined using VL-XT predictor. This was used as rationale to map the interaction site between OTUD5 and UBR5.

Structurally, OTUD5 contains both an OTU domain in its central region that is responsible for the catalytic activity, and a UIM (Ubiquitin Interacting Motif) at the C-terminus (21). In addition to the above disorder prediction, limited proteolysis assay was performed using the recombinant OTUD5 to test the predicted disorder structure. This experiment showed that trypsin digest on OTUD5 led to rapid degradation and produced a fragment with the approximate size of the central structured domain of OTUD5, the catalytic domain OTU (Figure 14).

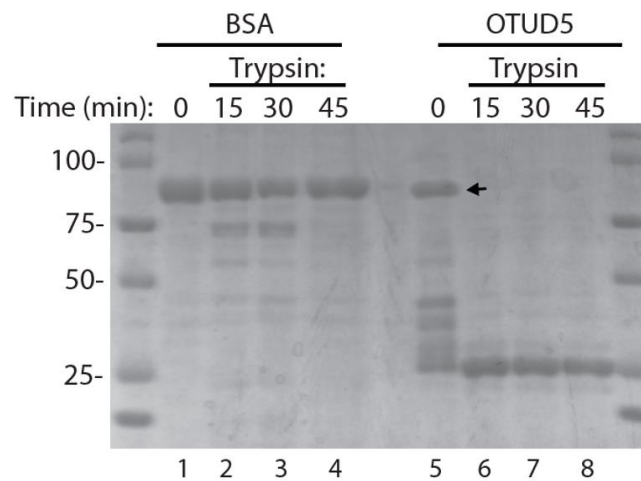


**Figure 14 – Limited Proteolysis of OTUD5.** Trypsin digestion of OTUD5 reveals a singular fragment of approximately 25kDa which corresponds to the predicted size of the OTU domain of OTUD5. OTUD5 was rapidly digested after addition of trypsin. BSA was used as a digestion control.

Using the disorder predictor and the domains found within OTUD5, a series of OTUD5 fragments were created to binding against UBR5. By PCR amplifying and cloning the desired OTUD5 fragment into pCMV 3xFLAG 9.0 vector, immunoprecipitation was performed to test narrow down the interaction site. Additionally, each constructed plasmid was reintroduced into OTUD5 KO cell line to test if it had the ability to stabilize UBR5 protein levels (Figure 15).

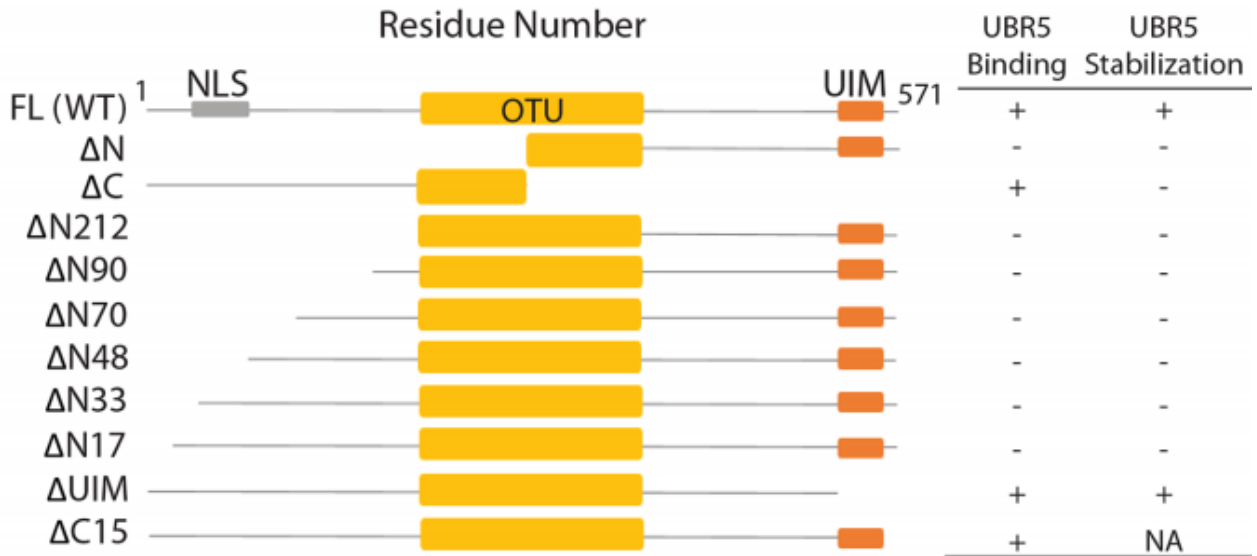


**Figure 15 – Mapping the interaction site of OTUD5-UBR5.** Schematic of all OTUD5 fragments tested against UBR5 binding and stability. The binding site was narrowed down to the N terminus of OTUD5, specifically the first 17 amino acids of OTUD5. OTUD5 ΔC15 was not tested against UBR5 stability.

Using this assay, it was found that OTUD5 uses its N-terminus to bind UBR5. The first 17 amino acids, which are conserved among many species that express OTUD5, were found to be crucial in both abilities to bind and stabilize UBR5 (Figure 16).

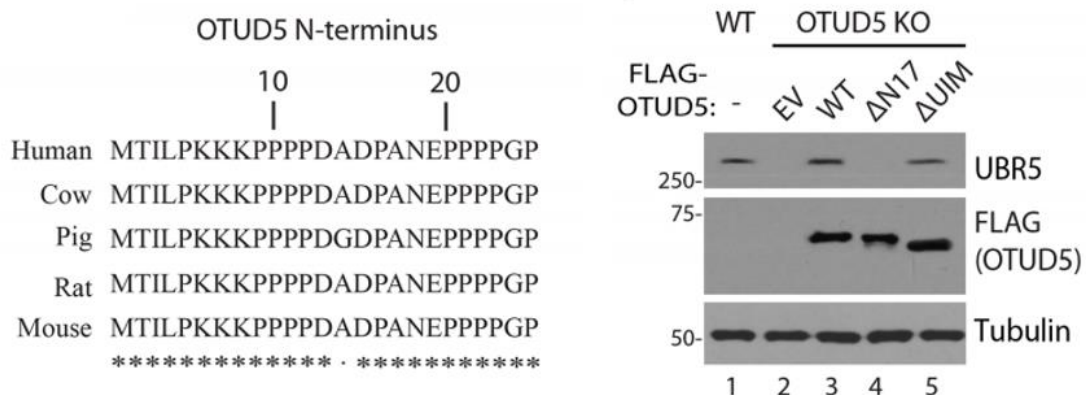


**Figure 16 – The N-Terminus of OTUD5 is required for UBR5 interaction and stability.** The N-terminus of OTUD5 is conserved across species (left). ΔN17 OTUD5 fails to stabilize UBR5 when introduced to OTUD5 KO cells. Although ΔUIM OTUD5 does not correctly identify ubiquitin chains, it still stabilizes UBR5 protein levels (right) when introduced into OTUD5 KO HeLa cells.

Using Proximity Ligation Assay (PLA) I was also able to confirm that the  $\Delta$ N17 fragments fails to interact with UBR5 while OTUD5 WT indeed produced PLA signal (Figure 17).

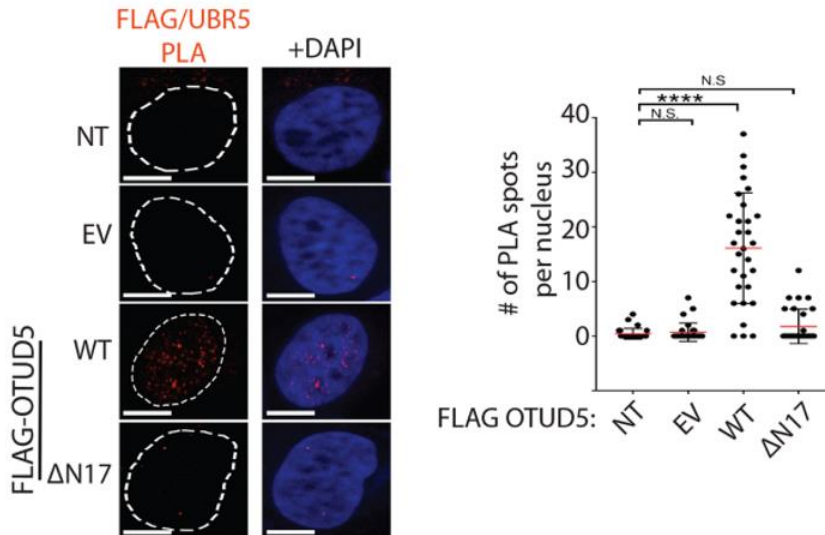


**Figure 17 – OTUD5 WT, but not OTUD5  $\Delta$ N17, interact with UBR5.** PLA between UBR5 and FLAG-OTUD5 (anti-Flag), shows that the  $\Delta$ N17 fragment fails to interact with UBR5. EV= Empty vector, used as a negative control for PLA signal. OTUD5 WT was used as a positive control for PLA signal.

### OTUD5 regulates transcriptional repression at double strand breaks

In a previous study, the Kee group showed that UBR5-BMI1 interaction is crucial for regulating transcriptional repression at damaged chromatin. We used the stable reporter cell line pTuner263 that was generated and used in Tang et al. and generously donated for our research. This cell line can induce and visualize DSBs by a fusion mCherry-LacI-FokI nuclease that is found on the LacO arrays placed kilobases upstream of the transcription sites codes for the fusion protein YFP-MS2. By inducing the stability of FokI fusion nuclease by addition of 4-OHT and Shield-1 and creating a double strand break, it was found that this suppresses the transcription of YFP-MS2. This can be visualized using immunofluorescent microscopy as YFP-

MS2 will localize to actively transcribe DNA, and upon suppression of transcription the over accumulation observed will be repressed (Figure 18).

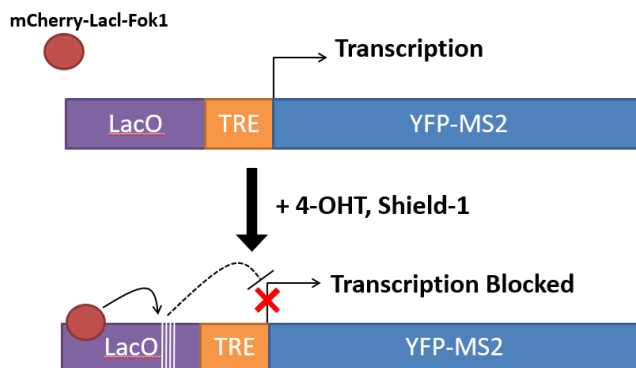


**Figure 18 – Schematic for pTuner263 reporter cell line.** The cell line contains a mCherry-LacI-Fok1 fusion nuclease that both allows localization to the LacO region where it will induce a double strand break and visualization via immunofluorescent microscopy. Fok1 is rapidly degraded and is only stabilized and imported into the nucleus upon the addition of 4-OHT and Shield-1. Further downstream there is the YFP-MS2 fusion protein. This fusion protein will only be expressed upon induction by Doxycycline and will localize to regions of active transcription. Upon Fok-1 stability, the double strand break will block transcription of YFP-MS2 gene. Cell line originally described in Shanbhag, et al, 2010 and cells were generously donated for us to use by Dr. Roger Greenberg.

Upon investigating the role of UBR5 and OTUD5 have on this system by means of siRNA targeting UBR5 and OTUD5, I discovered that both are essential to the Fok1 mediated repression of YFP-MS2 transcription (Figure 19A).

Other members of the OTU family were tested by means of siRNA knockdowns, but it was found that only OTUD5 and UBR5 have an effect of transcriptional repression. (Figure 19B). In addition to using the pTuner263 reporter cell line, de-repression of transcription was also observed by looking at localization of active RNA polymerase II (RPB1 pSerine-2 CTD) in OTUD5 and UBR5 depleted cells. Similarly, when cells (OTUD5 KO and UBR5 KO cell lines) were treated with bleomycin to induce double strand breaks, RNA Polymerase II was observed

to overlap with  $\gamma$ H2AX, a marker for double strand breaks. This overlap was not observed in the WT cell line (Figure 20).

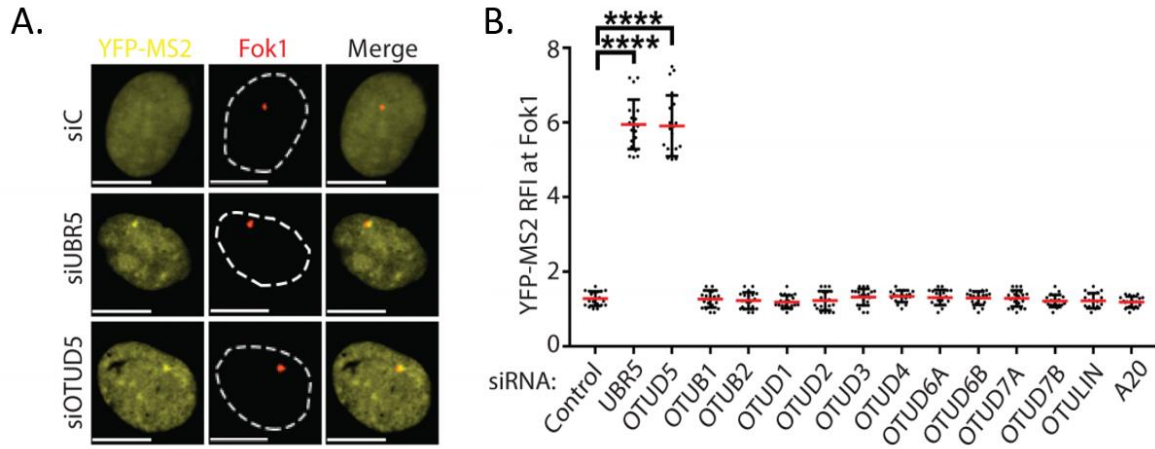


**Figure 19 – OTUD5 and UBR5 depletion leads to de-repression of transcription at double strand breaks.** **A.** Reporter cell line pTuner263 show accumulation of YFP-MS2 at mCherry-Fok1 induced double strand break when treated with siRNA targeting UBR5 or OTUD5. **B.** YFP-MS2 accumulation is specific to OTUD5 and UBR5 knockdowns, but not other members of the OTU family.

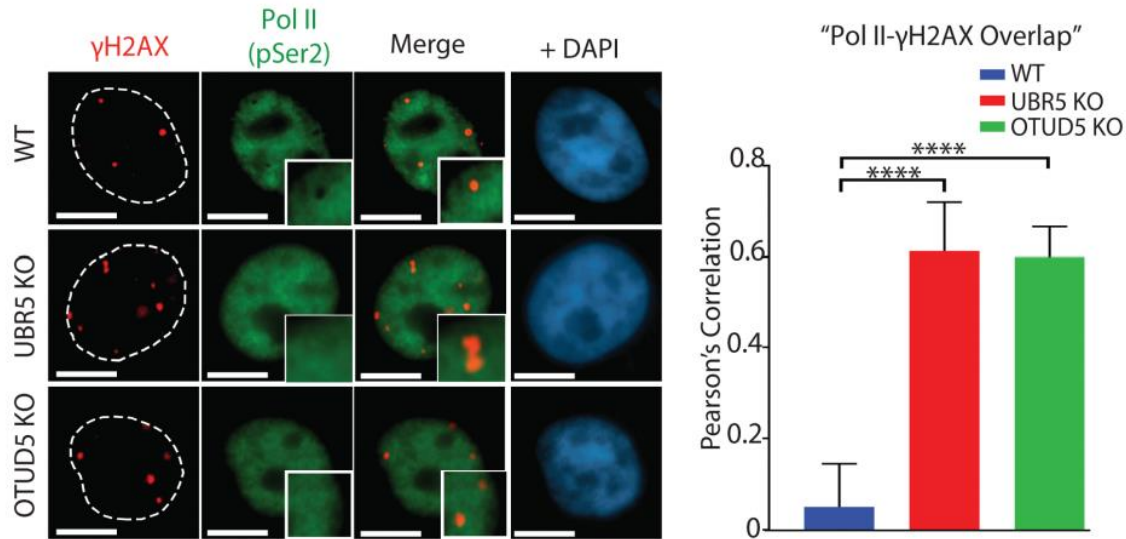


**Figure 20 – OTUD5 and UBR5 depletion lead to RNA Pol II overlap with  $\gamma$ H2AX.** Representative images of RNA Polymerase II and  $\gamma$ H2AX immunofluorescent staining. In UBR5, OTUD5 KO conditions there is observable overlap indicating de-repression of transcription (left). The results were quantified and presented as Pearson's correlations that indicate the overlap coefficient (right).

When testing staining of 5-EU (used to detect global transcription) in similar conditions, transcription is also excluded at bleomycin induced  $\gamma$ H2AX foci in the WT cells but not in the OTUD5 KO or UBR5 KO cells (Figures 21).

In a similar experiment, using siRNA to knockdown OTUD5 and UBR5 led to similar phenotypes with both RNA Polymerase II staining (Figure 22A) and 5-EU staining (Figure 22B). These results altogether suggest that UBR5 and OTUD5 induce transcriptional silencing at DSB lesions by controlling the PolII access.

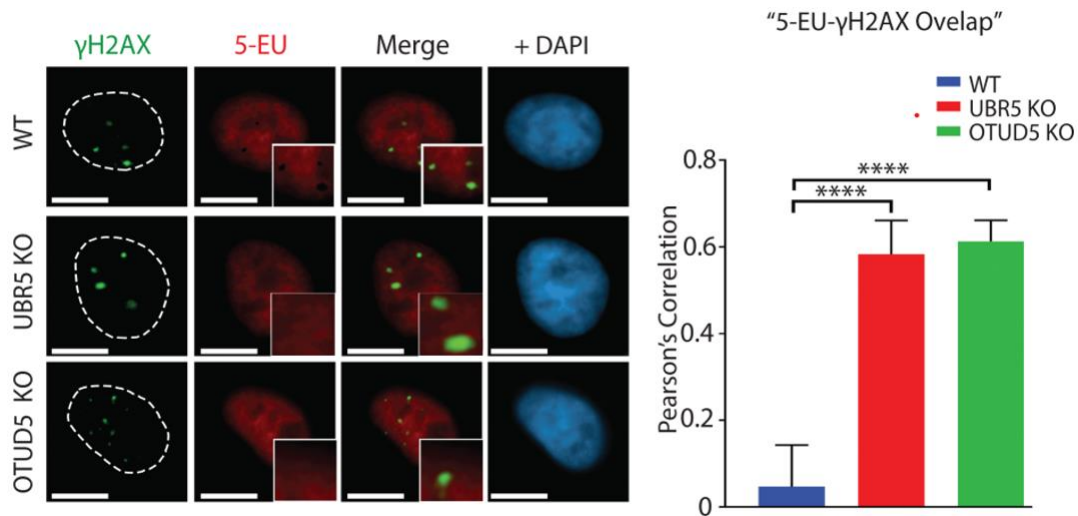


**Figure 21 – 5-EU stain in OTUD5, UBR5 KO cell lines reveal that transcription is not repressed at DSB sites.** Representative images for 5-EU staining show overlap between active transcription and double strand breaks (left). The results were quantified and presented as Pearson's correlations that indicate the overlap coefficient (right).

### OTUD5 interacts with histone chaperone SPT16

In a previous study by the Kee group, we showed that UBR5 interacts with SPT16 which along with SSRP1, form the FACT histone chaperon complex. We reasoned that OTUD5 could be involved in this interaction as well, and to test whether OTUD5 also interacts with SPT16, I performed FLAG-OTUD5 IP and GST-OTUD5 pulldown experiments from HeLa S3 cells and



subjected the eluate to mass spec analysis (Figure 23A). In both independent experiments, I found peptides derived from UBR5, a few RNA Pol II-associated factors, and the FACT components SPT16 and SSRP1. The interaction was confirmed by performing an immunoprecipitation experiment of endogenous SPT16, which co-purified both UBR5 and OTUD5 (Figure 23B). These lysates were pre-treated with benzonase to rule out that the observed interactions are DNA mediated.

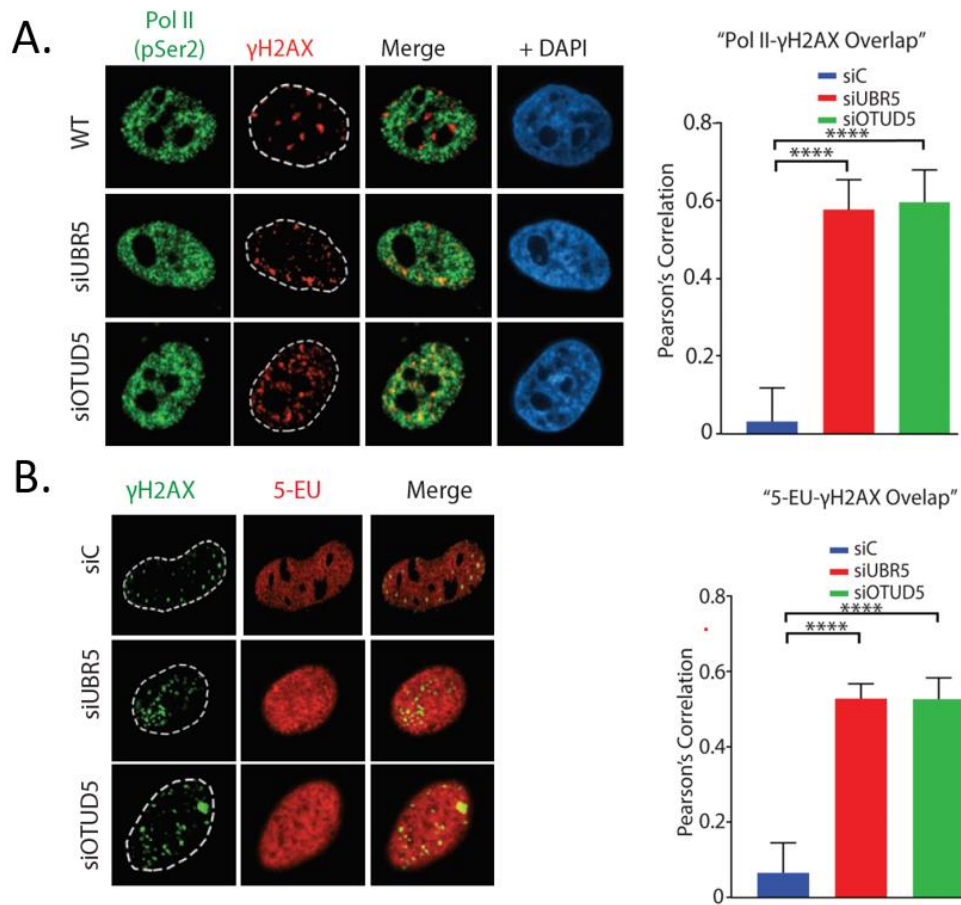


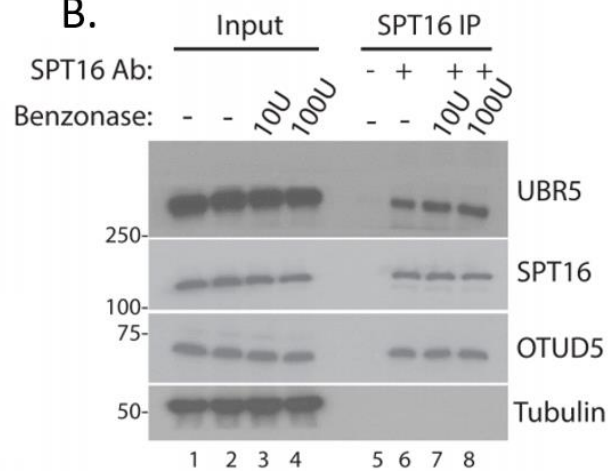
**Figure 22 – siRNA verification of de-repression phenotype. A.** siRNA targeting UBR5 and OTUD5 de-repress transcriptional repression as pSer2 RNA Pol II overlaps with  $\gamma$ H2AX. Representative images shown on left. Quantification of three independent experiment shown on the right. **B.** siRNA targeting UBR5 and OTUD5 de-repress transcriptional repression as 5-EU (active transcription site) overlaps with  $\gamma$ H2AX. Representative images shown on left. Quantification of three independent experiment shown on the right.

A.

Protein	Mass spec	
	Exp. #1	Exp. #2
OTUD5	14	15
UBR5	2	1
<b>SPT16</b>	7	2
<b>SSRP1</b>	4	1
POLR2A	5	6
POLR2B	3	4
POLR2C	2	1
POL2R2H	3	1
SUB1	4	1
NONO	8	3

Shown are unique peptide numbers

B.



C.

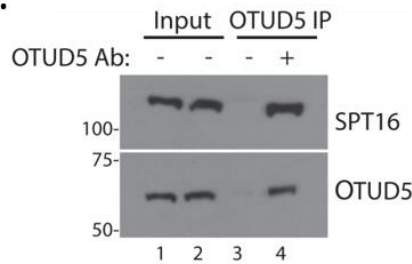


**Figure 23 – OTUD5 binds to SPT16.** **A.** Mass spec analysis of OTUD5 immunoprecipitation elution. Exp #1 represents a FLAG OTUD5 IP while Exp #2 represents GST-OTUD5 pulldown after being incubated with a S3 HeLa whole cell lysate. **B.** SPT16 IP confirms interaction with OTUD5. Benzonase was added to eliminate DNA, indicating this is not a DNA mediated interaction. Figure courtesy of Anthony Sanchez **C.** 293T cells were grown and lyzed and added OTUD5 antibody. Endogenous OTUD5 IP shows binding to SPT16.

Additionally, an IP of endogenous OTUD5 also co-precipitated SPT16 (Figure 23C).

To further investigate this novel interaction, using the pTuner263 cell line, I performed a localization experiment and found that SPT16 and OTUD5 co-localize to Fok1-induced DSB lesions (Figure 24A), in addition to the UVC-induced lesions (Figure 24B).

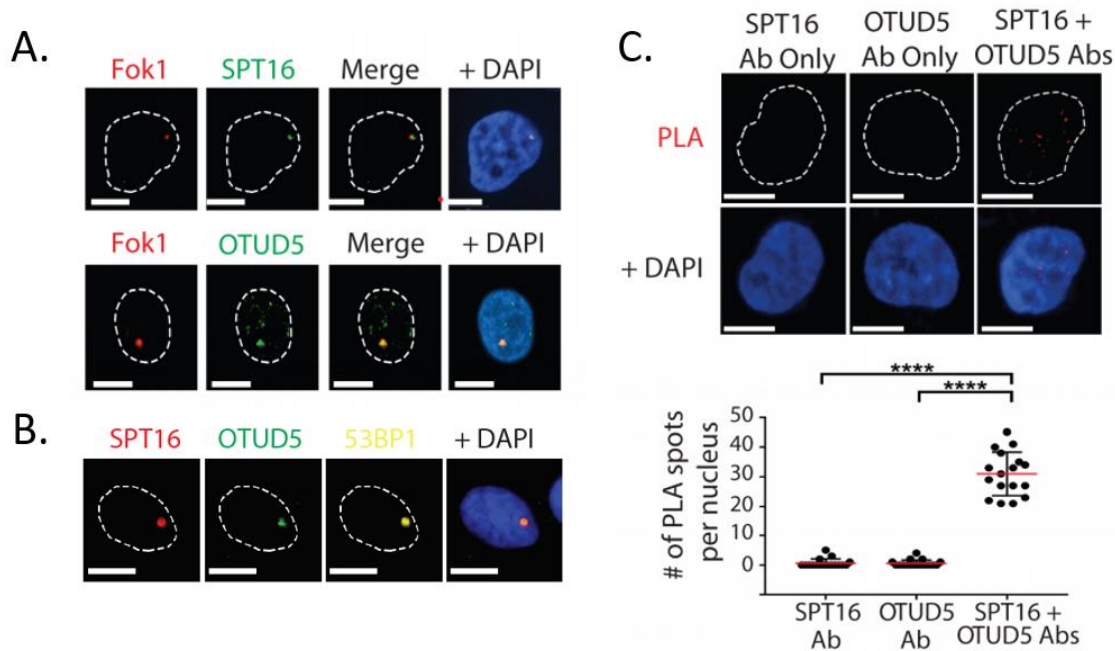


**Figure 24 – OTUD5 co-localizes with SPT16 at DSBs.** **A.** Using the reporter system Ptuner263, localization of SPT16 and OTUD5 was tested. SPT16 and OTUD5 both localize to Fok1 induced DSBs. **B.** OTUD5 and SPT16 co-localize to UV-C (3um micropore filter) induced 53BP1 damage marker. **C.** Proximity Ligation Assay between OTUD5 and SPT16 confirms interaction between the two proteins. Representative images shown on top. Quantification of three independent experiment shown below.

Further, the interaction between OTUD5 and SPT16 can be detected by PLA (Figure 24C). These PLA results were validated when depletion of each protein via siRNA treatment leads to abolishment of the PLA signal (Figure 25A). These results suggest that both OTUD5 and UBR5 interact with SPT16 within the chromatin. Additionally, the PLA signal between UBR5 and SPT16 was no longer observed in OTUD5 knockdown cells (Figure 25B), consistent with the observations that OTUD5 is necessary for UBR5 stabilization and thus the interaction with SPT16.

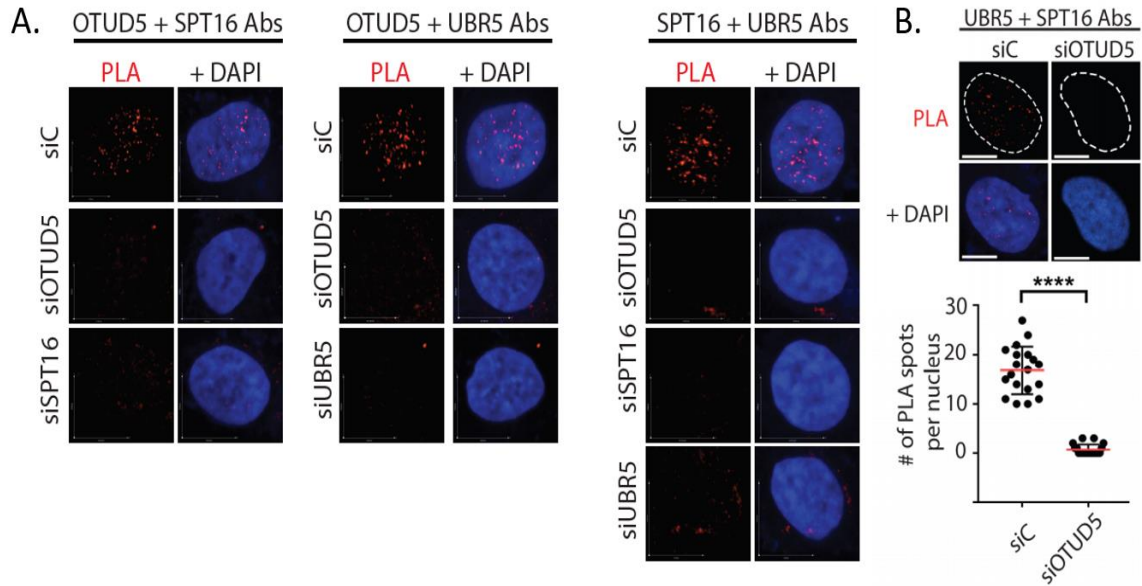


**Figure 25 – Verification Proximity Ligation Assay signal.** **A.** siRNA knockdown of each protein that was used in PLA to verify that observed signal is not false positive. **B.** siRNA knockdown of OTUD5 eliminates PLA signal between SPT16 and UBR5 as OTUD5 depletion leads to UBR5 depletion (Top). Quantification of 3 independent experiment (Bottom).

### OTUD5 interacts with SPT16 through its C-terminus.

Like the previous mapping of the interaction between OTUD5 and UBR5, I next attempted to identify the region of OTUD5 that interacts with SPT16. Using the same constructs that were generated to test UBR5 binding, SPT16 binding was tested. SPT16 interaction is retained in the  $\Delta N17$  but was lost when the C-terminus of OTUD5 was deleted, specifically the UIM motif (Figure 26A).

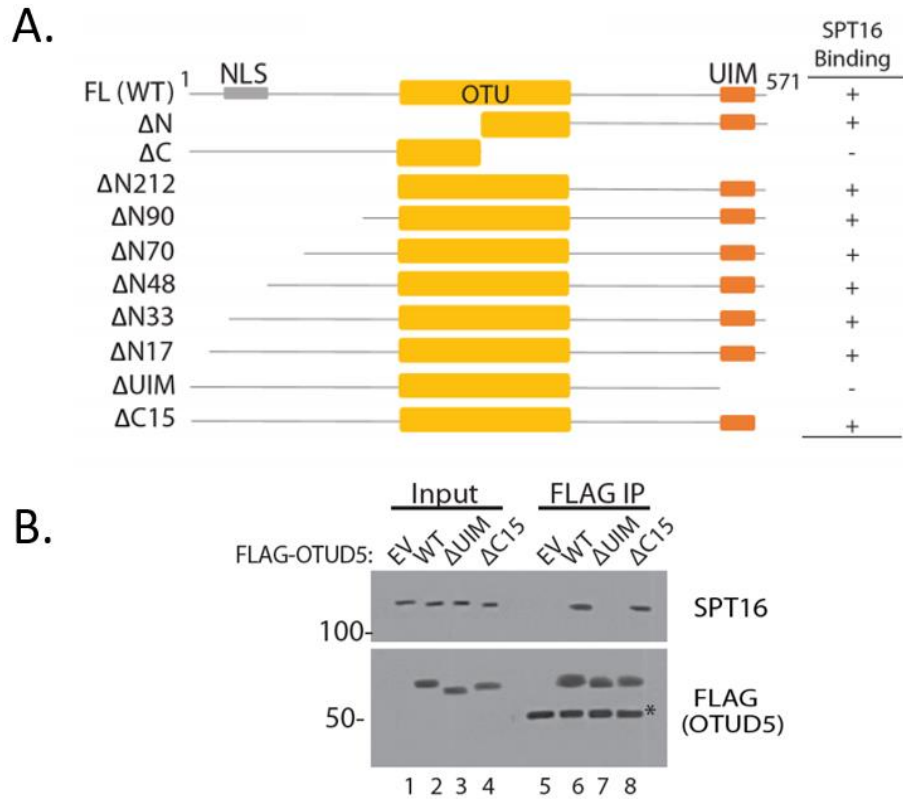


**Figure 26 – OTUD5 binds SPT16 through its UIM. A.** Schematic for OTUD5 fragments tested against SPT16 binding. OTUD5 binds SPT16 through its C-terminal tail, specifically through its UIM. **B.** Immunoprecipitation of FLAG-OTUD5 C-terminal fragments reveal that the UIM of OTUD5, but not the last 15 amino acids of OTUD5, are required for SPT16 binding.

Deletion of the final 15 amino acids downstream of the UIM did not disrupt SPT16 binding (Figure 26B), suggesting that it is the UIM specifically that interacts with SPT16. In addition, we tested recombinant GST-OTUD5 WT and GST-OTUD5  $\Delta$ UIM interaction with SPT16. This experiment provided further data that suggest that in fact the UIM of OTUD5 is required for SPT16 binding (Figure 27).

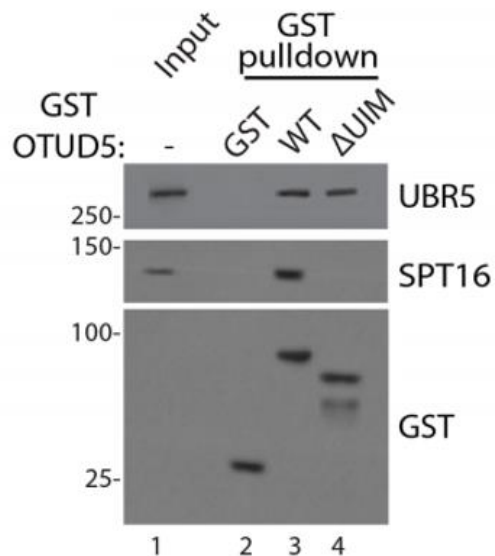


**Figure 27 – Recombinant GST-OTUD5  $\Delta$ UIM does not bind to SPT16.** Recombinant GST-OTUD5 WT and GST OTUD5  $\Delta$ UIM were purified and mix with 293T cell lysate. WT OTUD5 was able to bind both UBR5 and SPT16, but OTUD5  $\Delta$ UIM was only able to bind SPT16.

### Identification of a Nuclear Localization Signal in OTUD5

The  $\Delta$ N17 and  $\Delta$ UIM mutants still localized to the Fok1-induced DSB lesions as efficiently as WT, suggesting that these interactions are not required for the localization (Figure 28). Through the localization studies, we also found that OTUD5 is primarily localized in the nucleus and disrupting the residues within 33–70 a.a. inhibited its nuclear localization (Figure 29). These analyses also indicated that the nuclear localization and UBR5 interaction is separable.

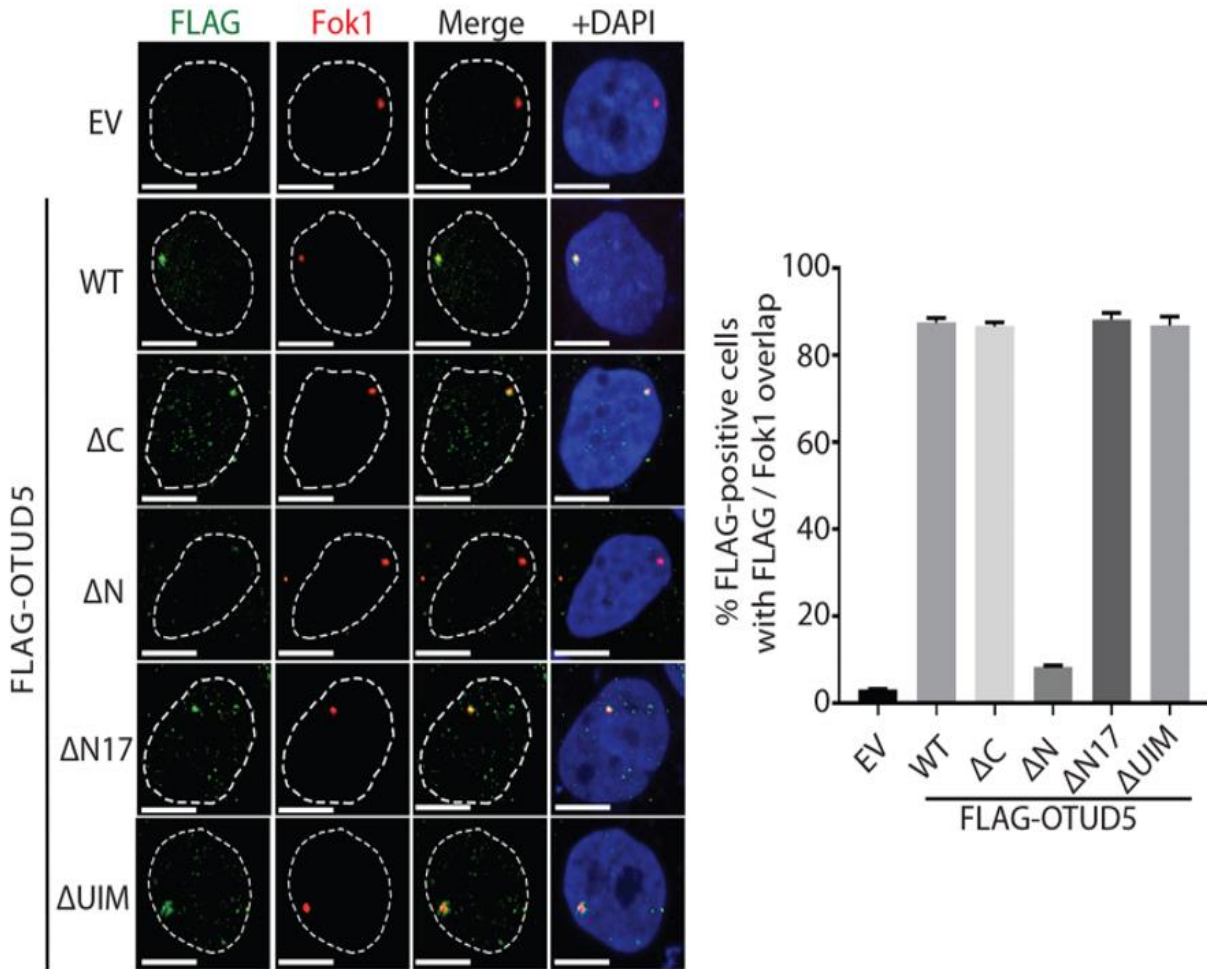


**Figure 28 – The interaction deficient mutant localizes to DSBs.** Using the pTuner263 reporter cell line, OTUD5 fragments were introduced and localization tested. The binding deficient OTUD5 mutants localize to the Fok-1 induced DSB.  $\Delta N$  mutant did not localize to the DSB. Representative image shown on the left. Quantification of three independent experiment shown on the right.

Altogether, these results demonstrate that OTUD5 interacts with UBR5 and SPT16 through two distinct regions, and that the UBR5-SPT16 interaction occurs indirectly through OTUD5.

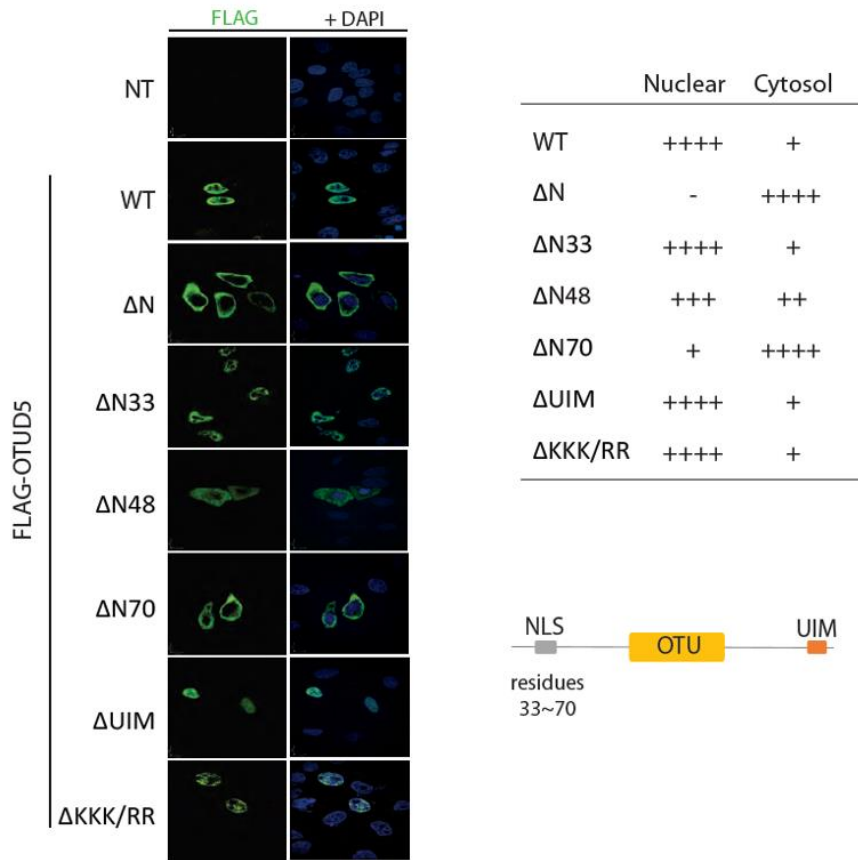


**Figure 29 – Localization study OTUD5 fragments.** Different OTUD5 fragments were introduced into HeLa cells and immunofluorescence microscopy using FLAG antibody was performed to test localization. Representative images shown on the left. Fragments were quantified based on location (cytosol or nuclear). The more protein observed in each compartment, the more + assigned (top right). Schematic of predicted nuclear localization signal (bottom right).

### OTUD5 regulates SPT16 enrichment

When I analyzed the effects of SPT16 foci at UV-C lesions using micropore filter (3μm), I observed that knockdown of both UBR5 and OTUD5 led to SPT16 foci enlargement at the sites of H2AX (Figure 30A). This experiment was repeated in the pTuner263 reporter cell line and the results were reproducible. SPT16 foci were enlarged at the Fok1-induced DSB nuclease (Figure 30B). This data suggests that UBR5 and OTUD5 have a repressive role on FACT and OTUD5 and UBR5 depletion leads to SPT16 enrichment at the damage sites.



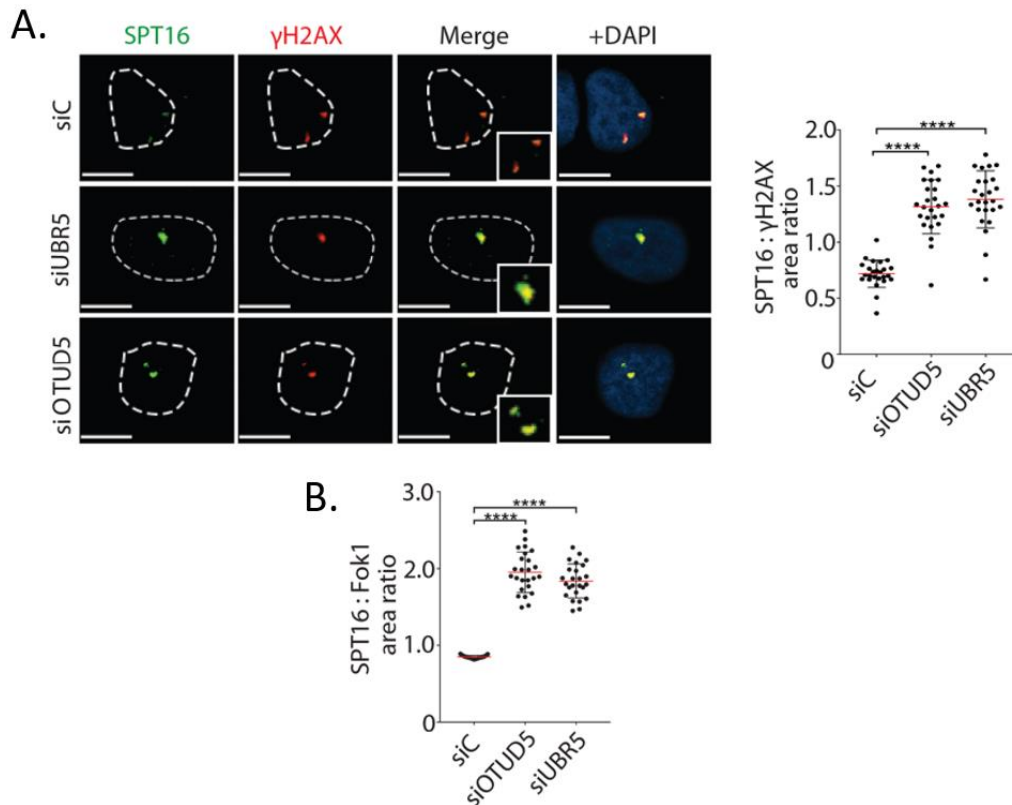


**Figure 30 – SPT16 foci is enlarged when OTUD5 or UBR5 are depleted. A.** HeLa cells were treated with UV-C (100J/M<sup>2</sup>) through a micropore filter (3μm). Representative images shown on left. Quantification of three independent experiments shown right. **B.** Ptuner263 reporter cells were to test SPT16 enlargement phenotype. SPT16 foci is enlarged in siOTUD5 and siUBR5 treated cells.

### Transcriptional repression at DSB is dependent on SPT16

Previously, the Kee group we showed that UBR5 ubiquitinates SPT16 and suggested that this may repress FACT activity. Consistently, accumulation of YFP-MS2 at Fok1-induced DSB sites in OTUD5 or UBR5 knockdown cells was reversed by additional SPT16 knockdown (Figure 31). This data suggest that RNA Polymerase II elongation at DSB caused by UBR5 or OTUD5 depletion depends on SPT16 protein levels.

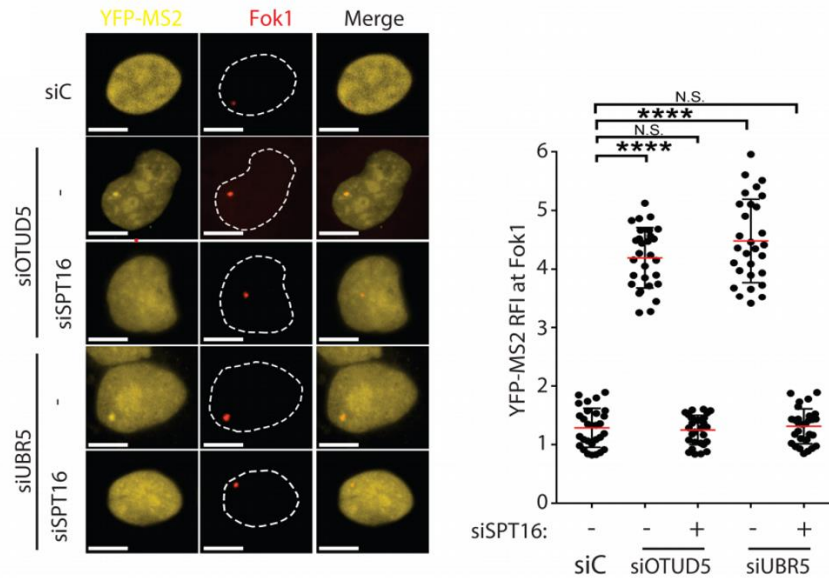


**Figure 31 – SPT16 depletion reverses OTUD5, UBR5 depletion phenotype.** When OTUD5 or UBR5 is depleted, MS2 accumulates at Fok1 sites indicating de-repression of transcription. Depleting SPT16 in these conditions reverses the observed de-repression of transcription (Left). Quantification of 3 independent experiment (Right).

### Interaction-deficient OTUD5 mutants cannot rescue the transcription phenotypes

With the binding sites between OTUD5/UBR5 and OTUD5/SPT16 found, I wanted to see if these interactions were needed to transcriptional repression. To investigate this, I performed a rescue experiment where I first treated pTuner263 cells with siRNA targeting OTUD5 followed by transfecting different OTUD5 fragments and mutations. I found that expressing the FLAG-OTUD5 WT reversed the accumulation of YFP-MS2 reporter at the Fok1- induced DSB sites in OTUD5 knockdown cells (Figure 32A). In addition, both  $\Delta N17$  and  $\Delta UIM$  OTUD5 mutant (both unable to bind either UBR5 or SPT16, respectively) still showed accumulation of YFP-MS2 at the Fok1-induced DSB, unable to rescue the phenotype even upon equal expression, and  $\Delta N17$  was not able to restore UBR5 protein levels (Figure 32B).

The expression of these fragments is similar to WT levels, suggesting that the ability to bind UBR5 and SPT16 is not required for its stability. These results suggest that the both

catalytic activity of OTUD5 (deubiquitinating UBR5) as well as the scaffolding ability of OTUD5 (binding to SPT16) are important in the process.

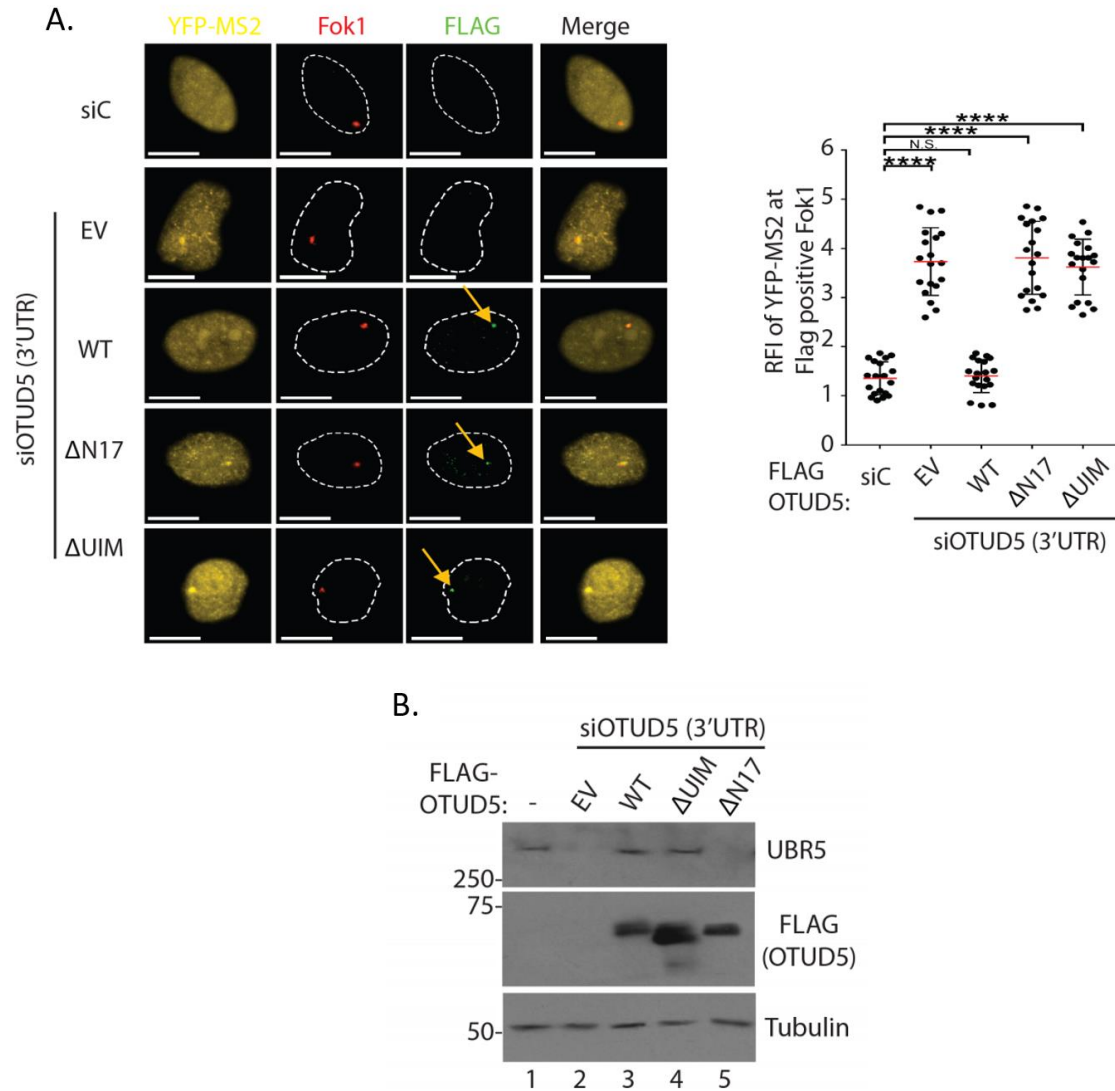


**Figure 32 – Interaction deficient mutant do not repress transcription. A.** Using the Ptuner263 reporter cell line, siOTUD5 and indicated OTUD5 fragments were treated. ΔN17 and ΔUIM both localized to DSB but do not repress transcription at DSB. Representative image shown on the left. Quantification of three independent experiments shown on right. **B.** Expression verification of the OTUD5 fragments.

### Cancer-associated OTUD5 missense mutation disrupts the FACT association

Numerous missense mutations for OTUD5 have been found in numerous cancers and reported to Cbioportal. However, none of these mutations have been studied and the role of

them is currently unknown. Interestingly, the D537 residue within the UIM is mutated to Ala in several reported cases of leukemia (Figure 33A). I decided to test the functional role of the D537 residue and mutate it to Ala and test whether this mutation was sufficient to bind SPT16. Through immunoprecipitation test I found that the D537A mutation disrupts the interaction with the FACT components SPT16 and SSRP1 (Figure 33B). This mutation did not disrupt the interaction with UBR5, further supporting that the OTUD5-FACT association is independent of UBR5. When the D537A mutant was tested against transcriptional repression in pTuner263 cell line, I saw that it failed to repress transcription at the Fok1-induced DSB (Figure 33C). Taken together, this data highly suggests that the OTUD5/SPT16 interaction (and FACT as a whole) is important for transcriptional regulation, and provide a new pathway of transcriptional repression previously undescribed. This data also provides a possible link between the how FACT misregulation can lead to transcriptional errors and how FACT contributes to tumor suppression.

### **OTUD5 depletion causes genome instability**

This work shows how OTUD5 works as a regulator of transcriptional activity at double strand breaks. Further investigation of downstream effects of de-repression of transcription shows that upon OTUD5 or UBR5 depletion, cells show sensitivity to Bleomycin (compared to siControl cells). However, the observed sensitivity is not as strong phenotype to the sensitivity observed in BRCA1 knockdown conditions. These phenotypes were observed in both U2OS cell (Figure 34A) and HeLa cells (Figure 34B). When OTUD5 knockdown was administered, it was observed that cells were sickly and would start to die. To test this, we collected siOTUD5 treated cells exposed to bleomycin. When testing the viability of these cells, they show increased apoptosis when OTUD5 is depleted (subG1 population) and this phenotype is

synergistic with bleomycin treatment (Figure 34C). I also observed that OTUD5 depletion had an increased in cell population during the S and G2/M phases.

This could be interpreted as DNA replication problem along with increased DNA damage, possibly due to unregulated DNA transcription. Further suggesting replication errors, I found that OTUD5 KO cells show an increased number of spontaneous RPA foci (Figure 34D).

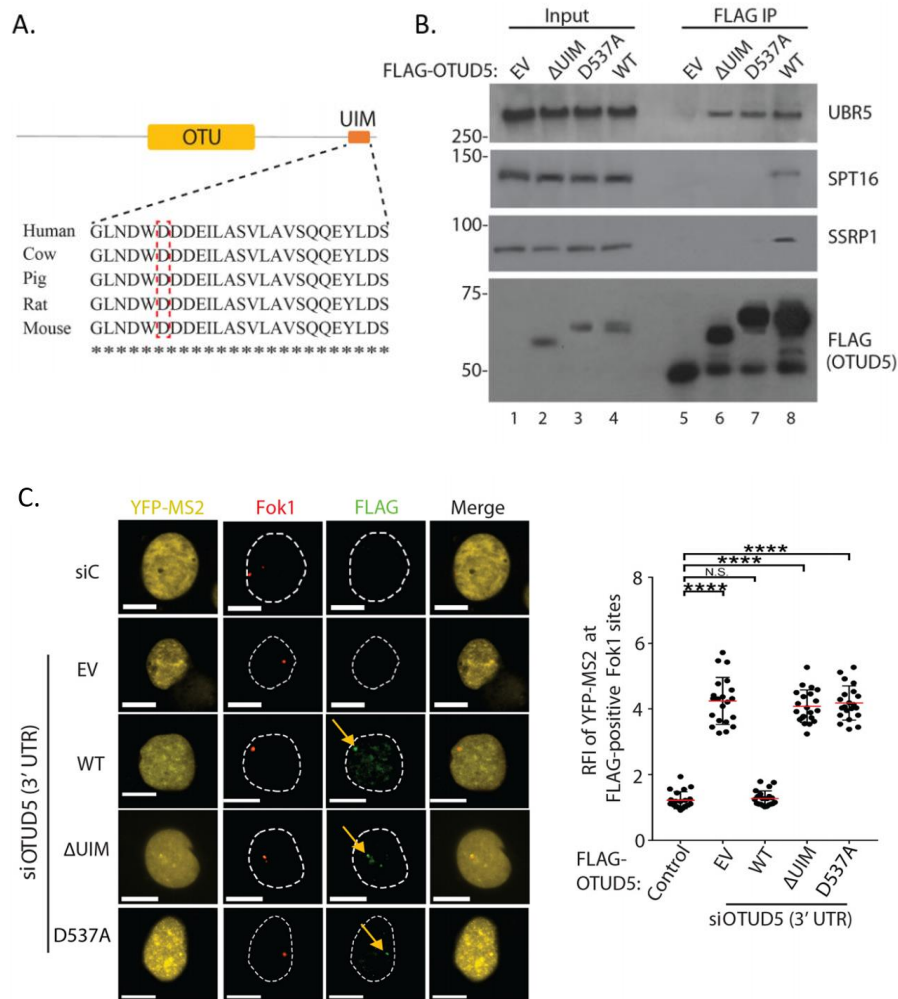


**Figure 33 – UIM mutant D537A does not repress transcription.** **A.** UIM sequence alignment between different species show that it is conserved. Red outline indicates mutated amino acid. **B.** Immunoprecipitation assay shows that OTUD5 D537A mutant does not bind SPT16. **C.** Using the Ptuner263 reporter cell line, siOTUD5 and indicated OTUD5 fragments were treated. D537A localized to DSB but does not repress transcription at DSB. Representative image shown on the left. Quantification of three independent experiments shown on right.

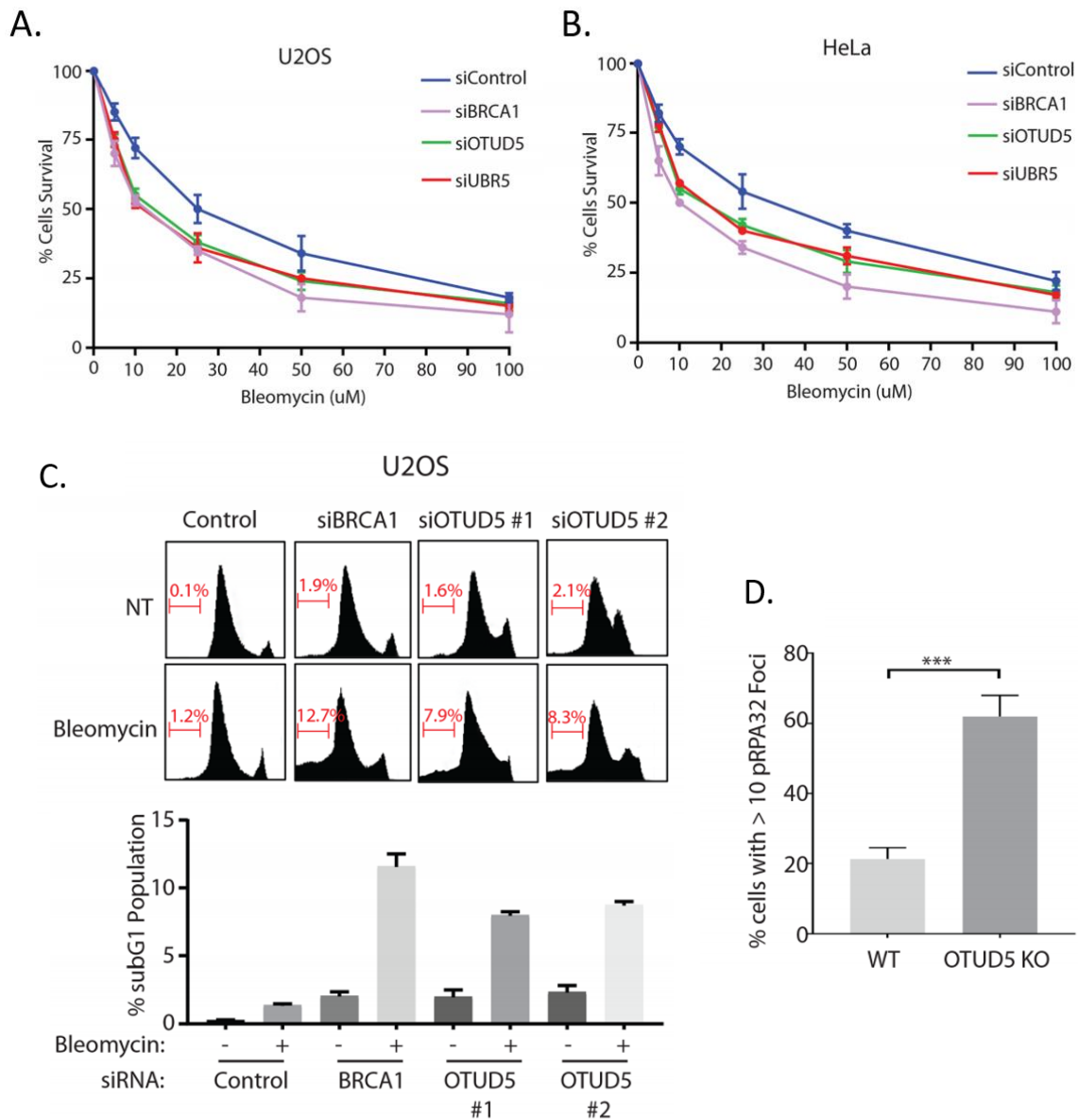


**Figure 34 – OTUD5 depletion causes genomic instability.** **A.** U2OS cells were treated with indicated siRNA then seeded at 100 cell per well. Cells were treated for 10 days with bleomycin at indicated dosage, then fixed and stained. Colometric assay was performed on stained cells. Data was normalized to Control no treatment. **B.** HeLa cells were used for survival assay as described in (A) **C.** U2OS cells were treated with indicated siRNA and analyzed using flow cytometry (top). Quantification of sub G1 population (bottom). **D.** HeLa WT and OTUD5 KO cells stained for pRPA32 and analyzed using immunofluorescence microscopy.

These data altogether suggest that OTUD5 is a bona fide regulator of the DNA damage response and is necessary for genomic integrity maintenance.

## Discussion

In this study, a new role for OTUD5 as a regulator of transcriptional repression at damaged chromatin was found. Initially found through a DUB siRNA screen, OTUD5 is a specific deubiquitinating enzyme that stabilizes the E3 ubiquitin ligase UBR5. OTUD5, as well as UBR5, localizes to damaged chromatin sites (DSBs) caused by UV-C and nuclease (Fok1), where they both interact. Through a series of truncations on OTUD5, the interaction site between OTUD5 and UBR5 was identified and analyzed. OTUD5 interacts with UBR5 through the N-terminal disordered tail region and deletion of the disordered N-terminal tail (first 17 amino acids,  $\Delta$ N17) eliminated resulted in lack of binding and UBR5 instability. On the opposite end of OTUD5, the C-terminal tail interacts with the FACT complex component the histone chaperon SPT16, specifically through the UIM. In this study I also show that OTUD5 depletion phenocopies UBR5 depletion in all aspects of the transcriptional regulation we tested, such as misregulation of Pol II elongation through Bleomycin and nuclease-induced DSB lesions, nascent RNA synthesis at the lesions and increased cellular sensitivity to Bleomycin. These phenotypes are seen to be dependent on SPT16, as depletion of either UBR5 or OTUD5 alongside SPT16 results in reversal of transcriptional de-repression. The transcriptional deregulation observed in the OTUD5-depleted cells was rescued by reintroduction of exogenous OTUD5 WT, but not by either of the interaction deficient OTUD5 mutant, OTUD5  $\Delta$ N17 or  $\Delta$ UIM. These data support a model, in which the OTUD5–UBR5 complex interacts with SPT16 causing it to be repressed at double strand breaks. When OTUD5 or UBR5 are depleted, SPT16 will accumulate at these damage sites. We propose that repression of FACT activity by the OTUD5–UBR5 complex is crucial for RNA Polymerase II stalling and gaining access to damaged DNA. However, the mechanism described in this study is distinct from the direct stalling of Pol II by the DNA lesions. The Shanbhag et al. study used the same system used in this study (Ptuner263 reporter cell line) and suggested that DSBs initiate a signaling

cascade that represses transcription distant from the lesion (99). This study proposes that FACT is an important factor in this in transcriptional regulation at double strand breaks, and that FACT (particularly SPT16) is subject to regulation by OTUD5–UBR5 complex in response to RNA Polymerase II stalling.

### **Future Direction**

The data shown in this study suggest that OTUD5 and UBR5 repress FACT histone exchange activity. However the mechanism of action is still largely unknown. There is evidence that UBR5 ubiquitinates SPT16, but the consequence of this modification is not known. Current literature has two models for FACT activity: 1. FACT can facilitate the eviction of H2A/H2B dimer by directly binding to them, or 2. Destabilization of the histone core complex to weaker the histone-DNA interaction (25–27,31–33). It is possible that OTUD5 prevents the FACT engagement on the histones or DNA, by directly binding to FACT. Alternatively, the ubiquitination of SPT16 by UBR5/OTUD5 could be a completely different method of regulation for FACT and could disrupt FACT access to nucleosomes. Further work is needed to understand the precise regulatory mechanism.

Although this study does investigate how OTUD5 is recruited to the damage sites, how this is achieved is unknown. Using different inhibitors and siRNA, I determined that recruitment to the DSB is not dependent on ATM, ATR, PARP, SPT16 or UBR5. Through the investigation of OTUD5 binding to UBR5 and SPT16, the OTUD5 fragments created did reveal a possible nuclear localization signal at the N-terminus of OTUD5 (amino acids 33-70, Figure 30). However, the exact signal for localization to the nucleus and DSB is unknown.

This study suggests that the OTUD5–SPT16 interaction through the UIM may be an important tumor suppressive mechanism, as shown for the case of D537A mutation (Figure 35).



FACT overexpression has been reported in certain cancers and undifferentiated cells (33,37,38). Based on the data from this study, I believe that accelerated FACT activity may contribute to the progression of cancer through various gene expression or general genomic instability. Because some tumors carry the OTUD5 D537A mutation, FACT hyper-activity (due to loss of repression in the OTUD5 D537A mutant) would be similar the effects of FACT overexpression. However, we cannot exclude a possibility that OTUD5 has a yet unknown function that could act as tumor suppressive function through interaction with other proteins. Multiple mechanisms have been proposed that regulate the process under different experimental settings (discussed in chapter 1). As OTUD5/UBR5/SPT16 also contributes to these experiment, we thought it might be linked to a previously describe mechanism. However, we have not yet been able to found evidence of crosstalk between the ATM or DNA-PK signaling pathway and the UBR5–OTUD5-FACT components in the transcriptional repression. I also tested if OTUD5 or UBR5 could contribute to the NELF-E regulatory pathway, but upon siRNA depletion of OTUD5 or UBR5 NELF-E protein levels remained stable. There is however evidence that UBR5 recruitment to DSB is dependent on the PRC1 complex, particularly BMI1 and RNF2. This suggests that these two pathways could be linked, but further analysis is needed to determine the mechanism of repression in the PRC1-UBR5 pathway.

## Chapter 4 – Uncoupling of OTUD5/FACT leads to replication stress and genomic instability

### **Introduction**

After the findings described in Chapter 4, I decided to further investigate the downstream effects of the genomic instability. Due to the results described in Figure 36C, I hypothesized that transcriptional de-repression observed in OTUD5 depleted cells could result in replication defects. Cells have developed mechanisms to avoid the collision between the transcription machinery and the replication machinery (47), and pathways such as Fanconi Anemia coordinate transcription and replication to prevent errors (102, 103). Transcription-Replication Conflicts (TRCs) is avoided by separating the two actions both by locations and by time (104). However, problems can arise in genes that are simply too large. When TRC occurs, higher levels of R-loops are observed. R-loops are RNA:DNA hybrid structures where RNA binds to a single stranded DNA and the other DNA strand is displaced (105). There is increasing amount of data that show that R-loops can contribute to genomic instability (106) and as such there have been new mechanism described that are responsible for processing R-loops (103). R-loops are generated from transcription and are more common to occur at common fragile sites (CFSs) (81). CFSs are genomic loci that are naturally subject to breaks upon replication stress and are often found in cancers (107).

In this study, I investigate the effects of unregulated transcription upon replication. I have found that OTUD5 depletion causes replication stress as evidenced by an increase in 53BP1 nuclear bodies and RPA32 foci. Upon further investigation, I discovered that OTUD5 accumulates at CFSs under replication stress and OTUD5 depletion increased R-loops and RNA polymerase II accumulation at CFS. Upon investigation of a HeLa OTUD5 D537A Knock in

cell line we found that uncoupling of the SPT16/OTUD5 interaction causes genomic stress, increases R-loops, RNA polymerase II accumulation at CFS and sensitivity to replication stress.

## **Results**

This study focuses on the effects of OTUD5 depletion and misregulation of FACT on replication.

### **OTUD5 depletion causes replication stress**

When investigating the effects of OTUD5 depletion, I noticed that 53BP1 foci were increased. 53BP1 nuclear foci in G1 phase have been previously reported to be a result of replication stress. When OTUD5 was depleted and cells stained for 53BP1 and CyclinA (to distinguish cell phases), 53BP1 nuclear bodies were observed to be increased when OTUD5 was depleted with two independent siRNAs (Figure 35A). When the number of 53BP1 nuclear bodies was quantified, it was found that OTUD5 depleted cells had a similar amount of nuclear bodies as FANCD2-depleted cells, known to cause replication stress when depleted (Figure 35B).

Due to the increase in 53BP1 nuclear bodies observed, I wondered if these were located at chromosome fragile sites (CFSs) since CFS are prone to break upon replication stress. To test this, I performed Chromatin Immunoprecipitation (ChIP) of three different CFS: FRA3B (I tested both a distal and central site for this loci), FRA7H, and FRA16D (Figure 36A). Upon OTUD5 knockdown and ChIP analysis of the CFSs, I indeed saw increased 53BP1 protein at these regions (Figure 36B).

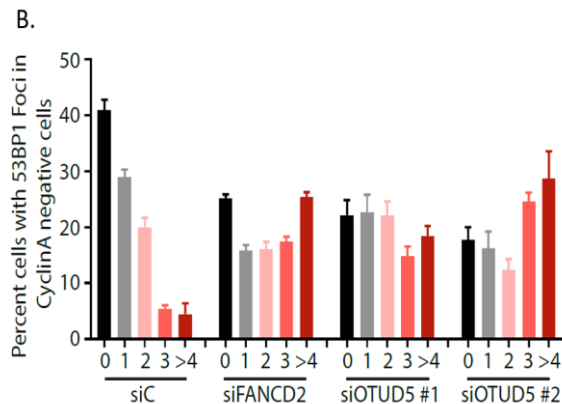
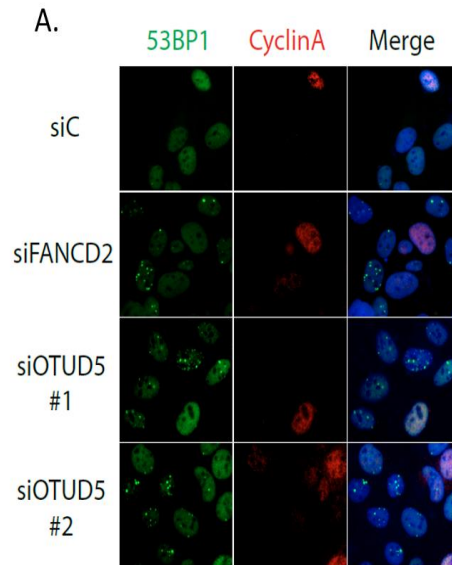


**Figure 35 – OTUD5 depletion increases G1 bodies.** **A.** U2OS cells were treated with indicated siRNA and stained for 53BP1 and CyclinA and analyzed using immunofluorescent microscopy. Representative images are shown. **B.** Quantification of (A). Only cells that were negative to cyclinA were counted, as cyclinA positive cells are not in G1 phase.

Additional investigation into OTUD5 knockdown revealed more replication stress phenotypes: RPA32 protein was increased at replication fork (Figure 37A), cells were sensitive to hydroxyurea (HU) when either OTUD5 or UBR5 was depleted (Figure 37B), and formation of micronuclei, a canonical replicative stress phenotype, was increased upon OTUD5 or UBR5 knockdown (Figure 37C). These data support the hypothesis that OTUD5 has a crucial role in preventing replication stress.

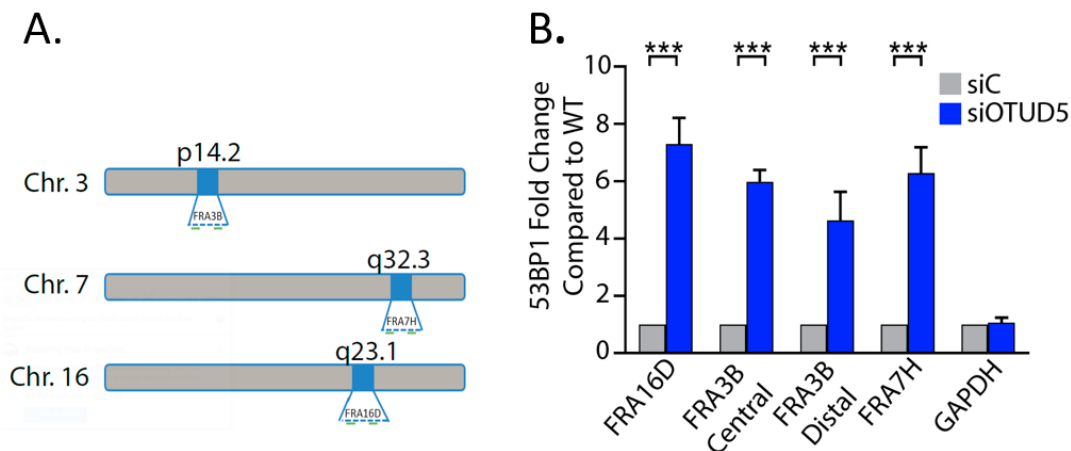


**Figure 36 - OTUD5 depletion causes accumulation of 53BP1 at CFS. A.** Schematic for ChIP analysis. Shown are the CFS that are tested. **B.** ChIP analysis of siC and siOTUD5 cells. 53BP1 accumulates at CFS under siOTUD5 conditions.

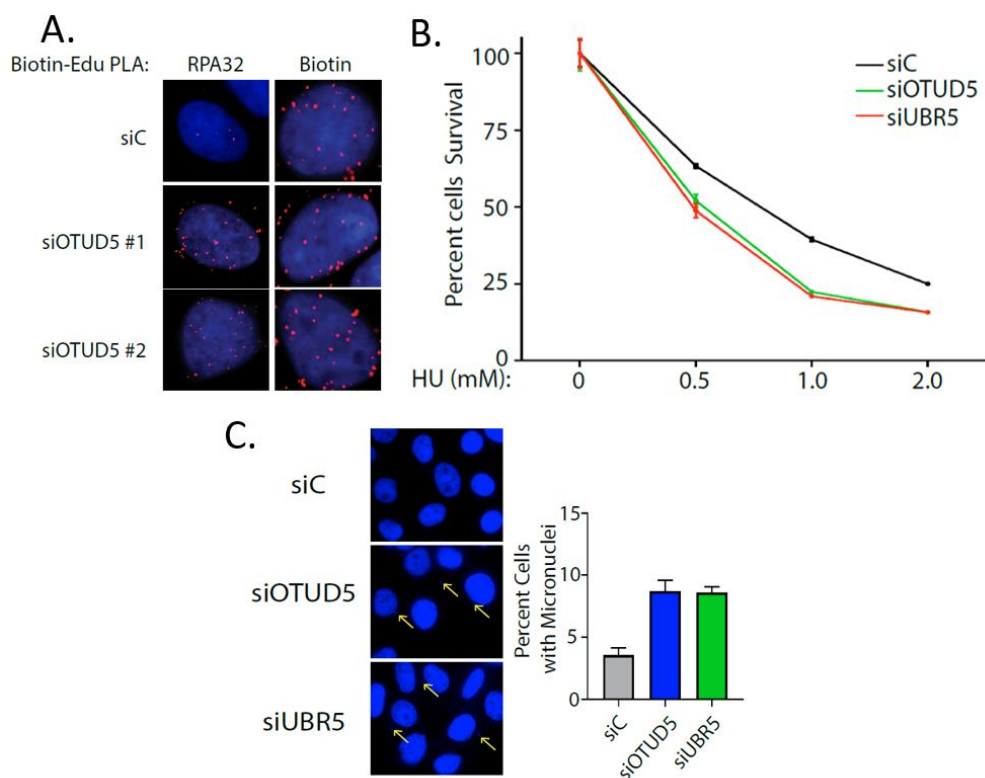


**Figure 37 – OTUD5 knockdown shows replication stress. A.** OTUD5 depletion shows increased PLA signal between Biotin-Edu labeled replication fork and RPA32. Biotin/Biotin PLA was used as a PLA signal control. **B.** Cell survival assay was performed on U2OS cells after siRNA mediated depletion of OTUD5 or UBR5. Both knockdowns show sensitivity to HU treatment. **C.** U2OS cells were treated with indicated siRNA and 72 hours later fixed and stained with DAPI. In both knockdown conditions, micronuclei formation is increased.

## OTUD5 depletion causes R-loop formation and accumulation at CFS

Because of the previous studies described in chapter 4, I hypothesized that the replication stress phenotype observed could be due to transcriptional deregulation. To test this, first I decided to check RNA Polymerase II levels at CFSs. Upon OTUD5 knockdown, ChIP analysis revealed a 5 to 12 fold increase of RNA Pol II occupancy levels at CFSs (Figure 38A). Because aberrant transcription can lead to formation of R-loops and R-loops have been found to be a source of replication stress, I also tested OTUD5 knockdown cells for accumulation of R-loops at CFS. To do this, I tested whether RNaseH1, the enzyme responsible for processing R-loops was accumulated at CFS. Indeed, when a catalytically inactive RNaseH1 was introduced into OTUD5 knockdown cells and tested with ChIP analysis, I found that RNaseH1 was increased at CFSs (Figure 38B).

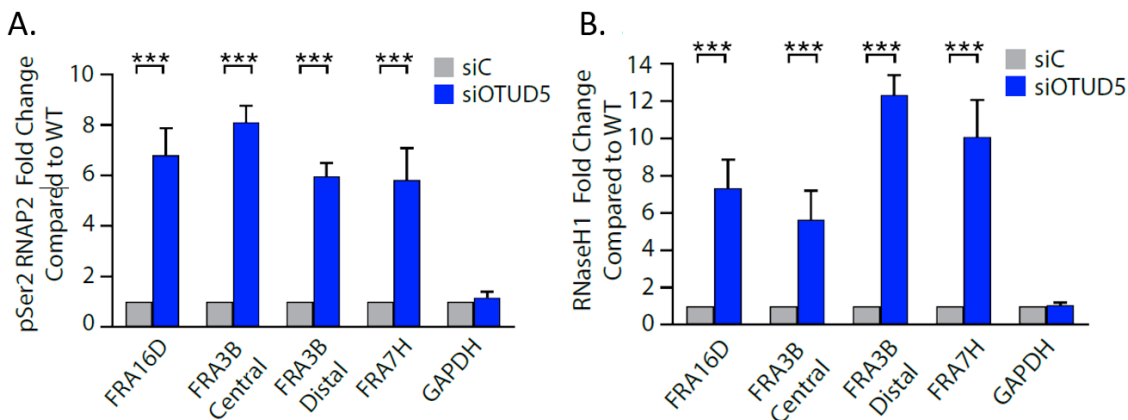


**Figure 38 – OTUD5 depletion leads to aberrant transcription at CFS.** A. ChIP analysis of OTUD5 depleted U2OS cells reveals RNA Polymerase II to accumulate at CFS. B. ChIP analysis of OTUD5 depleted U2OS cells reveals RNaseH1 to accumulate at CFS. RNaseH1 processes and removes R-loops.

Because of the accumulation of RNA Pol II at CFS, I hypothesized that transcription may perturb replication. First, to test if RNA Polymerase II physically collide with replication fork, I

performed PLA between pSer2 RNA Pol II and Biotin-labeled Edu (Edu is an analog to thymidine that allows for biotin labeling for visualization using immunofluorescent microscopy). This experiment shows that upon OTUD5 or UBR5 depletion, PLA signal between pSer2 RNA Pol II and Edu is increased (Figure 39A), suggesting that the transcription machinery is present at the replication fork. Similarly, an additional PLA was performed between PCNA and pSer2 RNA Pol II which showed similar results (Figure 39B).

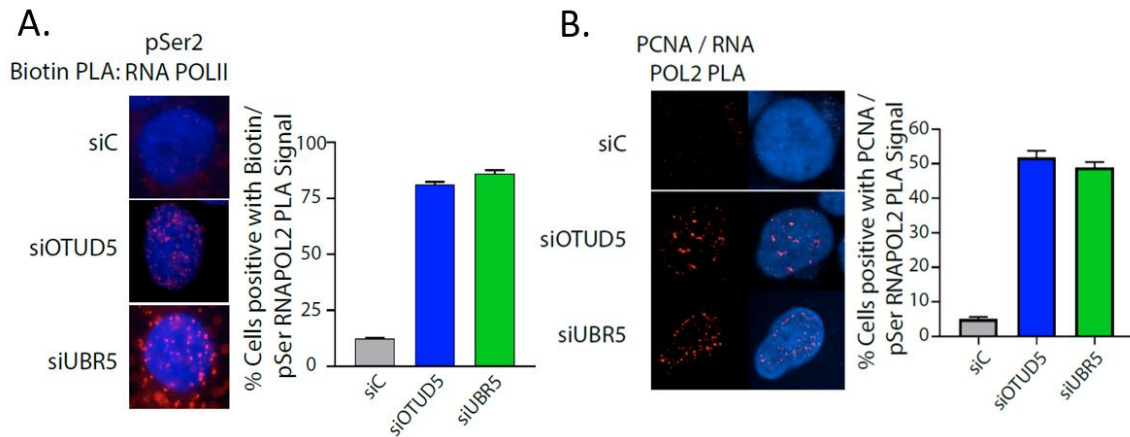


**Figure 39 – PLA analysis of OTUD5, UBR5 depleted cells reveals TRC phenotype. A.** PLA assay between Biotin-Edu labeled replication fork and pSer2 RNA Polymerase II shows increased signal, suggesting TRC. **B.** PLA assay between PCNA and pSer2 RNA Polymerase II shows increased signal, suggesting TRC.

To try to explain this phenotype, I performed ChIP analysis to determine if OTUD5 was present at the CFS. This experiment showed that OTUD5 was present at CFSs, and accumulates at CFSs in response to replication stress (in the form of HU treatment, Figure 40A). Lastly, the OTUD5 mutants that fail to bind UBR5 or SPT16 were introduced into OTUD5 depleted cells to test if they would rescue G1 body formation. While the introduction of WT

OTUD5 did reverse the phenotype, neither the  $\Delta$ N17 nor the D537A OTUD5 mutant were able to reverse the 53BP1 nuclear bodies formation (Figure 40B).

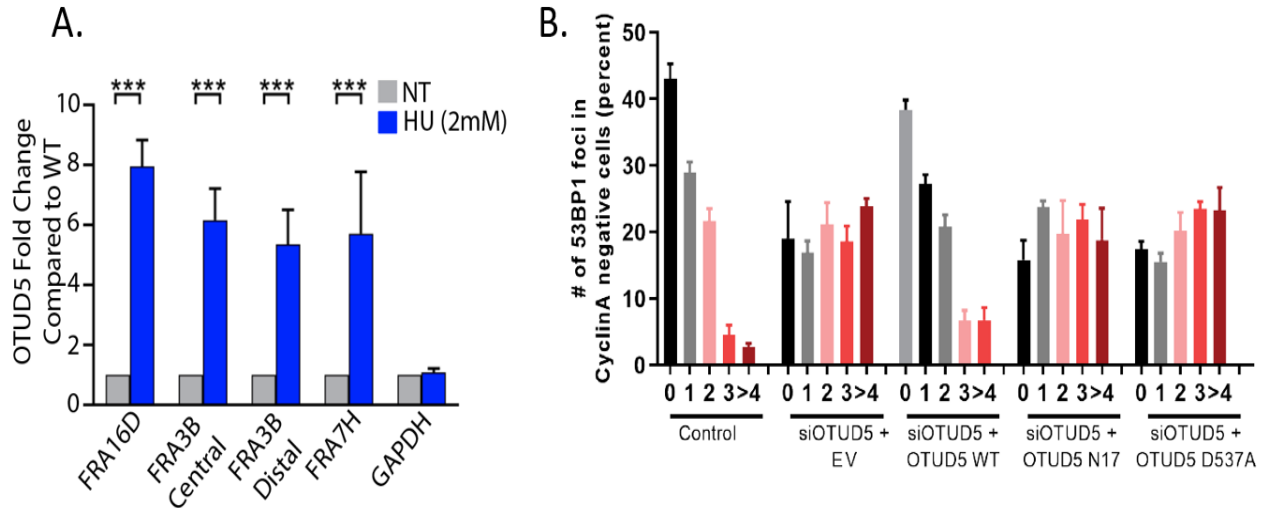


**Figure 40 – OTUD5 binding to UBR5-SPT16 is important to prevent replication stress. A.** ChIP analysis of HU treated U2OS cells reveals OTUD5 to accumulate and is enriched at CFS after replication stress. **B.** Quantification of G1 body analysis using OTUD5 mutants to rescue. Only WT OTUD5 was able to reduce number of G1 bodies observed. Only cells that were negative to cyclinA were counted, as cyclinA positive cells are not in G1 phase.

### Validation of OTUD5 D537A knock in cell line

To further investigate the effects that uncoupling of OTUD5-SPT16 have on the cell, 4 different OTUD5<sup>D537A</sup> knock in HeLa clones were generated. The knock ins were confirmed by genomic sequencing (Figure 41). OTUD5<sup>D537A</sup> knock in HeLa clones were generated by Genome Engineering & iPSC Center at Washington University in St. Louis.



WT HeLa 1594 1647

Allele 1: tttccttctcctcgcgccagcaggtctgaacgattggGATgatgatgagatcctagcttcggtgctggcagtgctcc

Allele 2: tttccttctcctcgcgccagcaggtctgaacgattggGATgatgatgagatcctagcttcggtgctggcagtgctcc

D537A Clone 1

Allele 1: tttccttctcctcgcgccagcaggtctgaacgattggGCCgatgatgagatcctagcttcggtgctggcagtgctcc

Allele 2: tttccttctcctcgcgccagcaggtctgaacgattggGCCgatgatgagatcctagcttcggtgctggcagtgctcc

D537A Clone 2

Allele 1: tttccttctcctcgcgccagcaggtctgaacgattggGCCgatgatgagatcctagcttcggtgctggcagtgctcc

Allele 2: tttccttctcctcgcgccagcaggtctgaacgattggGCCgatgatgagatcctagcttcggtgctggcagtgctcc

D537A Clone 3

Allele 1: tttccttctcctcgcgccagcaggtctgaacgattggGCCgatgatgagatcctagcttcggtgctggcagtgctcc

Allele 2: tttccttctcctcgcgccagcaggtctgaacgattggGCCgatgatgagatcctagcttcggtgctggcagtgctcc

D537A Clone 4

Allele 1: tttccttctcctcgcgccagcaggtctgaacgattggGCCgatgatgagatcctagcttcggtgctggcagtgctcc

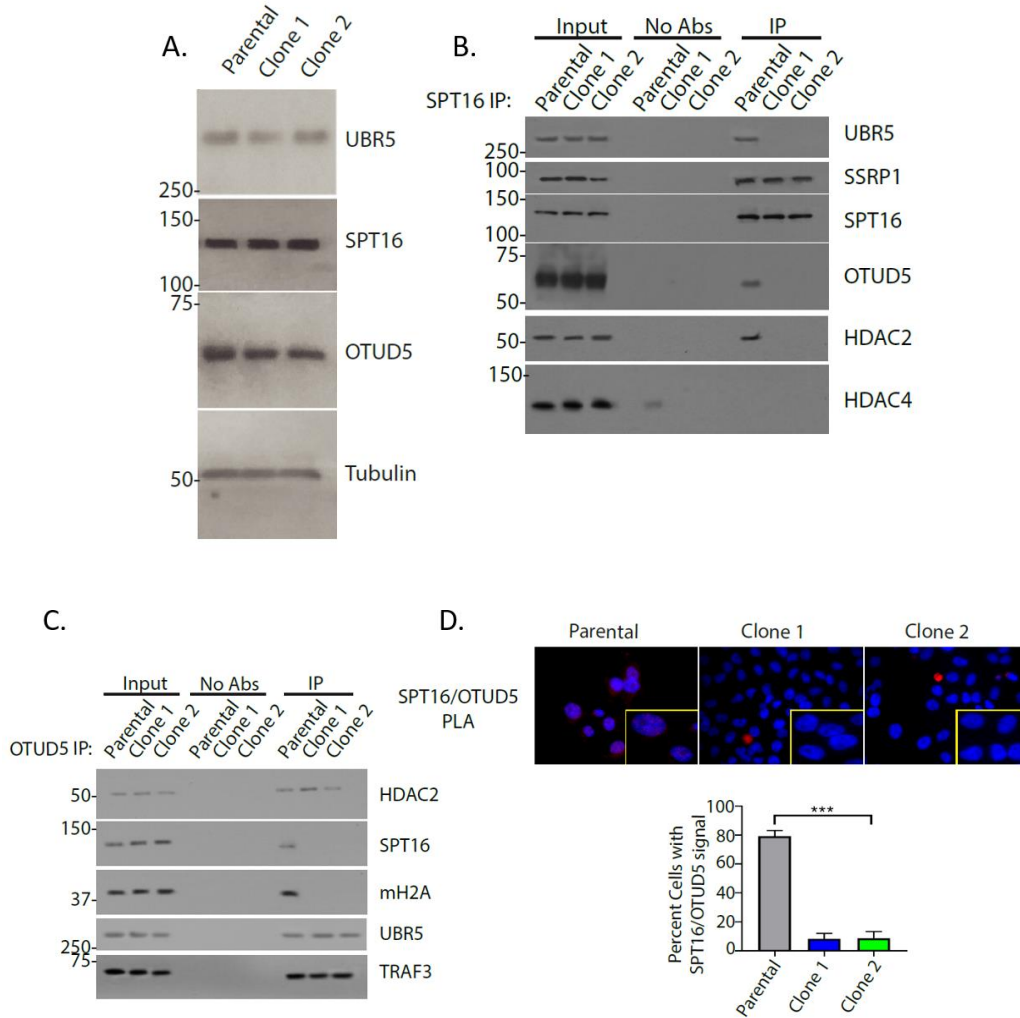
Allele 2: tttccttctcctcgcgccagcaggtctgaacgattggGCCgatgatgagatcctagcttcggtgctggcagtgctcc

**Figure 41 – Genomic sequencing of OTUD5 D537A Knock in cell lines.** Stable knock in of OTUD5 D537A were generated in HeLa cells. Four different clones were generated and sequenced. Cell lines generated by Genome Engineering & iPSC Center at Washington University in St. Louis.

To validate the clones, expression levels for OTUD5 and SPT16 were tested and verified to be unchanged compared to parental cells (Figure 42A). Importantly, the lack of binding between OTUD5 and SPT16 was verified in the two clones tested, confirming the earlier results which used the overexpressed OTUD5 from plasmid transfections. When two clones were tested using immunoprecipitation, the binding between OTUD5 and SPT16 was still disrupted (Figure 42B for SPT16 IP, Figure 42C for OTUD5 IP). The interaction was also tested using PLA between OTUD5 and SPT16 in two of the clones (Figure 42D). These results provide confidence that the newly created knock in cell lines are an acceptable model of study.

To determine if the OTUD5<sup>D537A</sup> Knock in cell lines also exhibit the TRC phenotypes, different assays were employed: first, the presence of micronuclei was tested. When testing the

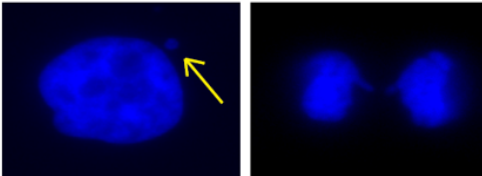
4 different clones for micronuclei, I noticed that in addition to the increased micronuclei, I observed increased nuclear bridges (Figure 43).



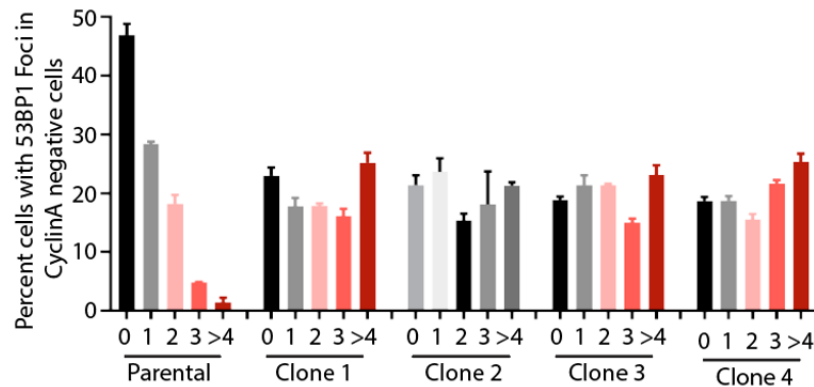
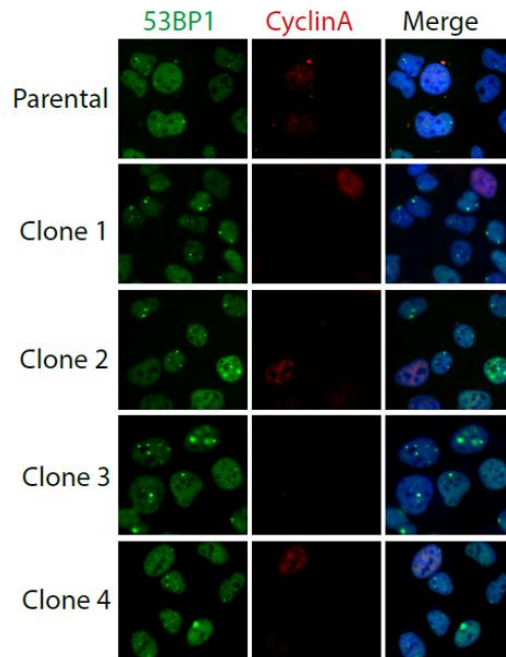
**Figure 42 – Validation of OTUD5 D537A Knock in cell line.** **A.** Western blot showing that expression levels of OTUD5, UBR5 and SPT16 are equal in clones 1 and 2. **B.** Endogenous SPT16 in clone 1 and 2 of the OTUD5<sup>D537A</sup> knock in cell line confirm lack of binding between OTUD5 and SPT16. SSRP1 binding remains intact. **C.** Endogenous OTUD5 in clone 1 and 2 of the OTUD5<sup>D537A</sup> knock in cell line confirm lack of binding between OTUD5 and SPT16. UBR5 binding remains intact. **D.** PLA analysis of clone 1 and 2 of the OTUD5<sup>D537A</sup> knock in cell line confirm lack of signal. Representative image top. Quantification of three independent experiments shown in bottom.

These bridges have been shown to be a result from incomplete replication, usually because of replication stress. Next, immunofluorescent microscopy was performed to test if G1 bodies were elevated. When staining for 53BP1 and CyclinA, I observed that most of the knock in cells had G1 bodies present, with many of them presenting with multiple nuclear bodies (Figure 44).

	Micronuclei	Bridges
Parental	24/608 = 3.94%	6/608 = 0.98%
Clone #1	85/765 = 10.45%	32/765 = 4.18%
Clone #2	73/639 = 11.4%	26/639 = 4.07%
Clone #3	88/681 = 12.9%	41/681 = 6.02%
Clone #4	68/578 = 11.7%	38/578 = 6.57%

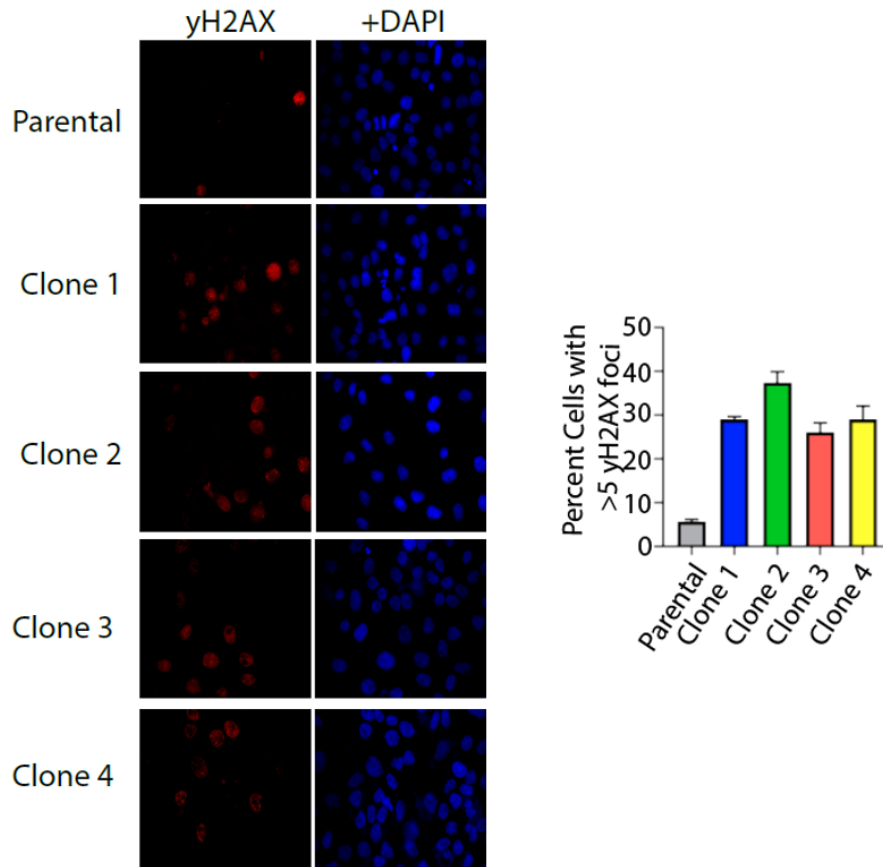
  


**Figure 43 – OTUD5<sup>D537A</sup> Knock in clones show increased replication defects.** WT and OTUD5<sup>D537A</sup> KI clones were fixed and stained with DAPI. Immunofluorescent reveals increased formation of micronuclei in the KI clones, as well as increased anaphase bridge formation. These two phenotypes are indicate of replication defects. Number of cells with and without aberrations were counted and quantified. A representative image for each condition is shown at the bottom.



**Figure 44 – OTUD5<sup>D537A</sup> Knock in cell lines have increased G1 bodies.** OTUD5<sup>D537A</sup> cells were fixed and stained for 53BP1, CyclinA and DAPI and analyzed using immunofluorescent microscopy. Representative images are shown in top. Quantification of three independent experiments shown in bottom.

In a similar experiment, spontaneous  $\gamma$ H2AX levels were tested in the OTUD5<sup>D537A</sup> knock in clones. Indeed, the OTUD5<sup>D537A</sup> knock in clones have increased levels of  $\gamma$ H2AX foci (Figure 45).



**Figure 45 - OTUD5<sup>D537A</sup> Knock in cell lines show spontaneous yH2AX foci.** OTUD5<sup>D537A</sup> cells were fixed and stained for yH2AX and DAPI and analyzed using immunofluorescent microscopy. yH2AX is a modified histone responsible for initiating double strand break repair.

Lastly, two clones were used for cell survival assay against different chemical agents. When dosed with aphidocolin (APH), AZ20 (ATR inhibitor), HU, or bleomycin, these clones showed sensitivity to these treatments (Figure 46). These data consistently suggest that the D537A mutation in OTUD5 is crucial for maintaining proper replication within cells.

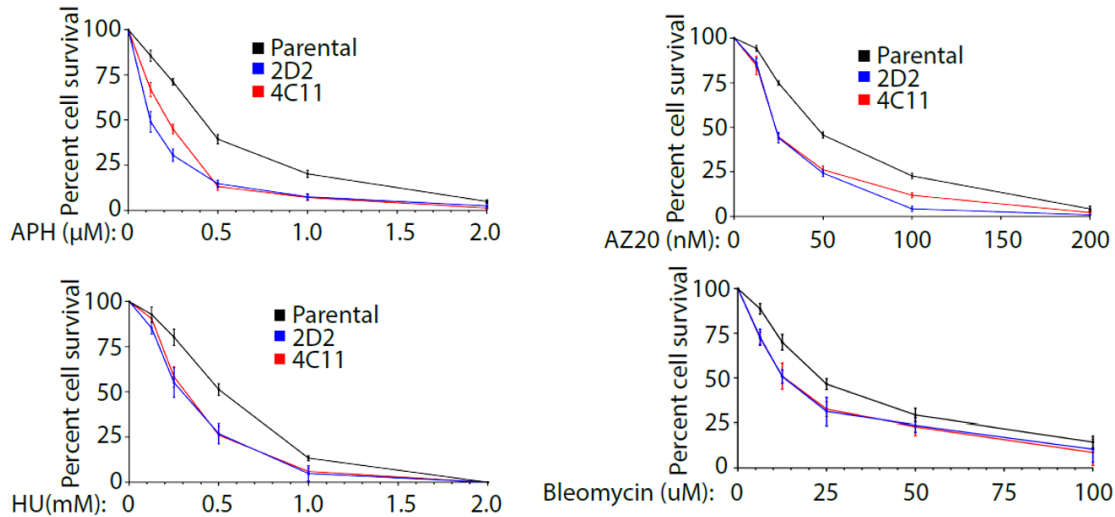


**Figure 46 - OTUD5<sup>D537A</sup> Knock in cell lines are sensitive to a variety of different damage.** OTUD5<sup>D537A</sup> Knock in cells were seeded at 100 cell per well. Cells were treated for 10 days with either APH, AZ20 (ATR inhibitor), HU, or Bleomycin at indicated dosage, then fixed and stained. Colometric assay was performed on stained cells. Data was normalized to Parental no treatment.

### OTUD5 is a direct binding partner of SPT16

To determine why the OTUD5<sup>D537A</sup> knock in cell lines show such phenotypes, I decided to further investigate the binding between OTUD5 and SPT16. Previously described work (Chapter 4) indicated that OTUD5<sup>D537A</sup> cannot bind SPT16 in vivo, however the question remains whether OTUD5 directly interacts with the FACT complex and if so, to which subunit it directly binds to. To test this, both OTUD5 WT and a  $\Delta$ UIM mutant were purified using DH5a *E. coli*. Additionally, SPT16 and SSRP1 were purified using baculovirus method by infecting SF9 cells and amplifying the virus, eventually infecting a large number of cells to overexpress FLAG-SPT16 or 6xHis SSRP1. When purified OTUD5 WT and SPT16 were mixed together, they both were present after pulldown. As expected, OTUD5  $\Delta$ UIM failed to bind SPT16. Interestingly, neither the OTUD5 WT nor the  $\Delta$ UIM were able to bind SSRP1. However, when SPT16 was added to this reaction, OTUD5 WT, SPT16 and SSRP1 were able to be pulldown (Figure 47A). Using a 293T FLAG-SPT16 knock in cell lysate as bait, purified GST-OTUD5 WT,  $\Delta$ UIM and

D537A proteins were mixed, resulting in only GST OTUD5 WT to be able to pulldown SPT16 (Figure 47B).

Finally, I wanted to test if the C-terminus of OTUD5 (amino acids 500-571) is sufficient to bind SPT16. By purifying the UIM of OTUD5 fused with GST tag and mixing it with a FLAG SPT16 cell lysate (as described above), I was able to determine that the UIM of OTUD5 is sufficient to facilitate the binding between OTUD5 and SPT16 (Figure 48).

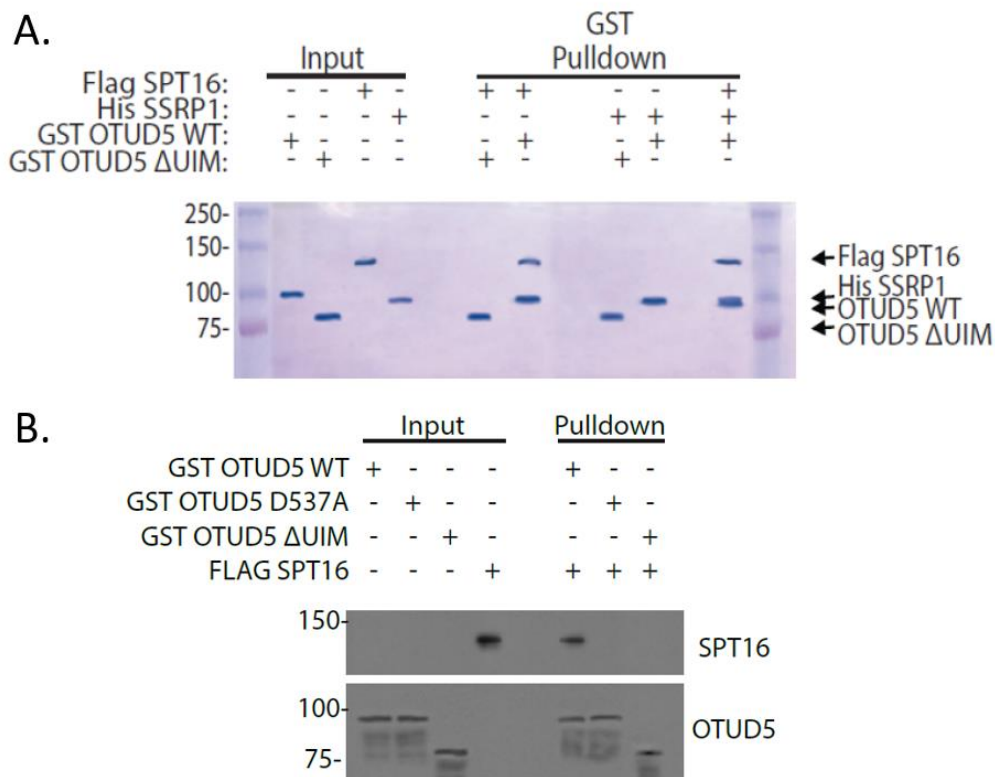


**Figure 47 – OTUD5 binds directly to SPT16. A.** Recombinant GST-OTUD5 WT, GST-OTUD5 ΔUIM, FLAG-SPT16, and 6xHis-SSRP1 were purified in either bacteria or SF9 insect cells. FLAG-SPT16 and 6xHis-SSRP1 were eluted off beads and mixed with indicated proteins and a pulldown was performed. **B.** Purified recombinant GST-OTUD5 WT, GST-OTUD5 D537A and GST-OTUD5 ΔUIM were mixed with a 293T FLAG-SPT16 knock in lysate. Pulldown analysis reveals that only GST-OTUD5 WT was able to bind FLAG-SPT16.

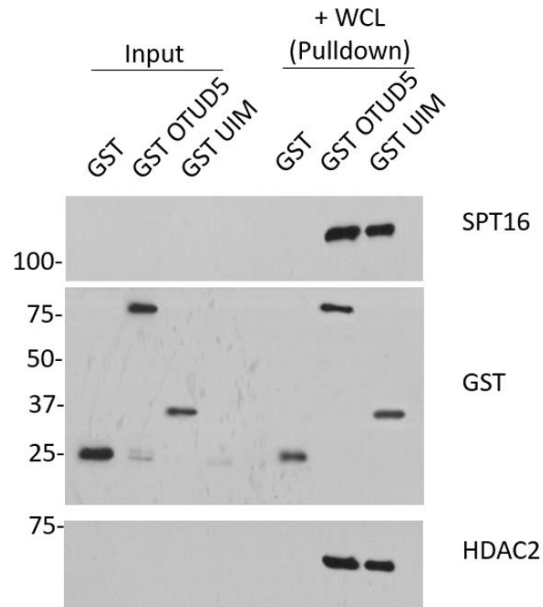


**Figure 48 – The C-term of OTUD5 is sufficient to bind SPT16.** Recombinant GST-OTUD5 WT and GST-UIM were purified from bacteria and mixed with a 293T FLAG-SPT16 knock in lysate. Pulldown analysis reveals that both GST-OTUD5 WT and GST-UIM were able to bind SPT16.

#### **OTUD5<sup>D537A</sup> knock in cell line exhibit TRC**

To determine if the replication defects observed are a result of aberrant transcriptional regulation described in Chapter 4, I decided to explore phenotypes associated with Transcription Replication Conflict. With the hypothesis that SPT16 is not restrained in OTUD5<sup>D537A</sup> knock in cells, I tested whether SPT16 occupancy at CFSs is altered. To do this, I used the OTUD5<sup>D537A</sup> knock in cells to perform a ChIP experiment to analyze if SPT16 accumulates at CFSs. Interestingly, the ChIP experiment showed that SPT16 was increased at CFSs (Figure 49).



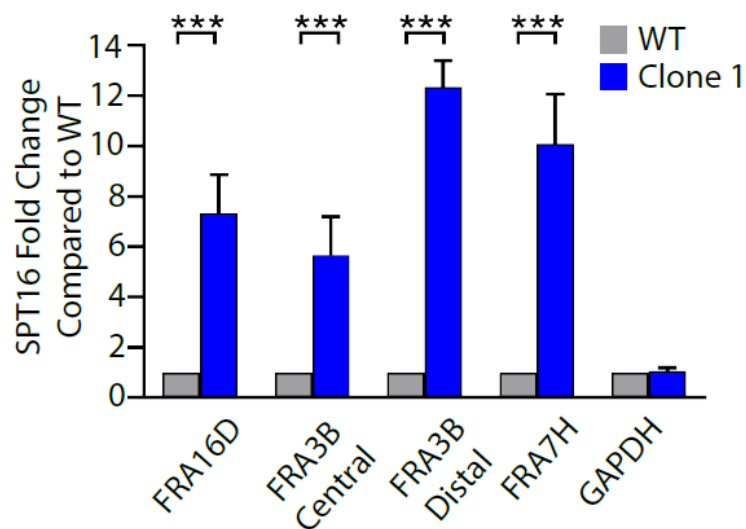


**Figure 49 – SPT16 accumulates at CFSs in OTUD5 D537A Knock in cells.** ChiP analysis reveals a 6 to 12 fold increase of SPT16 accumulation at CFSs in OTUD5<sup>D537A</sup> cells compared to parental cells. GAPDH is used as a loading control.

Observing that SPT16 is accumulating at CFSs, the next question I had was what the consequences of this accumulation were. Using both the Knock out system and the Knock in lines, I tested whether R-loop formation at the CFSs was affected. With the help of Anthony Sanchez, ChIP analysis confirmed that OTUD5 KO and UBR5 KO cells have increased R-loop formation at the CFS (Figure 50A). Similarly, when the same experiment was performed using the OTUD5 D537A knock in cell lines, ChIP analysis revealed increased R-loop formation at the CFSs (Figure 50B).

Next, I wanted study if there were any replication fork phenotypes. To do this, I employed PLA between Biotin-Edu labeled replication fork and pSer2 RNA Polymerase II. If the phenotypes observed are due to aberrant transcriptional regulation, I expect to see increased transcriptional machinery at the replication fork, resulting in collisions between the two structures.

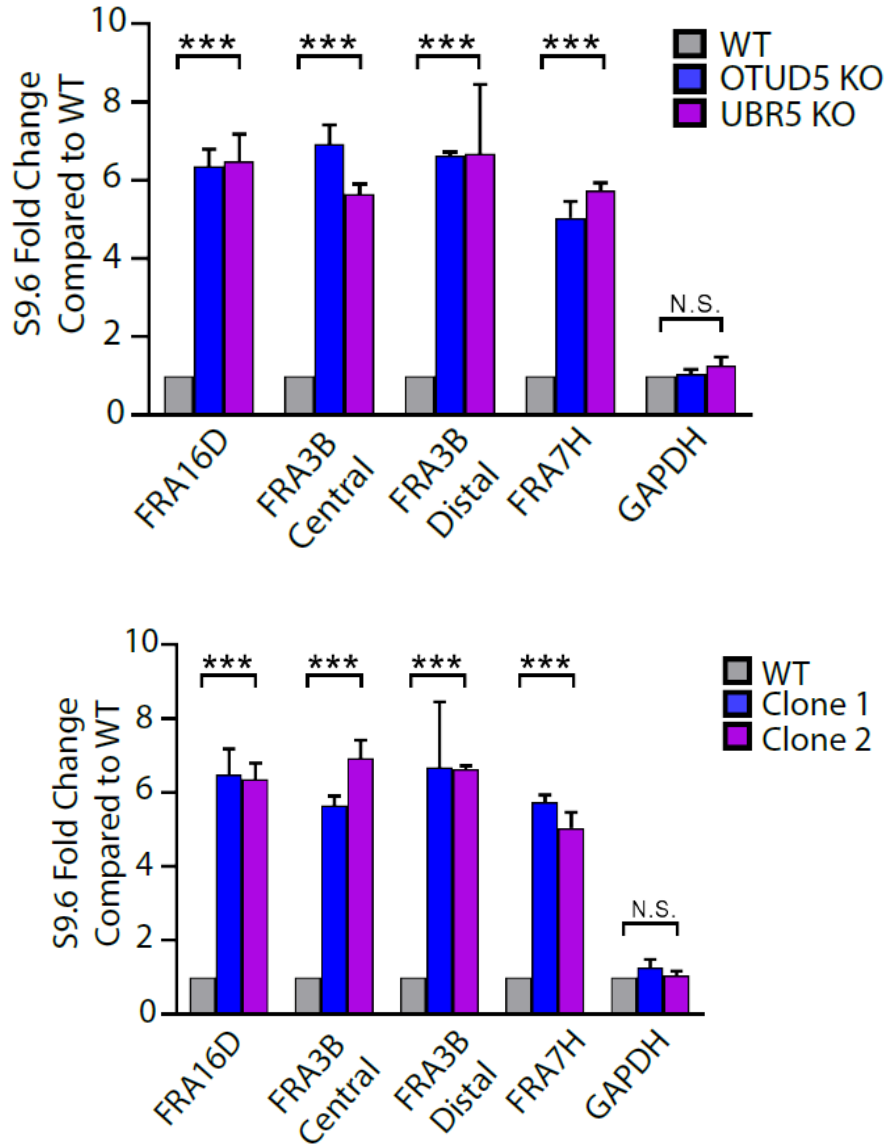


**Figure 50 – R-loop formation at CFS is increased in cells with unregulated transcription A.** ChiP analysis of OTUD5 KO and UBR5 KO HeLa cells reveals an increase of R-loop formation at CFSs. GAPDH is used as a loading control. **B.** ChiP analysis of two OTUD5 D537A knock in HeLa clones reveals an increase of R-loop formation at CFSs. GAPDH is used as a loading control. Data courtesy of Anthony Sanchez.

When the OTUD5 D537A knock in cell lines were tested for this, I saw an increased PLA signal in the knock ins compared to the WT (Figure 51A). This phenotype was accompanied by an increased PLA signal between Biotin-Edu labeled replication fork and SPT16 (Figure 51B), suggesting that aberrant SPT16 activity associated with increased collisions.

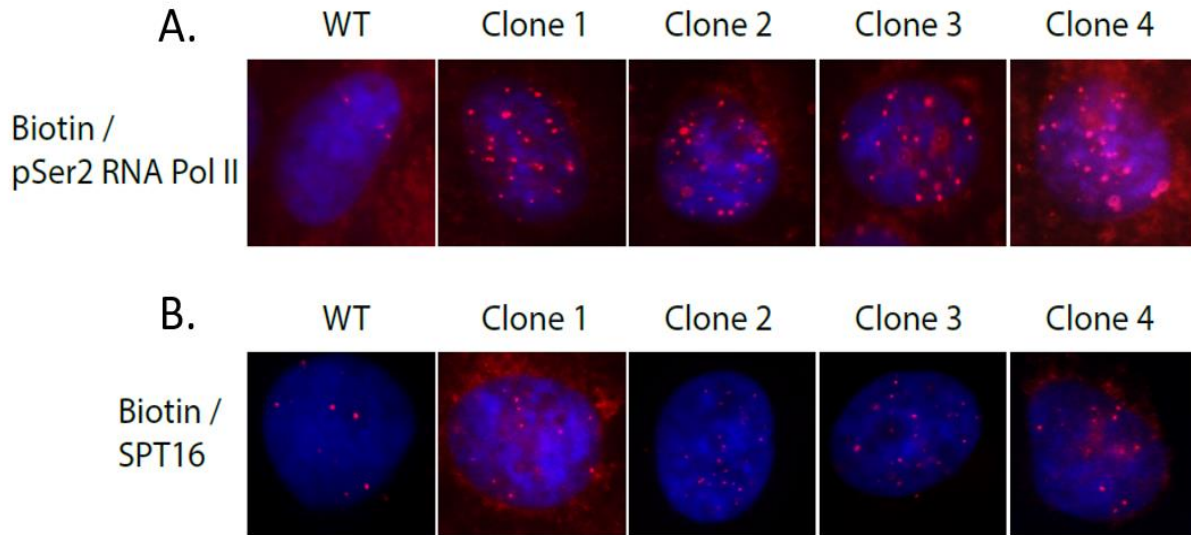


**Figure 51 – OTUD5<sup>D537A</sup> knock in cell line show increased PLA signal between replication fork and transcription.** **A.** PLA between Biotin-Edu and pSer2 RNA Polymerase II was performed in the OTUD5 D537A knock in cell lines, resulting in increased signal in the knock in lines. **B.** PLA between Biotin-Edu and SPT16 was performed in the OTUD5 D537A knock in cell lines, resulting in increased signal in the knock in lines.

Growing number of evidence suggest that the Fanconi Anemia pathway is involved in resolution of R-loop. To test whether the Fanconi Anemia pathway is activated in the OTUD5 D537A knock in cell lines, I looked at presence FANCD2 foci. I found that FANCD2 foci was both increased and had increased overlap with RPA32, a marker for single stranded DNA (Figure 52).

Altogether, these data suggest that the TRC observed in OTUD5 D537A knock in cell lines is associated with unregulated SPT16 activity due to the uncoupling of the OTUD5-SPT16 interaction.

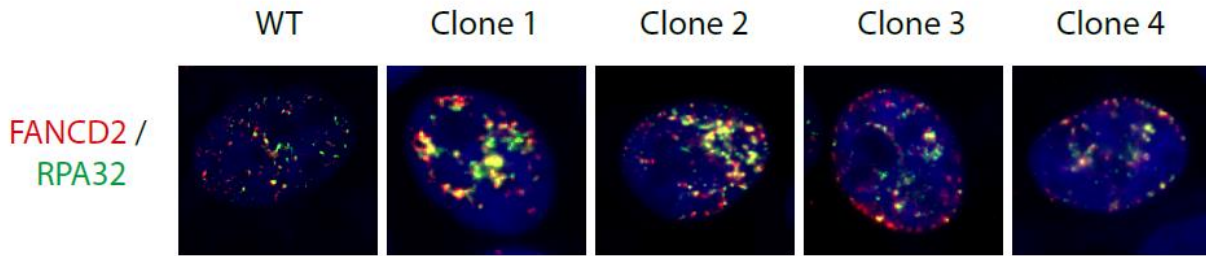


**Figure 52 - OTUD5<sup>D537A</sup> knock in cell have increased FANCD2 foci.** OTUD5 D537A knock in cell lines were fixed and stained for FANCD2 and RPA32. The clones show an increased both in foci for both FANCD2 and RPA32, but also in overlap.

### **SPT16 interacts with HDAC1/HDAC2 through OTUD5**

To further understand the mechanism of action that is responsible for TRC, I decided to investigate other OTUD5 interacting partners. It was recently described by Beck et al. (Preprint) that OTUD5 uses its C-terminal tail to interact with the Histone deacetylase HDAC2 amongst a few other proteins. Due to the role histone deacetylases play in chromatin regulation, we hypothesized that HDAC2 could be a negative regulator of SPT16 mediated transcription. To investigate this, I first performed an immunoprecipitation assay to determine if SPT16 interacts with HDAC2. I found that in the WT HeLa cells, HDAC2 did co-IP with SPT16. However, this interaction was lost in the two tested OTUD5 D537A knock in clones (Figure 53A) suggesting that the interaction between SPT16 and HDAC2 is mediated by OTUD5. The IP analysis was also performed under benzonase conditions to confirm that the interactions were not DNA mediated (Figure 53B).

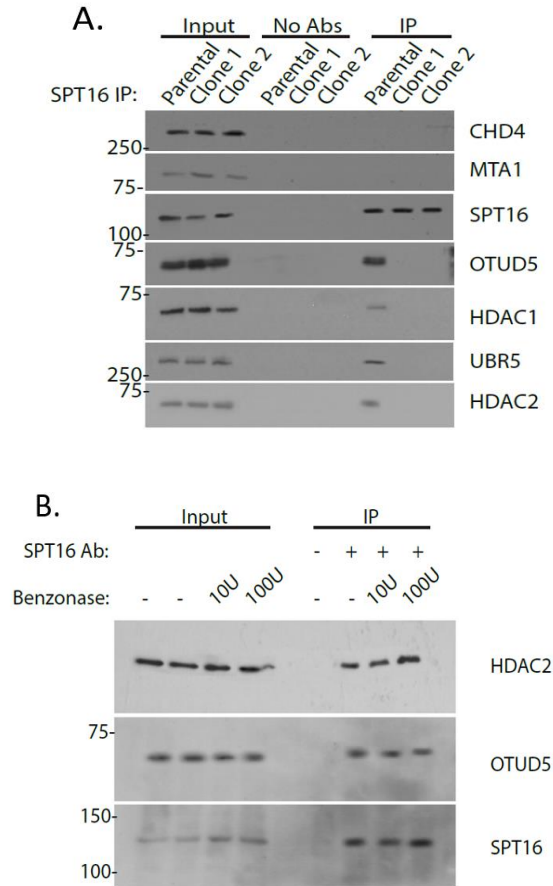


**Figure 53 – OTUD5 mediates the interaction of HDAC1/2 with SPT16.** **A.** SPT16 immunoprecipitation was performed in HeLa WT and two OTUD5 D537A knock in clones. SPT16 only was able to interact with HDAC1 and HDAC2 in the WT setting. **B.** SPT16 immunoprecipitation was performed in HeLa WT and treated with benzonase revealing that the interaction is not DNA dependent.

To verify the results of the immunoprecipitation assay, PLA between SPT16 and HDAC1 or HDAC2 was performed. Although the PLA signal between SPT16 and HDAC1/2 to be weak, the PLA signal was completely abrogated in the OTUD5 knock in cell line (Figure 55), supporting the co-IP results.

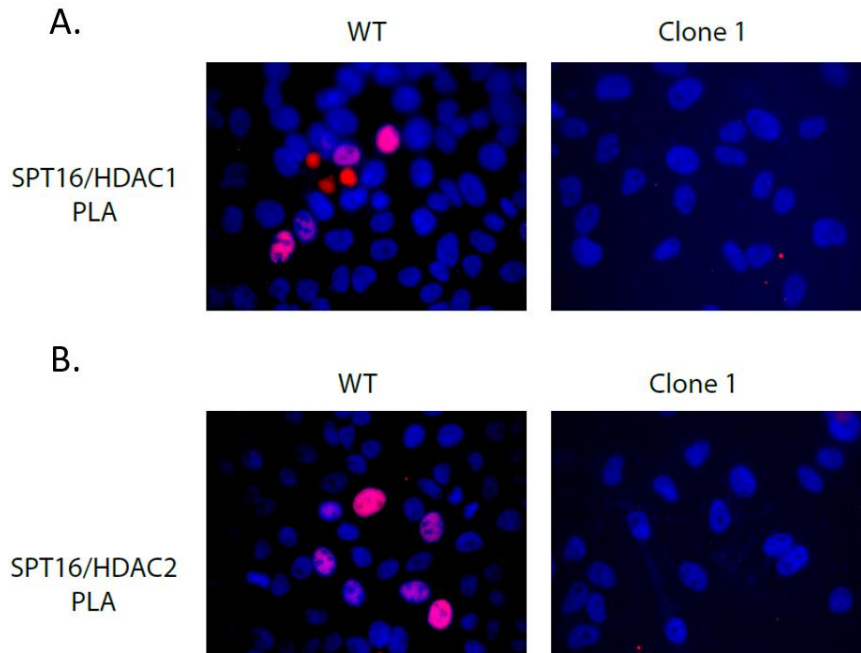


**Figure 54 – PLA analysis between SPT16 and HDAC1/2 reveals lack of signal in OTUD5 D537A Knock in cell line.** PLA between SPT16 and either HDAC1 or HDAC2 was performed in the OTUD5 D537A knock in cell line, resulting in decreased signal in the knock in line.

## Discussion

In this study we describe a novel role for OTUD5 in which it prevents TRC through the suppression of FACT mediated transcription. When OTUD5 is depleted or it loses the ability to bind to SPT16 (OTUD5 D537A mutant) exhibit signs of replication stress: G1 body formation, micronuclei formation, and R-loop formation and accumulation. Using CHIP, I was able to analyze accumulation of replication stress markers such 53BP1 or RNaseH1 at CFSs. I also found that OTUD5 was increased at CFS under replication stress, and when the OTUD5/SPT16 binding is perturbed SPT16, RNA Pol II, and R-loop accumulates at CFSs. To measure TRC, I used PLA analysis and observed increased occurrence of these events, which are increased in the OTUD5 depleted cells or OTUD5 D537A knock in cell lines. These cells also show sensitivity to various types of damage, such as double strand break or inhibition of ATR or

replication. Taken together, these results indicate that the interaction between OTUD5 and SPT16 is crucial in protecting the cell against genomic instability, and it does this by preventing Transcription-Replication Conflicts.

In chapter 4 I described the role of OTUD5 in transcriptional regulation at sites of double strand break. Here we extend that study into replication and genomic stability in more physiological setting where the aberrant DNA structures (R-loops) and replication fork perturbation are monitored on CFSs of the genome, and how the effects of unregulated transcription affect replication. In a study by Beck et al., they found that OTUD5 is a binding partner and responsible for the stability of HDAC2 (86). Histone deacetylases are known to remove acetyl modification from chromatin, resulting in condensed chromatin and thus inhibiting transcription (87). Here I confirm the interaction between OTUD5 and HDAC2, and explore the interaction further, showing that OTUD5 also interacts with HDAC1 and allows SPT16 to indirectly interact with HDAC1/2. These interactions could be a new mechanism by which cells repress transcription to avoid genomic instability and TRC.

### **Future Directions**

While this study explores the downstream effects transcriptional deregulation has, little new information on the mechanism was given. This study explores the interaction of OTUD5/FACT with a new binding partner, HDAC1/2. However, there is little known about how HDAC1/2 are contributing to this mechanism. HDAC1/2, as discussed in chapter 1, are involved in a number of different complexes with different roles. It is unclear if the described function is associated with an already known role of chromatin compaction or if this is an entirely new function of HDAC1/2. Further investigation is necessary.

Additionally, OTUD5 depletion was shown to cause TRC and replication stress. This can be further investigated by looking directly at the replication fork progression using a fibre assay. This will allow me to determine if OTUD5 depletion affects replication fork speed or collapsing replication forks.

Finally, another point of investigation is how SPT16 binds to OTUD5. Finding the binding site of SPT16 to OTUD5 may reveal further insight into how OTUD5 suppresses transcription. For instance, OTUD5 may physically bar SPT16 from binding to histones, thus preventing transcription.



### Works Cited

1. Suresh,B., Lee,J., Kim,K.-S. and Ramakrishna,S. (2016) The Importance of Ubiquitination and Deubiquitination in Cellular Reprogramming. *Stem Cells Int.*, **2016**, 6705927.
2. Nandi,D., Tahiliani,P., Kumar,A. and Chandu,D. (2006) The ubiquitin-proteasome system. *J. Biosci.*, **31**, 137–155.
3. Mevissen,T.E.T. and Komander,D. (2017) Mechanisms of deubiquitinase specificity and regulation. *Annu. Rev. Biochem.*, **86**, 159–192.
4. Mevissen,T.E.T., Hospenthal,M.K., Geurink,P.P., Elliott,P.R., Akutsu,M., Arnaudo,N., Ekkebus,R., Kulathu,Y., Wauer,T., El Oualid,F., *et al.* (2013) OTU Deubiquitinases Reveal Mechanisms of Linkage Specificity and Enable Ubiquitin Chain Restriction Analysis. *Cell*, **154**, 169–184.
5. Komander,D. (2009) The emerging complexity of protein ubiquitination. *Biochem. Soc. Trans.*, **37**, 937–953.
6. Pickart,C.M. (2001) Mechanisms Underlying Ubiquitination. *Annu. Rev. Biochem.*, **70**, 503–533.
7. Wolf,D.H. (2004) Ubiquitin-proteasome system. *Cell. Mol. Life Sci.*, **61**, 1601–1614.
8. Ma,T., Keller,J.A. and Yu,X. (2011) RNF8-dependent histone ubiquitination during DNA damage response and spermatogenesis. *Acta Biochim. Biophys. Sin. (Shanghai)*, **43**, 339–345.
9. Haglund,K., Sigismund,S., Polo,S., Szymkiewicz,I., Di Fiore,P.P. and Dikic,I. (2003) Multiple monoubiquitination of RTKs is sufficient for their endocytosis and degradation. *Nat. Cell*

*Biol.*, **5**, 461–466.

10. Dye, B.T. and Schulman, B.A. (2007) Structural Mechanisms Underlying Posttranslational Modification by Ubiquitin-Like Proteins. *Annu. Rev. Biophys. Biomol. Struct.*, **36**, 131–150.
11. Citterio, E. (2015) Fine-tuning the ubiquitin code at DNA double-strand breaks: deubiquitinating enzymes at work. *Front. Genet.*, **6**, 282.
12. Kee, Y., Muñoz, W., Lyon, N. and Huibregtse, J.M. (2006) The Deubiquitinating Enzyme Ubp2 Modulates Rsp5-dependent Lys63-linked Polyubiquitin Conjugates in *Saccharomyces cerevisiae*. *J. Biol. Chem.*, **281**, 36724–36731.
13. Thorslund, T., Ripplinger, A., Hoffmann, S., Wild, T., Uckelmann, M., Villumsen, B., Narita, T., Sixma, T.K., Choudhary, C., Bekker-Jensen, S., *et al.* (2015) Histone H1 couples initiation and amplification of ubiquitin signalling after DNA damage. *Nature*, **527**, 389–393.
14. Ehlers, M.D. (2003) Activity level controls postsynaptic composition and signaling via the ubiquitin-proteasome system. *Nat. Neurosci.*, **6**, 231–242.
15. Bence, N.F., Sampat, R.M. and Kopito, R.R. (2001) Impairment of the Ubiquitin-Proteasome System by Protein Aggregation. *Science (80- )*, **292**, 1552 LP – 1555.
16. Ravid, T. and Hochstrasser, M. (2008) Diversity of degradation signals in the ubiquitin-proteasome system. *Nat. Rev. Mol. Cell Biol.*, **9**, 679–689.
17. Ciechanover, A. (1994) The ubiquitin-proteasome proteolytic pathway. *Cell*, **79**, 13–21.
18. Strous, G.J. and Govers, R. (1999) The ubiquitin-proteasome system and endocytosis. *J. Cell Sci.*, **112**, 1417 LP – 1423.
19. Berndsen, C.E. and Wolberger, C. (2014) New insights into ubiquitin E3 ligase mechanism. *Nat. Struct. Mol. Biol.*, **21**, 301–307.

20. Munoz,M.A., Saunders,D.N., Henderson,M.J., Clancy,J.L., Russell,A.J., Lehrbach,G., Musgrove,E.A., Watts,C.K.W. and Sutherland,R.L. (2007) The E3 ubiquitin ligase EDD regulates S-phase and G2/M DNA damage checkpoints. *Cell Cycle*, **6**, 3070–3077.
21. Shearer,R.F., Iconomou,M., Watts,C.K.W. and Saunders,D.N. (2015) Functional Roles of the E3 Ubiquitin Ligase UBR5 in Cancer. *Mol. Cancer Res.*, **13**, 1523–1532.
22. Zhang,T., Cronshaw,J., Kanu,N., Snijders,A.P. and Behrens,A. (2014) UBR5-mediated ubiquitination of ATMIN is required for ionizing radiation-induced ATM signaling and function. *Proc. Natl. Acad. Sci. U. S. A.*, **111**, 12091–12096.
23. Gudjonsson,T., Altmeyer,M., Savic,V., Toledo,L., Dinant,C., Grøfte,M., Bartkova,J., Poulsen,M., Oka,Y., Bekker-Jensen,S., *et al.* (2012) TRIP12 and UBR5 Suppress Spreading of Chromatin Ubiquitylation at Damaged Chromosomes. *Cell*, **150**, 697–709.
24. Sanchez,A., De Vivo,A., Uprety,N., Kim,J., Stevens,S.M. and Kee,Y. (2016) BMI1-UBR5 axis regulates transcriptional repression at damaged chromatin. *Proc. Natl. Acad. Sci. U. S. A.*, **113**, 11243–11248.
25. Zhang,X., Pfeiffer,H., Thorne,A. and McMahon,S.B. (2008) USP22, an hSAGA subunit and potential cancer stem cell marker, reverses the polycomb-catalyzed ubiquitylation of histone H2A. *Cell Cycle*, **7**, 1522–1524.
26. Tang,B., Tang,F., Li,B., Yuan,S., Xu,Q., Tomlinson,S., Jin,J., Hu,W. and He,S. (2015) High USP22 expression indicates poor prognosis in hepatocellular carcinoma. *Oncotarget*, **6**, 12654–12667.
27. Hicke,L., Schubert,H.L. and Hill,C.P. (2005) Ubiquitin-binding domains. *Nat. Rev. Mol. Cell Biol.*, **6**, 610–621.

28. Komander,D., Clague,M.J. and Urbé,S. (2009) Breaking the chains: Structure and function of the deubiquitinases. *Nat. Rev. Mol. Cell Biol.*, **10**, 550–563.
29. Park,S.Y., Choi,H.K., Choi,Y., Kwak,S., Choi,K.C. and Yoon,H.G. (2015) Deubiquitinase OTUD5 mediates the sequential activation of PDCD5 and p53 in response to genotoxic stress. *Cancer Lett.*, **357**, 419–427.
30. Kayagaki,N., Phung,Q., Chan,S., Chaudhari,R., Quan,C., O’Rourke,K.M., Eby,M., Pietras,E., Cheng,G., Bazan,J.F., *et al.* (2007) DUBA: A deubiquitinase that regulates type I interferon production. *Science (80-. )*, **318**, 1628–1632.
31. Rutz,S., Kayagaki,N., Phung,Q.T., Eidenschenk,C., Noubade,R., Wang,X., Lesch,J., Lu,R., Newton,K., Huang,O.W., *et al.* (2015) Deubiquitinase DUBA is a post-translational brake on interleukin-17 production in T cells. *Nature*, **518**, 417–421.
32. Ciccia,A. and Elledge,S.J. (2010) The DNA Damage Response: Making It Safe to Play with Knives. *Mol. Cell*, **40**, 179–204.
33. Houtgraaf,J.H., Versmissen,J. and van der Giessen,W.J. (2006) A concise review of DNA damage checkpoints and repair in mammalian cells. *Cardiovasc. Revascularization Med.*, **7**, 165–172.
34. Heyer,W.-D., Ehmsen,K.T. and Liu,J. (2010) Regulation of Homologous Recombination in Eukaryotes. *Annu. Rev. Genet.*, **44**, 113–139.
35. Hill,S.J., Rolland,T., Adelmant,G., Xia,X., Owen,M.S., Dricot,A., Zack,T.I., Sahni,N., Jacob,Y., Hao,T., *et al.* (2014) Systematic screening reveals a role for BRCA1 in the response to transcription-associated DNA damage. *Genes Dev.*, **28**, 1957–1975.
36. Ouchi,T., Monteiro,A.N.A., August,A., Aaronson,S.A. and Hanafusa,H. (1998) BRCA1

- regulates p53-dependent gene expression. *Proc. Natl. Acad. Sci.*, **95**, 2302 LP – 2306.
37. Arizti,P., Fang,L., Park,I., Yin,Y., Solomon,E., Ouchi,T., Aaronson,S.A. and Lee,S.W. (2000) Tumor suppressor p53 is required to modulate BRCA1 expression. *Mol. Cell. Biol.*, **20**, 7450–7459.
38. Kruhlak,M., Crouch,E.E., Orlov,M., Montañó,C., Gorski,S.A., Nussenzweig,A., Misteli,T., Phair,R.D. and Casellas,R. (2007) The ATM repair pathway inhibits RNA polymerase I transcription in response to chromosome breaks. *Nature*, **447**, 730–734.
39. Pengelly,A.R., Kalb,R., Finkl,K. and Müller,J. (2015) Transcriptional repression by PRC1 in the absence of H2A monoubiquitylation. *Genes Dev.*, **29**, 1487–1492.
40. Buchwald,G., van der Stoop,P., Weichenrieder,O., Perrakis,A., van Lohuizen,M. and Sixma,T.K. (2006) Structure and E3-ligase activity of the Ring-Ring complex of polycomb proteins Bmi1 and Ring1b. *EMBO J.*, **25**, 2465–2474.
41. Chagraoui,J., Hébert,J., Girard,S. and Sauvageau,G. (2011) An anticlastogenic function for the Polycomb Group gene Bmi1. *Proc. Natl. Acad. Sci.*, **108**, 5284 LP – 5289.
42. Harding,S.M., Boiarsky,J.A. and Greenberg,R.A. (2015) ATM Dependent Silencing Links Nucleolar Chromatin Reorganization to DNA Damage Recognition. *Cell Rep.*, **13**, 251–259.
43. Dong,C., West,K.L., Tan,X.Y., Li,J., Ishibashi,T., Yu,C.H., Sy,S.M.H., Leung,J.W.C. and Huen,M.S.Y. (2020) Screen identifies DYRK1B network as mediator of transcription repression on damaged chromatin. *Proc. Natl. Acad. Sci. U. S. A.*, **117**, 17019–17030.
44. Meisenberg,C., Pinder,S.I., Hopkins,S.R., Wooller,S.K., Benstead-Hume,G., Pearl,F.M.G., Jeggo,P.A. and Downs,J.A. (2019) Repression of Transcription at DNA Breaks Requires Cohesin throughout Interphase and Prevents Genome Instability. *Mol. Cell*, **73**, 212-

223.e7.

45. De Vivo,A., Sanchez,A., Yegres,J., Kim,J., Emly,S. and Kee,Y. (2019) The OTUD5-UBR5 complex regulates FACT-mediated transcription at damaged chromatin. *Nucleic Acids Res.*, **47**, 729–746.
46. Wei,X., Samarabandu,J., Devdhar,R.S., Siegel,A.J., Acharya,R. and Berezney,R. (1998) Segregation of Transcription and Replication Sites Into Higher Order Domains. *Science (80-. )*, **281**, 1502 LP – 1505.
47. Hamperl,S. and Cimprich,K.A. (2016) Conflict Resolution in the Genome: How Transcription and Replication Make It Work. *Cell*, **167**, 1455–1467.
48. Wu,W., Hickson,I.D. and Liu,Y. (2020) The prevention and resolution of DNA replication–transcription conflicts in eukaryotic cells. *Genome Instab. Dis.*, **1**, 114–128.
49. Bermejo,R., Lai,M.S. and Foiani,M. (2012) Preventing replication stress to maintain genome stability: resolving conflicts between replication and transcription. *Mol. Cell*, **45**, 710–718.
50. Pomerantz,R.T. and O’Donnell,M. (2008) The replisome uses mRNA as a primer after colliding with RNA polymerase. *Nature*, **456**, 762–766.
51. Stirling,P.C., Chan,Y.A., Minaker,S.W., Aristizabal,M.J., Barrett,I., Sipahimalani,P., Kobor,M.S. and Hieter,P. (2012) R-loop-mediated genome instability in mRNA cleavage and polyadenylation mutants. *Genes Dev.* , **26**, 163–175.
52. Gan,W., Guan,Z., Liu,J., Gui,T., Shen,K., Manley,J.L. and Li,X. (2011) R-loop-mediated genomic instability is caused by impairment of replication fork progression. *Genes Dev.* , **25**, 2041–2056.
53. Wahba,L., Koshland,D., Costantino,L., Tan,F.J., Zimmer,A. and Koshland,D. (2016) S1-

- DRIP-seq identifies high expression and polyA tracts as major contributors to R-loop formation. *Genes Dev.* , **50**, 1327–1338.
54. Castellano-Pozo,M., García-Muse,T. and Aguilera,A. (2012) R-loops cause replication impairment and genome instability during meiosis. *EMBO Rep.*, **13**, 923–929.
55. Chakraborty,P. and Grosse,F. (2011) Human DHX9 helicase preferentially unwinds RNA-containing displacement loops (R-loops) and G-quadruplexes. *DNA Repair (Amst.)*, **10**, 654–665.
56. Hatchi,E., Skourti-Stathaki,K., Ventz,S., Pinello,L., Yen,A., Kamieniarz-Gdula,K., Dimitrov,S., Pathania,S., McKinney,K.M., Eaton,M.L., *et al.* (2015) BRCA1 Recruitment to Transcriptional Pause Sites Is Required for R-Loop-Driven DNA Damage Repair. *Mol. Cell*, **57**, 636–647.
57. Sollier,J., Stork,C.T., García-Rubio,M.L., Paulsen,R.D., Aguilera,A. and Cimprich,K.A. (2014) Transcription-coupled nucleotide excision repair factors promote R-loop-induced genome instability. *Mol. Cell*, **56**, 777–785.
58. Nudler,E. (2012) RNA Polymerase Backtracking in Gene Regulation and Genome Instability. *Cell*, **149**, 1438–1445.
59. Azvolinsky,A., Giresi,P.G., Lieb,J.D. and Zakian,V.A. (2009) Highly Transcribed RNA Polymerase II Genes Are Impediments to Replication Fork Progression in *Saccharomyces cerevisiae*. *Mol. Cell*, **34**, 722–734.
60. Luger,K., Mäder,A.W., Richmond,R.K., Sargent,D.F. and Richmond,T.J. (1997) Crystal structure of the nucleosome core particle at 2.8 Å resolution. *Nature*, **389**, 251–260.
61. Tremethick,D.J. (2007) Higher-order structures of chromatin: the elusive 30 nm fiber. *Cell*,

128, 651–654.

62. Burgess,R.J. and Zhang,Z. (2013) Histone chaperones in nucleosome assembly and human disease. *Nat. Struct. Mol. Biol.*, **20**, 14–22.
63. Belotserkovskaya,R., Oh,S., Bondarenko,V.A., Orphanides,G., Studitsky,V.M. and Reinberg,D. (2003) FACT Facilitates Transcription-Dependent Nucleosome Alteration. *Science (80-. )*, **301**, 1090 LP – 1093.
64. Orphanides,G., LeRoy,G., Chang,C.-H., Luse,D.S. and Reinberg,D. (1998) FACT, a Factor that Facilitates Transcript Elongation through Nucleosomes. *Cell*, **92**, 105–116.
65. Marcianó,G., Da Vela,S., Tria,G., Svergun,D.I., Byron,O. and Huang,D.T. (2018) Structure-specific recognition protein-1 (SSRP1) is an elongated homodimer that binds histones. *J. Biol. Chem.*, **293**, 10071–10083.
66. Orphanides,G., Wu,W.H., Lane,W.S., Hampsey,M. and Reinberg,D. (1999) The chromatin-specific transcription elongation factor FACT comprises human SPT16 and SSRP1 proteins. *Nature*, **400**, 284–288.
67. Formosa,T., Eriksson,P., Wittmeyer,J., Ginn,J., Yu,Y. and Stillman,D.J. (2001) Spt16-Pob3 and the HMG protein Nhp6 combine to form the nucleosome-binding factor SPN. *EMBO J.*, **20**, 3506–3517.
68. Brewster,N.K., Johnston,G.C. and Singer,R.A. (2001) A Bipartite Yeast SSRP1 Analog Comprised of Pob3 and Nhp6 Proteins Modulates Transcription. *Mol. Cell. Biol.*, **21**, 3491 LP – 3502.
69. Stuwe,T., Hothorn,M., Lejeune,E., Rybin,V., Bortfeld,M., Scheffzek,K. and Ladurner,A.G. (2008) The FACT Spt16 ‘peptidase’ domain is a histone H3-H4 binding module. *Proc. Natl.*



*Acad. Sci. U. S. A.*, **105**, 8884–8889.

70. VanDemark,A.P., Xin,H., McCullough,L., Rawlins,R., Bentley,S., Heroux,A., Stillman,D.J., Hill,C.P. and Formosa,T. (2008) Structural and functional analysis of the Spt16p N-terminal domain reveals overlapping roles of yFACT subunits. *J. Biol. Chem.*, **283**, 5058–5068.
71. Winkler,D.D. and Luger,K. (2011) The histone chaperone FACT: Structural insights and mechanisms for nucleosome reorganization. *J. Biol. Chem.*, **286**, 18369–18374.
72. Tsunaka,Y., Fujiwara,Y., Oyama,T., Hirose,S. and Morikawa,K. (2016) Integrated molecular mechanism directing nucleosome reorganization by human FACT. *Genes Dev.*, **30**, 673–686.
73. Zhang,W., Zeng,F., Liu,Y., Shao,C., Li,S., Lv,H., Shi,Y., Niu,L., Teng,M. and Li,X. (2015) Crystal Structure of Human SSRP1 Middle Domain Reveals a Role in DNA Binding. *Sci. Rep.*, **5**, 1–12.
74. Brewster,N.K., Johnston,G.C. and Singer,R.A. (1998) Characterization of the CP complex, an abundant dimer of Cdc68 and Pob3 proteins that regulates yeast transcriptional activation and chromatin repression. *J. Biol. Chem.*, **273**, 21972–21979.
75. Tsunaka,Y., Toga,J., Yamaguchi,H., Tate,S., Hirose,S. and Morikawa,K. (2009) Phosphorylated intrinsically disordered region of FACT masks its nucleosomal DNA binding elements. *J. Biol. Chem.*, **284**, 24610–24621.
76. Formosa,T. (2008) FACT and the reorganized nucleosome. *Mol. Biosyst.*, **4**, 1085–1093.
77. Biswas,D., Yu,Y., Prall,M., Formosa,T. and Stillman,D.J. (2005) The yeast FACT complex has a role in transcriptional initiation. *Mol. Cell. Biol.*, **25**, 5812–5822.
78. Jamai,A., Puglisi,A. and Strubin,M. (2009) Histone chaperone spt16 promotes redeposition

- of the original h3-h4 histones evicted by elongating RNA polymerase. *Mol. Cell*, **35**, 377–383.
79. Dinant,C., Ampatziadis-Michailidis,G., Lans,H., Tresini,M., Lagarou,A., Grosbart,M., Theil,A.F., van Cappellen,W.A., Kimura,H., Bartek,J., *et al.* (2013) Enhanced chromatin dynamics by FACT promotes transcriptional restart after UV-induced DNA damage. *Mol. Cell*, **51**, 469–479.
80. Pavri,R., Zhu,B., Li,G., Trojer,P., Mandal,S., Shilatifard,A. and Reinberg,D. (2006) Histone H2B Monoubiquitination Functions Cooperatively with FACT to Regulate Elongation by RNA Polymerase II. *Cell*, **125**, 703–717.
81. Kim,J., Sturgill,D., Sebastian,R., Khurana,S., Tran,A.D., Edwards,G.B., Kruswick,A., Burkett,S., Hosogane,E.K., Hannon,W.W., *et al.* (2018) Replication Stress Shapes a Protective Chromatin Environment across Fragile Genomic Regions. *Mol. Cell*, **69**, 36-47.e7.
82. Han,J., Li,Q., McCullough,L., Kettelkamp,C., Formosa,T. and Zhang,Z. (2010) Ubiquitylation of FACT by the cullin-E3 ligase Rtt101 connects FACT to DNA replication. *Genes Dev.*, **24**, 1485–1490.
83. Choudhary,C., Kumar,C., Gnad,F., Nielsen,M.L., Rehman,M., Walther,T.C., Olsen,J. V and Mann,M. (2009) Lysine Acetylation Targets Protein Complexes and Co-Regulates Major Cellular Functions. *Science (80-. )*, **325**, 834 LP – 840.
84. ALLFREY,V.G., FAULKNER,R. and MIRSKY,A.E. (1964) ACETYLATION AND METHYLATION OF HISTONES AND THEIR POSSIBLE ROLE IN THE REGULATION OF RNA SYNTHESIS. *Proc. Natl. Acad. Sci. U. S. A.*, **51**, 786–794.
85. Kelly,R.D.W. and Cowley,S.M. (2013) The physiological roles of histone deacetylase

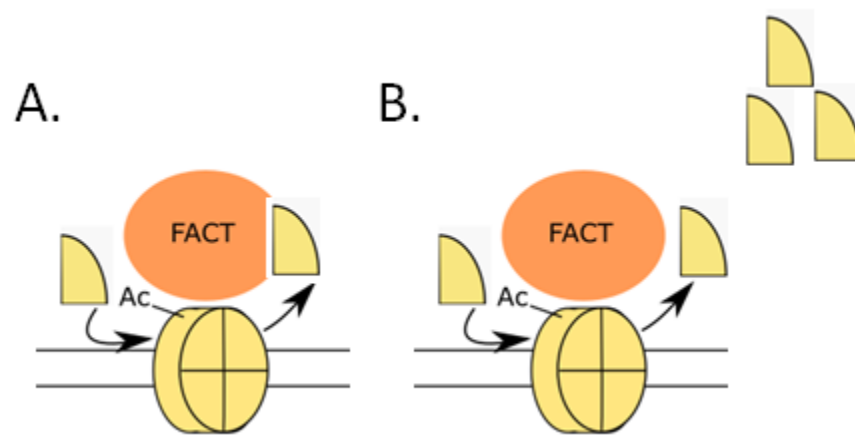
- (HDAC) 1 and 2: Complex co-stars with multiple leading parts. *Biochem. Soc. Trans.*, **41**, 741–749.
86. Beck,D., Basar,M., Asmar,A., Thompson,J., Oda,H., Uehara,D., Saida,K., D’Souza,P., Bodurtha,J., Mu,W., *et al.* (2020) Regulation of human development by ubiquitin chain editing of chromatin remodelers. 10.1101/2020.01.23.917450.
87. Zhang,Y., Ng,H.H., Erdjument-Bromage,H., Tempst,P., Bird,A. and Reinberg,D. (1999) Analysis of the NuRD subunits reveals a histone deacetylase core complex and a connection with DNA methylation. *Genes Dev.*, **13**, 1924–1935.
88. Cowley,S.M., Iritani,B.M., Mendrysa,S.M., Xu,T., Cheng,P.F., Yada,J., Liggitt,H.D. and Eisenman,R.N. (2005) The mSin3A chromatin-modifying complex is essential for embryogenesis and T-cell development. *Mol. Cell. Biol.*, **25**, 6990–7004.
89. Laherty,C.D., Yang,W.M., Sun,J.M., Davie,J.R., Seto,E. and Eisenman,R.N. (1997) Histone deacetylases associated with the mSin3 corepressor mediate mad transcriptional repression. *Cell*, **89**, 349–356.
90. Reyes-Turcu,F.E., Ventii,K.H. and Wilkinson,K.D. (2009) Regulation and Cellular Roles of Ubiquitin-Specific Deubiquitinating Enzymes. *Annu. Rev. Biochem.*, **78**, 363–397.
91. Kee,Y. and Huibregtse,J.M. (2007) Regulation of catalytic activities of HECT ubiquitin ligases. *Biochem. Biophys. Res. Commun.*, **354**, 329–333.
92. Nijman,S.M.B., Luna-Vargas,M.P.A., Velds,A., Brummelkamp,T.R., Dirac,A.M.G., Sixma,T.K. and Bernards,R. (2005) A Genomic and Functional Inventory of Deubiquitinating Enzymes. *Cell*, **123**, 773–786.
93. Kee,Y. and Huang,T.T. (2016) Role of Deubiquitinating Enzymes in DNA Repair. *Mol. Cell.*

*Biol.*, **36**, 524–544.

94. Nakada,S., Tai,I., Panier,S., Al-Hakim,A., Iemura,S.I., Juang,Y.C., O'Donnell,L., Kumakubo,A., Munro,M., Sicheri,F., *et al.* (2010) Non-canonical inhibition of DNA damage-dependent ubiquitination by OTUB1. *Nature*, **466**, 941–946.
95. Sun,X.-X., Challagundla,K.B. and Dai,M.-S. (2012) Positive regulation of p53 stability and activity by the deubiquitinating enzyme Otubain 1. *EMBO J.*, **31**, 576–592.
96. Zhao,Y., Majid,M.C., Soll,J.M., Brickner,J.R., Dango,S. and Mosammaparast,N. (2015) Noncanonical regulation of alkylation damage resistance by the OTUD4 deubiquitinase. *EMBO J.*, **34**, 1687–1703.
97. Somesh,B.P., Reid,J., Liu,W.-F., Søgaaard,T.M.M., Erdjument-Bromage,H., Tempst,P. and Svejstrup,J.Q. (2005) Multiple Mechanisms Confining RNA Polymerase II Ubiquitylation to Polymerases Undergoing Transcriptional Arrest. *Cell*, **121**, 913–923.
98. Geijer,M.E. and Marteijn,J.A. (2018) What happens at the lesion does not stay at the lesion: Transcription-coupled nucleotide excision repair and the effects of DNA damage on transcription in cis and trans. *DNA Repair (Amst.)*, **71**, 56–68.
99. Shanbhag,N.M., Rafalska-Metcalf,I.U., Balane-Bolivar,C., Janicki,S.M. and Greenberg,R.A. (2010) ATM-Dependent Chromatin Changes Silence Transcription In cis to DNA Double-Strand Breaks. *Cell*, **141**, 970–981.
100. Chou,D.M., Adamson,B., Dephoure,N.E., Tan,X., Nottke,A.C., Hurov,K.E., Gygi,S.P., Colaiácovo,M.P. and Elledge,S.J. (2010) A chromatin localization screen reveals poly (ADP ribose)-regulated recruitment of the repressive polycomb and NuRD complexes to sites of DNA damage. *Proc. Natl. Acad. Sci.*, **107**, 18475 LP – 18480.

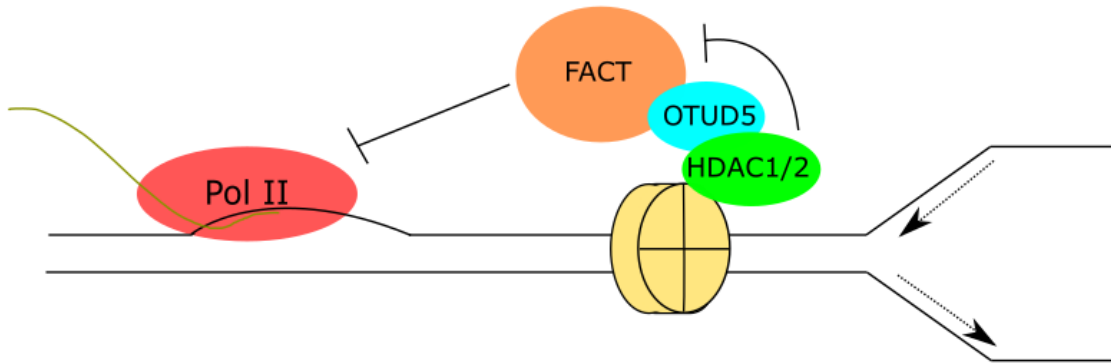
101. Im, J.-S., Keaton, M., Lee, K.Y., Kumar, P., Park, J. and Dutta, A. (2014) ATR checkpoint kinase and CRL1 $\beta$ TRCP collaborate to degrade ASF1a and thus repress genes overlapping with clusters of stalled replication forks. *Genes Dev.*, **28**, 875–887.
102. Michl, J., Zimmer, J. and Tarsounas, M. (2016) Interplay between Fanconi anemia and homologous recombination pathways in genome integrity. *EMBO J.*, **35**, 909–923.
103. Schwab, R.A., Nieminuszczy, J., Shah, F., Langton, J., Lopez Martinez, D., Liang, C.-C., Cohn, M.A., Gibbons, R.J., Deans, A.J. and Niedzwiedz, W. (2015) The Fanconi Anemia Pathway Maintains Genome Stability by Coordinating Replication and Transcription. *Mol. Cell*, **60**, 351–361.
104. Saponaro, M., Kantidakis, T., Mitter, R., Kelly, G.P., Heron, M., Williams, H., Söding, J., Stewart, A. and Svejstrup, J.Q. (2014) RECQL5 Controls Transcript Elongation and Suppresses Genome Instability Associated with Transcription Stress. *Cell*, **157**, 1037–1049.
105. Puget, N., Miller, K.M. and Legube, G. (2019) Non-canonical DNA/RNA structures during Transcription-Coupled Double-Strand Break Repair: Roadblocks or Bona fide repair intermediates? *DNA Repair (Amst.)*, **81**, 102661.
106. Kotsantis, P., Silva, L.M., Irscher, S., Jones, R.M., Folkes, L., Gromak, N. and Petermann, E. (2016) Increased global transcription activity as a mechanism of replication stress in cancer. *Nat. Commun.*, **7**, 1–13.
107. Sanchez, A., de Vivo, A., Tonzi, P., Kim, J., Huang, T.T. and Kee, Y. (2020) Transcription-replication conflicts as a source of common fragile site instability caused by BMI1-RNF2 deficiency. *PLoS Genet.*, **16**, 1–23.

Appendix I: Supplementary Information

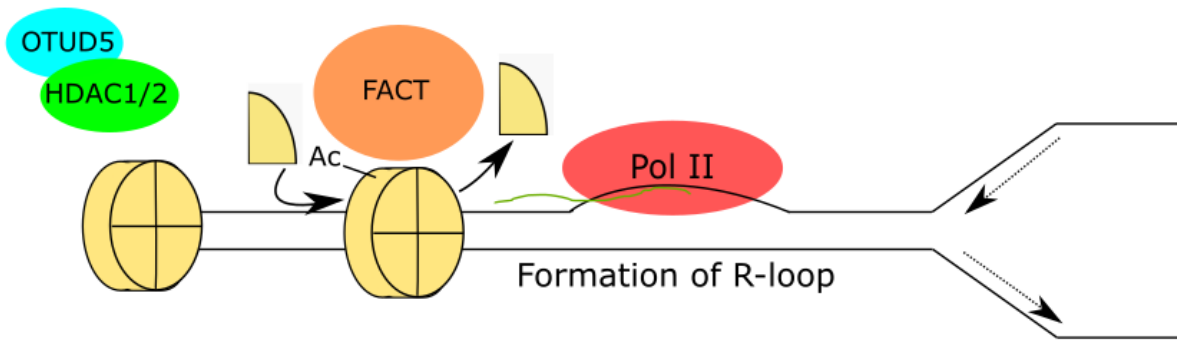


**Supplementary Figure 1A – FACT histone Eviction Model.** There have been two proposed mechanisms of action for FACT: when FACT removed a histone and reintegrates the same histone into the chromatin **(A)** or when FACT removes a histone and integrates a new histone based on an available free floating pool **(B)**

## Normal Conditions



## Uncoupling FACT/OTUD5



**Supplementary Figure 2A – Model for Repression.** Based on the data presented, transcription is repressed by HDAC1/2 acting upon acetylated chromatin while OTUD5 acts as a linker protein between HDAC1/2 and FACT. Upon uncoupling of OTUD5 and FACT (through OTUD5<sup>D537A</sup>), FACT no longer is repressed allowing RNA Polymerase II to continue transcribing DNA, potentially colliding with the replication fork.